NMR INVESTIGATIONS ON SOLUTIONS AND SINGLE CRYSTALS OF ALKALI RADICAL ION PAIRS

G. W. CANTERS

NMR INVESTIGATIONS ON SOLUTIONS AND SINGLE CRYSTALS OF ALKALI RADICAL ION PAIRS

PROMOTOR:

PROF. DR. E. DE BOER

NMR INVESTIGATIONS ON SOLUTIONS AND SINGLE CRYSTALS OF ALKALI RADICAL ION PAIRS

PROEFSCHRIFT

TER VERKRIJGING VAN DE GRAAD VAN
DOCTOR IN DE WISKUNDE EN NATUURWETENSCHAPPEN
AAN DE KATHOLIEKE UNIVERSITEIT TE NIJMEGEN,
OP GEZAG VAN DE RECTOR MAGNIFICUS MR. W. C. L. VAN DER GRINTEN,
HOOGLERAAR IN DE FACULTEIT DER RECHTSGELEERDHEID,
VOLGENS BESLUIT VAN DE SENAAT
IN HET OPENBAAR TE VERDEDIGEN OP VRIJDAG 3 OKTOBER 1969,
DES NAMIDDAGS TE 2 UUR

door

GERARDUS WILHELMUS CANTERS

Geboren te 's-Gravenhage

1969

DRUKKERIJ WED. G. VAN SOEST N.V. - AMSTERDAM

Aan mijn grootvader

Aan mijn ouders

Aan Minke en Hanneke

ACKNOWLEDGMENT

The author is much indebted to MR. A. A. K. KLAASSEN and DRS. B. M. P. HENDRIKS for their skilful assistance in the performance of the experiments.
Valuable discussions with DR. H. VAN WILLIGEN are gratefully acknowledged. DR. C. CORVAJA is thanked for helpful discussions about the sign of the alkali metal spin density in the alkali radical ion pairs. PROFESSOR T. R. TUTTLE, JR. is thanked for his interest in this work.
Technical assistance was lended by the electronics department, the instrument workshop and the glassworks of the Faculty of Science. The drawing and reproduction of the figures was provided for by the departments of reproduction and photography. The assistance of all these departments is gratefully acknowledged.
Part of the investigations described in this study have been carried out under the auspices of the Netherlands Foundation for Chemical Research (S.O.N.) and with the aid of the Netherlands Organization for the Advancement of Pure Research (Z.W.O.).

CONTENTS

INTRODUCTION

It has been known since long [1, 2] that it is possible to prepare negative ions of polycyclic aromatic hydrocarbons, like naphthalene and anthracene, by reducing the neutral compound (Ar) in a water- and oxygen-free environment with an alkali metal (Me) according to the reaction

$$Ar + Me \rightarrow Ar^- + Me^+$$

As the electron which is transferred to the aromatic compound in this reaction remains unpaired, the aromatic ions Ar^- are paramagnetic and it should in principle be possible to observe the electron spin resonance (ESR) signal of these unpaired electrons. WEISSMAN et al. in 1953 [3] were the first to succeed in observing such a signal. However, instead of one single resonance line they measured an ESR spectrum which was characterized by a rich hyperfine structure. They ascribed this hyperfine structure to the interaction of the magnetic moment of the unpaired electron with the nuclear magnetic moments of the hydrogen atoms in the aromatic molecule. It appeared that by describing the π-electron system of the aromatic ion by simple Hückel molecular orbital (M.O.) theory a satisfactory quantitative explanation of the observed hyperfine pattern could be given [4, 5]. However, for some radicals, like the negative ion of pyrene, serious discrepancies existed between the ESR spectra and the simple M.O. theory [6]. The difficulties were circumvented by the concept of negative spindensities [7, 8]. While Hückel theory would always predict a distribution of the unpaired electron over the radical according to which only non-negative spindensities could occur in the electronic π-system of the radical, more refined calculations, taking into account electronic correlation by means of a configuration interaction (C.I.) procedure, would predict also negative spin densities, particularly at sites in the molecule for which Hückel theory predicted a small or zero spin density [7]. In this way nice agreement was found between an overwhelming amount of measured ESR spectra of free radicals and the theory [9].

In 1961 ATHERTON and WEISSMAN discovered in the ESR spectrum of a solution of Na naphthalene apart from the normal proton hyperfine splitting pattern an additional hyperfine splitting which, contrary to the proton splitting, appeared to be very sensitive towards changes in solvent and temperature [10]. They were able to show that this additional splitting was caused by the interaction of the unpaired electron with the nucleus of the alkali ion, which they assumed to be associated with the naphthalene ion. In fact their experiments proved that the unpaired electron is not delocalized only over the aromatic molecule, but also over the alkali ion, which results in the presence of a small spin density at the metal nucleus. The observed variation of the alkali hyperfine splitting with solvent and temperature could be satisfactorily explained on the basis of the theory of ion pairing. The explanation appeared to be consistent with the interpretation given by HOIJTINK and coworkers [11] of conductivity experiments performed on similar solutions of aromatic alkali salts.

In the early discussions of the alkali metal hyperfine splittings no mention was made of the sign of the spin density at the metal nucleus. As in the early discussions about the spin density distribution in π-radicals, in fact it was tacitly assumed that this sign would be always positive.

This assumption had to be abandoned when DE BOER in 1965 discovered the anomalous temperature dependence of the alkali splitting in the ESR spectrum of a solution of Cs pyracene [12]. Starting at high temperatures he observed a decrease of the Cs splitting with a decrease of the temperature until the metal splitting became zero at a well defined temperature, after which again an increase of the Cs splitting occurred upon a further decrease of the temperature. DE BOER explained this phenomenon by assuming that the spin density at the metal nucleus may have a negative as well as a positive sign and that in the Cs pyracene ion pairs in fact a change of sign with the temperature was observed when the Cs splitting passed zero.

For a theoretical description of the spin density at the metal nucleus the situation appeared to be less favourable than earlier for the description of the spin density distribution in a π-radical, mainly because no detailed knowledge about the ion pair structure was available. However, DE BOER indicated that the occurrence of a negative spin density at the metal nucleus might be explained in a

qualitative way by a similar procedure as had been used to explain the occurrence of negative spin densities in π-electron radicals, viz. by taking into account electronic correlation between the π-electrons of the radical ion and the core electrons of the metal.
Later on similar phenomena were observed for other systems viz. Na biphenyl in the solvents 2-methyltetrahydrofuran [13] and tetrahydropyran [14], and Li and Na fluorenone in tetrahydrofuran and 1,2-dimethoxyethane [15, see also fig. 1].

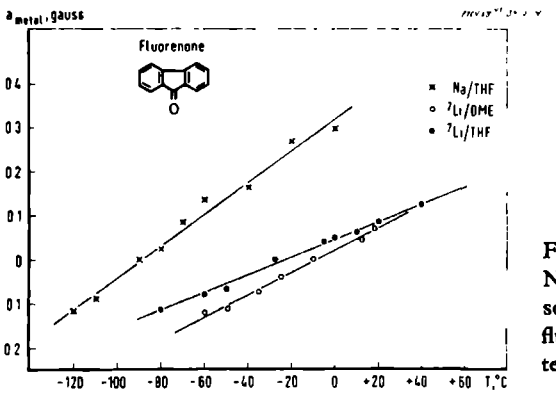

Fig. 1. ESR h.f.s.c. of Na and Li, measured on solutions of their respective fluorenone salts, *versus* temperature.

Unfortunately the ESR spectrum of a radical ion pair does not give direct evidence about the sign of the spindensity at the metal nucleus. In theory the alkali NMR spectrum of the ion pair might give the desired information: the presence of a non-zero spin density at the metal nucleus would cause the NMR signal of the alkali nucleus to be shifted by an amount of which sign and magnitude would be directly determined by the sign and the magnitude of the spin density at the metal nucleus [7, 16, 17].
The NMR method had been successfully applied already in the study of the sign of the proton hyperfine splitting constants (h.f.s.c.) in aromatic radicals [17]. As it had been assumed in these cases that the signals in the proton spectra of the pure radicals would be too broad to be observable, a procedure had been adopted by which the spectra of slightly reduced solutions of the aromatic compounds were measured. Due to the electron transfer reaction between reduced (Ar^-) and unreduced (Ar) molecules

$$Ar^- + Ar \leftrightarrows Ar + Ar^-$$

the proton signals of the diamagnetic unreduced compounds were slightly broadened and shifted in the directions of the respective resonance positions of the protons in the pure radicals. As it could be expected on theoretical grounds that the observed shifts would be proportional to the degree of reduction of the solutions, extrapolation to 100% reduction provided the resonance positions of the protons in the pure radicals, from which sign and magnitude of the proton h.f.s.c. could be established directly.

It was the purpose of this study to investigate the possibility to measure sign and magnitude of the spin density at the alkali nucleus in radical ion pairs by the NMR method in order to test the hypothesis of DE BOER about the sign and the sign reversal of this spin density. According to a suggestion of VAN WILLIGEN and DE BOER the experiments should be performed, in analogy with the proton experiments described above, by observing the alkali NMR signal of a solution of a diamagnetic alkali salt to which a small amount of a paramagnetic alkali radical salt would have been added. It could be expected that due to the cation exchange reaction

$$Me^+Ar^- + Me^+ \leftrightarrows Me^+ + Ar^-Me^+$$

the alkali NMR signal would be shifted with respect to the signal of the solution of the pure diamagnetic salt and that magnitude and direction of the shift would provide directly information about sign and magnitude of the spin density at the metal nucleus in the radical ion pair.

The first experiments which were performed in this way, namely on solutions of LiBr in THF to which small amounts of Li fluorenone had been added, proved unsuccessful in so far as no shift of the Li signal could be detected [18]. However, the experiments demonstrated that a study of the alkali linewidth might provide information about the relaxation mechanisms and the intramolecular interactions of the alkali nuclei in the ion pairs and thus about the ion pair structure. Another experimental approach could be applied after it had proved possible to measure the proton spectra of radicals in solution directly by using a sufficiently high radical concentration and an adapted experimental technique [19, 20]. From then the NMR spectra of the alkali nuclei in radical ion pairs were measured directly by using

concentrated solutions of these radical ion pairs. In this way it proved possible to study, apart from the proton spectra of aromatic radical ions like biphenyl$^-$, fluorenone$^-$ and phenanthrene$^-$, the signals of the seven most current alkali isotopes, viz. ^{6}Li, ^{7}Li, ^{23}Na, ^{39}K, ^{85}Rb, ^{87}Rb and ^{133}Cs, in reduced solutions of aromatic compounds like biphenyl, fluorenone and naphthalene. Sign and magnitude of the proton as well as of the alkali h.f.s.c. could be established and the hypothesis of the sign reversal of the metal spin density with the temperature in radical ion pairs could be tested [21, 22]. Moreover it appeared that the study of the proton and the alkali NMR linewidths provided information about the nuclear relaxation processes and the corresponding correlation times, and about the intramolecular interactions within the ion pairs. In this way information about the ion pair structure could be obtained.
During the course of this study we found in our samples for some systems single crystals. Since this was not found before for alkali radical complexes, we thought it would be very interesting to investigate these single crystals in order to obtain further information about structure and properties of alkali radical ion pairs.

The results of the investigations on the solutions and the single crystals of the alkali radical salts are reported in respectively Part I and Part II of this study.
Part I consists of the chapters two to six, of which chapter two contains the theory which is needed for the interpretation of the experimentally observed shifts and widths of the proton and the alkali NMR signals. Also in this chapter a quantum mechanical description of the spin density at the metal nucleus is given. In chapter three a description and a discussion of the experimental procedure is given, followed by the presentation of the experimental data in chapter four. In chapter five the experimental results are analysed and discussed. Part I is ended with a conclusion, presented in chapter six.
Part II consists of the single chapter seven, in which a short description is given of the preparation and the analysis of the single crystals of a number of different alkali biphenyl salts together with the results of some preliminary ESR and NMR investigations on these crystals.

PART I. NMR investigations on solutions of alkali radical ion pairs

CHAPTER 2

THEORY

2.0. SPIN HAMILTONIAN

(i). Introduction

The spin Hamiltonian of a nucleus **I** in a paramagnetic ion pair which is placed in a homogeneous magnetic field **H** along the Z-axis can be given by

$$\mathscr{H} = \mathscr{H}_0 + \mathscr{H}_{D,tot}(t) + \mathscr{H}_Q(t) \equiv \mathscr{H}_0 + \mathscr{H}_1(t) \tag{1}$$

$\mathscr{H}_0$ represents the nuclear Zeeman energy and is given by

$$\mathscr{H}_0 = -\gamma_N \hbar H I_z (1-\sigma) \tag{2}$$

in which γ_N is the gyromagnetic ratio of the nucleus, $\hbar$ is the constant of Planck divided by 2π and σ is the screening constant of the nucleus of which the value depends on the chemical compound under consideration [23].

$\mathscr{H}_{D,tot}(t)$ represents the magnetic dipole-dipole interaction between the nucleus and the magnetic moments in the complex.
$\mathscr{H}_Q(t)$ represents the interaction of the quadrupole moment of the nucleus with the field gradient at the site of the nucleus.

$\mathscr{H}_{D,tot}(t)$ will be dominated by the interaction between the nucleus and the unpaired electron **S**. Neglecting other dipole-dipole interactions, $\mathscr{H}_{D,tot}(t)$ can be given by

$$\mathscr{H}_{D,tot}(t) = \mathbf{I} \,.\, \mathbf{D}(t) \,.\, \mathbf{S}(t) \tag{3}$$

$\mathbf{D}(t)$ is a second rank tensor, which can be decomposed into an isotropic part and an anisotropic traceless part by

$$\mathbf{D}(t) = A \,.\, \mathbf{1} + \mathbf{T}(t) \tag{4}$$

in which A is a scalar, $\mathbf{1}$ is the unit dyadic and $\mathbf{T}(t)$ is a second rank traceless tensor.

(ii). The Fermi contact interaction

The parameter A in eq. (4) represents the Fermi contact interaction constant and is given by [24]

$$A = \frac{8\pi}{3} \gamma_e \gamma_N \hbar^2 \varrho(\mathbf{r}_N) \tag{5}$$

in which γ_e is the gyromagnetic ratio of the electron, defined as a positive quantity, $\varrho(\mathbf{r})$ is the spin density at the point $\mathbf{r}$ in space and $\mathbf{r}_N$ is the radiusvector of the nucleus. A is related to the hyperfine splitting constant (h.f.s.c.) a, measured in the ESR spectrum of the ion pair, by the formula

$$A = \gamma_e \hbar a \tag{6}$$

A has the dimension of an energy and a the dimension of a magnetic field strength. The sign of A and a depends on the sign of ϱ and γ_N. For the nuclei investigated in this study γ_N is positive so the sign of the h.f.s.c. is for these nuclei the same as the sign of $\varrho(\mathbf{r}_N)$.
As for two isotopes I and II of the same element, occupying identical sites in a given compound, $\varrho(\mathbf{r}_N)$ is the same, it follows from eqs. (5) and (6) that

$$\frac{a_I}{a_{II}} = \frac{A_I}{A_{II}} = \frac{\gamma_I}{\gamma_{II}} \tag{7}$$

(iii). The anisotropic dipolar interaction

$\mathbf{T}(t)$ represents the anisotropic dipolar interaction between the magnetic moments of the nucleus and the unpaired electron.
Using the concept of the spin density matrix [25] and following the procedure indicated by McConnell and Strathdee [26], the elements of $\mathbf{T}$ can be found from

$$\mathbf{T} = Tr(\boldsymbol{\rho} \,.\, \mathbf{T}) = \sum_{a,b} \varrho_{ab} \mathbf{T}_{ba} \tag{8}$$

in which $\boldsymbol{\rho}$ is the spin density matrix characterizing the spin density distribution of the unpaired electron in space, and $\mathbf{T}_{ba}$ is defined by

$$\mathbf{T}_{ba} \equiv < \varphi_b \,|\, \mathbf{T}_{op} \,|\, \varphi_a > \tag{9}$$

$\mathbf{T}_{op}$ is given by

$$\mathbf{T}_{op} \equiv \gamma_e \gamma_N \hbar^2 \frac{\mathbf{I}}{r^3}\left(\mathbf{1} - 3\frac{\mathbf{rr}}{r^2}\right) \tag{10}$$

in which $\mathbf{r}$ is given by $\mathbf{r} \equiv \mathbf{r}_e - \mathbf{r}_N$, $\mathbf{r}_e$ being the radius vector of the unpaired electron. The set $\{\varphi_a\}$ is the set of atomic orbitals (A.O.'s) from which the molecular orbital (M.O.) wavefunction of the unpaired electron can be constructed. In the present case $\{\varphi_a\}$ consists of the set $\{\varphi_i\}$ of the $2p_z$-A.O.'s of the aromatic carbon atoms and the set $\{\varphi_\nu\}$ of the A.O.'s of the alkali metal.
In the laboratory frame work the elements of $\mathbf{T}$ are a function of the direction cosines of $\mathbf{r}$. Tumbling of the complex therefore causes $\mathbf{T}$ to be a function of the time. Because of spin-lattice and spin-spin relaxation processes also the orientation of the electron spin is a function of the time. In concentrated radical solutions the time dependence of $\mathbf{S}(t)$ is determined mainly by the time dependent exchange interactions between electronic spins on different radicals.

(iv). The quadrupolar interaction

The Hamiltonian $\mathscr{H}_Q(t)$ of the quadrupolar interaction can be given by [27, 28]

$$\mathscr{H}_Q(t) = \frac{eQ}{2I(2I-1)}\mathbf{I}.\mathbf{V}(t).\mathbf{I} \qquad (11)$$

in which eQ is the nuclear quadrupole moment, I is the nuclear spin quantum number and $\mathbf{V}(t)$ is the traceless tensor of the field gradient at the site of the nucleus. It is pointed out that in this formula the Sternheimer correction [28], which takes into account the polarization of the metal core by the field gradient and the quadrupole moment, has not yet been applied. This will be discussed in sec. 2.2.2.
In the laboratory frame work the elements of $\mathbf{V}$ are a function of the direction cosines of the principal axes of $\mathbf{V}$. Tumbling of the complex therefore causes $\mathbf{V}$ to be a function of the time.

(v). Conclusion

Defining now

$$\mathscr{H}_{Fc} \equiv A\mathbf{I}.\mathbf{S}(t) \qquad (12)$$

$$\mathscr{H}_D \equiv \mathbf{I}.\mathbf{T}(t).\mathbf{S}(t) \qquad (13)$$

one finds from eqs. (1), (3), (4), (11), (12) and (13)

$$\mathscr{H}_1(t) = \mathscr{H}_{Fc}(t) + \mathscr{H}_D(t) + \mathscr{H}_Q(t) = \\ = A\mathbf{I}.\mathbf{S}(t) + \mathbf{I}.\mathbf{T}(t).\mathbf{S}(t) + \frac{eQ}{2I(2I-1)}\mathbf{I}.\mathbf{V}(t).\mathbf{I} \qquad (14)$$

2.1. THE CONTACT SHIFT AND THE HYPERFINE SPLITTING CONSTANT (H.F.S.C.)

In the following sections first general formulae for the contact shift will be derived. Next the methods which can be used to calculate sign and magnitude of the h.f.s.c. from a theoretical point of view, and the influence of solvent, temperature and concentration on the h.f.s.c., will be discussed for the protons and for the alkali nuclei in separate sections.

(i). Nucleus in a radical

The energy levels of a nucleus in a radical ion pair can be calculated from the spin Hamiltonian of eq. (1). As the ion pair is rapidly tumbling in the solution, the terms in the Hamiltonian which depend on the traceless tensors **T** and **V** can be neglected in the calculation. Therefore the energy levels can be calculated from the Hamiltonian

$$\mathscr{H} = -\gamma_N \hbar H I_z (1-\sigma) + A\,\mathbf{I}.\mathbf{S}(t) \tag{15}$$

If the external magnetic field is large, so that the second term in eq. (15) may be considered as a perturbation on the Zeeman term, and if the variation with the time of $\mathbf{S}(t)$ is characterized by a correlation time τ_e much shorter than $A.\hbar^{-1}$, eq. (15) reduces to [7]

$$\mathscr{H} = -\gamma_N \hbar H I_z (1-\sigma) + A I_z \langle S_z(t)\rangle$$

$$= -\gamma_N \hbar I_z \left[H(1-\sigma) + \frac{A}{\gamma_N \hbar}\,\frac{\gamma_e \hbar H}{3kT}\,S(S+1)\right] \tag{16}$$

in which k is the Boltzmann constant, T is the absolute temperature and S is the electron spin quantum number.
Performing an experiment by irradiating the sample with electromagnetic waves of frequency ω and assuming that the radical is in a doublet state with $S = 1/2$, the resonance condition is given by

$$\gamma_N \hbar \left[H_r (1-\sigma) + \frac{A}{\gamma_N \hbar}\,\frac{\gamma_e \hbar H_r}{4kT}\right] = \hbar\omega \tag{17}$$

in which H_r is the value of the applied external field, the nucleus being at resonance.
Performing the experiments by holding the frequency constant at a value ω_0 and varying the magnetic field, the resonance condition for a nucleus in a paramagnetic compound becomes

$$H_p (1-\sigma_p) + \frac{A}{\gamma_N \hbar}\,\frac{\gamma_e \hbar H_p}{4kT} = \frac{\omega_0}{\gamma_N} \tag{18}$$

The resonance condition for a nucleus in a diamagnetic reference compound becomes

$$H_0 (1-\sigma_0) = \frac{\omega_0}{\gamma_N} \tag{19}$$

Defining the contact shift δ_c^0 by

$$\delta_c^0 \equiv H_p - H_0 - H_p\sigma_p + H_0\sigma_0 \tag{20}$$

one finds from the eqs. (18) - (20)

$$\delta_c^0 = -\frac{A}{\gamma_N \hbar} \frac{\gamma_e \hbar H_p}{4kT} =$$

$$= -\frac{\gamma_e}{\gamma_N} a \frac{\gamma_e \hbar H_p}{4kT} \tag{21}$$

From the eqs. (5) and (21) it appears that the contact shift is independent of γ_N, so that the sign of the spin density $\varrho(\mathbf{r}_N)$ can be inferred directly from the sign of the contact shift: a high field shift indicates a negative $\varrho(\mathbf{r}_N)$, a low field shift indicates a positive $\varrho(\mathbf{r}_N)$.

(ii). Influence of an exchange equilibrium

In the case the nucleus participates in a chemical exchange equilibrium, formula (21) must be modified. Assuming that a fraction f_p of the nuclei occupies identical paramagnetic sites, and a fraction $(1-f_p)$ identical diamagnetic sites, then, provided the exchange between the two sites is rapid, the contact shift δ_c is given by

$$\delta_c = f_p \, . \, \delta_c^0 \tag{22}$$

in which δ_c^0 is given by eq. (21).
This situation occurs for instance for the aromatic protons in a partly reduced solution of an aromatic molecule Ar. Due to the electron transfer reaction

$$Ar + Ar^- \leftrightarrows Ar^- + Ar \tag{23}$$

the protons are part of the time in a paramagnetic and part of the time in a diamagnetic environment. Another example is found when one considers the alkali nuclei in a solution of radical ion pairs to which a certain amount of a diamagnetic alkali salt has been added [18] (see also chapter 1).

(iii). Conclusion

From eqs. (21) and (22) it follows that if the temperature, the shift of the NMR signal and the external field are measured, and for the case the nucleus participates in a chemical exchange between paramagnetic and diamagnetic sites, also f_p, the sign and the magnitude of the h.f.s.c. can be determined.
In working out the experimental data H_p in eq. (21) was for practical reasons set equal to H_0. This produced negligeably small errors in the final results.

2.1.1. PROTON H.F.S.C.

Since the distribution of the unpaired electron over the aromatic molecule is an intrinsic property of the electronic structure of the radical, the influence of the temperature, solvent and concentration on the proton h.f.s.c. will be small. Therefore it is not expected that the NMR method will give results which differ markedly from the ESR results, even though the concentrations used for the NMR experiments are three to four orders of magnitude larger than those used for the ESR measurements.
Theoretical values for the proton h.f.s.c. a_i can be calculated from the spin densities ϱ_i which are present in the $2p_z$-orbitals φ_i on the respective adjacent carbon atoms, by using the McConnell-Weissman relation [29, 30]

$$a_i = \mathcal{Q}\,\varrho_i \tag{24}$$

in which $\mathcal{Q}$ is a constant.
The spin densities ϱ_i can be calculated by the method of McLachlan [9] or by a combined S.C.F. and C.I. procedure.
The NMR method to determine the proton h.f.s.c. has the advantage

over the ESR method that not only the absolute value, but also the sign of the h.f.s.c. can be determined. This may facilitate the assignment of the proton h.f.s.c., because it is possible now to compare the experimentally determined sign of the h.f.s.c. with the theoretically calculated sign.

2.1.2. ALKALI METAL H.F.S.C.

(i). Introduction

In contrast with the calculation of the proton h.f.s.c. a general theory which describes the magnitude and the sign of the alkali h.f.s.c. in detail has not yet been developed, mainly because a detailed knowledge about the structure of alkali radical ion pairs is lacking. The theories which describe the influence of the temperature, solvent and concentration on the metal h.f.s.c. have been developed on the basis of ESR experiments and necessarily bear a more or less phenomenological character. In the following paragraphs the sign of the metal h.f.s.c. will be discussed and a brief survey of the theories used to explain the dependence of the metal h.f.s.c. upon the temperature, solvent and concentration will be given.

(ii). Sign of the metal h.f.s.c.

In his description of the spin density at the alkali nucleus in the alkali pyracene ion pairs DE BOER used an M.O. description in which the M.O.'s were constructed as linear combinations of the $2p_z$-A.O.'s $\{\varphi_t\}$ of the aromatic carbon atoms and the A.O.'s $\{\varphi_\nu\}$ of the alkali metal [12]. For the present case the M.O.'s will be divided into „aromatic" M.O.'s $\{\Phi_k\}$ and „metallic" M.O.'s $\{\Phi_\nu\}$. An aromatic M.O. Φ_k will consist mainly of the π-M.O. $\Phi_k^0 = \sum_t c_{k,t}\varphi_t$ of the neutral aromatic molecule into which small amounts of the A.O.'s $\{\varphi_\nu\}$ of the alkali metal are admixed, while a metallic M.O. Φ_ν will consist mainly of the metal A.O. φ_ν into which small amounts of the π-M.O.'s $\{\Phi_k^0\}$ are admixed.

The doublet ground state wave function ${}^2\Psi_N$ can be written in a zero order approximation as a single determinant wavefunction

$$^2\Psi_N = \left| \Phi_1 \bar{\Phi}_1 \ldots\ldots \Phi_k \bar{\Phi}_k \Phi_{k+1} \Phi_{1s} \bar{\Phi}_{1s} \ldots\ldots \Phi_\varkappa \bar{\Phi}_\varkappa \right|$$

in which the aromatic orbitals $\Phi_1 \ldots . \Phi_k$ are the bonding type aromatic M.O.'s and Φ_{k+1} is the first antibonding type aromatic M.O. and in which the metallic M.O.'s $\Phi_{1s} \ldots . \Phi_\varkappa$ are related to the metal core A.O.'s $\varphi_{1s} \ldots . \varphi_\varkappa$. A bar above an M.O. denotes an orbital with a beta spin, an M.O. without a bar denotes an orbital with an alpha spin.

Using the wavefunction $^2\Psi_N$ the zero order contribution $\varrho^0(\mathbf{r}_M)$ to the total spin density $\varrho(\mathbf{r}_M)$ at the metal nucleus is given by $\varrho^0(\mathbf{r}_M) = \left| \Phi_{k+1}(\mathbf{r}_M) \right|^2$, in which $\mathbf{r}_M$ is the radius vector of the alkali nucleus. This spin density is always positive and it will be determined mainly by the amount of admixture of the metal valence *ns*-orbital φ_{ns} into Φ_{k+1}.

In order to obtain negative spin densities DE BOER used a C.I. procedure. In this way he obtained a first order corrected wavefunction $^2\Psi'_N$ for the groundstate

$$^2\Psi'_N = {}^2\Psi_N + \sum_i \lambda_i {}^2\Psi_i$$

in which the summation over i runs over all the singly excited configurations. The excited configurations give a first order contribution $\varrho'(\mathbf{r}_M)$ to the zero order spin density, which may be negative. This possibly negative contribution will dominate the sign and the magnitude of the spin density at the metal nucleus only if the zero order spin density $\varrho^0(\mathbf{r}_M)$ is very small or equals zero. This will be the case if the admixture of φ_{ns} in the M.O. Φ_{k+1} is small. To explain the occurrence of a negative spin density $\varrho(\mathbf{r}_M)$ DE BOER therefore assumed that the alkali ion in the pyracene ion pair is in a plane which is at the same time a symmetry plane of the pyracene molecule as well as a nodal plane of the π-M.O. Φ^0_{k+1} of the neutral pyracene molecule. In that case the admixture of φ_{ns} in Φ_{k+1} is zero because of symmetry reasons.

The temperature dependence of the metal h.f.s.c. was explained by taking into account the vibration of the alkali metal in and out of the nodal plane. At an out of plane position of the metal nucleus the admixture of φ_{ns} in the M.O. Φ_{k+1} would be allowed, so that there would be a positive contribution to the spin density at the nucleus. In this way the total spin density would be the sum of a positive contribution from $\varrho^0(\mathbf{r}_M)$ and a negative contribution from

$\varrho'(\mathfrak{r}_M)$, whose relative magnitudes would vary with the position of the alkali nucleus with respect to the radical. An increase of the temperature would increase the amplitude of the vibration of the alkali ion, which would result in a shorter mean residence time of the alkali nucleus in the nodal plane and an accompanying increase of the metal h.f.s.c.

In his calculation of $\varrho'(\mathfrak{r}_M)$ DE BOER took into account configurations which were obtained from the zero order wavefunction ${}^2\Psi_N$ by exciting an electron from an occupied metallic core M.O. Φ_ν into an empty metallic valence or higher situated M.O. Φ_μ. As an example the contribution to $\varrho'(\mathfrak{r}_M)$ was calculated from the configuration ${}^2\Psi_t$ which represented the excitation of an electron from the core type M.O. $\Phi_{(n-1)s}$ to the valence type M.O. Φ_{ns}. Denoting this contribution by $\varrho'_t(\mathfrak{r}_M)$ the result can be given by

$$\varrho'_t(\mathfrak{r}_M) = \frac{4\lambda_t}{\sqrt{6}}\,\varphi_{(n-1)s}(\mathfrak{r}_M)\,\varphi_{ns}(\mathfrak{r}_M)$$

λ_t, which was calculated by a C.I. procedure, can be presented in good approximation by

$$\lambda_t = \frac{\sqrt{6}}{2}\,\frac{|c_{k+1,np}|^2 \left\langle \varphi_{np}(1)\,\varphi_{(n-1)s}(1)\left|\frac{e^2}{r_{12}}\right|\varphi_{np}(2)\,\varphi_{ns}(2)\right\rangle}{E_t - E_N}$$

in which E_t and E_N are the zero order energies of the configurations ${}^2\Psi_N$ and ${}^2\Psi_t$, φ_{np} is the valence np-A.O. of the alkali metal, $c_{k+1,np}$ is the coefficient by which φ_{np} is admixed in the M.O. Φ_{k+1} and $\mathfrak{r}_{12} \equiv \mathfrak{r}_1 - \mathfrak{r}_2$, $\mathfrak{r}_1$ and $\mathfrak{r}_2$ being the radius vectores of the electrons 1 and 2.

These results can be generalized by taking into account all the singly excited configurations ${}^2\Psi_j$ which represent the excitation of an electron from a metallic M.O. Φ_ν to a metallic M.O. Φ_μ. As the energy difference $E_j - E_N$ is nearly equal to the energy $E_{\nu\to\mu}$ needed for the excitation of an electron in the free alkali atom from φ_ν to φ_μ, $E_j - E_N$ will be replaced by $E_{\nu\to\mu}$ in the expression for λ_j. The total first order correction to the spin density $\varrho'(\mathfrak{r}_M)$ is then presented by

$$\varrho'(\mathfrak{r}_M) = \sum_j \varrho'_j(\mathfrak{r}_M) =$$

$$= \left| c_{k+1,np} \right|^2 \sum_{\nu,\mu} \frac{2 \langle \varphi_{np}(1)\, \varphi_\nu(1) \left| \frac{e^2}{r_{12}} \right| \varphi_{np}(2)\, \varphi_\mu(2) \rangle}{E_{\nu \to \mu}} \times$$

$$\times \varphi_\nu(\mathfrak{r}_M)\, \varphi_\mu(\mathfrak{r}_M) \qquad (25)$$

If $\varrho^0(\mathfrak{r}_M)$ is zero, the total spin density at the metal nucleus, $\varrho(\mathfrak{r}_M)$, will in first order be given by eq. (25).

A measure for $\varrho'(\mathfrak{r}_M)$ can be found by considering the spin density at the alkali nucleus in the n^2P state of the free alkali atom $\varrho_{n^2P}(\mathfrak{r}_M)$. In fact the sum over ν, μ in eq. (25) is a first order approximation of this spin density. By pursuing the calculation of $\varrho(\mathfrak{r}_M)$ to higher orders of approximation $\{\varrho(\mathfrak{r}_M) - \varrho^0(\mathfrak{r}_M)\} / \left| c_{k+1,np} \right|^2$ may approach $\varrho_{n^2P}(\mathfrak{r}_M)$ to any desired degree of precision. Assuming that $\varrho^0(\mathfrak{r}_M)$ is zero, one may put therefore $\varrho(\mathfrak{r}_M)$ equal to

$$\varrho(\mathfrak{r}_M) = \left| c_{k+1,np} \right|^2 \varrho_{n^2P}(\mathfrak{r}_M)$$

Substituting this expression for $\varrho(\mathfrak{r}_M)$ in eq. (5) one finds for the Fermi contact interaction constant of the alkali nucleus

$$A = \left| c_{k+1,np} \right|^2 A(np)$$

in which $A(np)$ is the Fermi contact interaction constant in the n^2P state of the free alkali atom.

Values of $A(np)$, calculated from the positions of the spectral terms in the n^2P state of the free alkali atoms [31], are presented in table 1, together with the Fermi contact interaction constants $A(ns)$ in the n^2S ground state of the free alkali atoms.

	^{6}Li	^{7}Li	^{23}Na	^{39}K	^{85}Rb	^{87}Rb	^{133}Cs
$A(ns).h^{-1}$, Mc/s	152.1	401.8	886	231	1 012	3 417	2 298
$A(np).h^{-1}$, Mc/s	−12.0	−31.6	−0.5[1])	−0.2[1])	2	8	

[1]) The sign of $A(np)$ is uncertain.
The following references were used in the calculation of $A(ns)$ and $A(np)$. $A(ns)$: [32]; $A(np)$: Li [33]; Na [34]; K [35]; Rb [36, 37].

Table 1: Isotropic hyperfine splitting constants in the n^2S and n^2P states of the free alkali atoms.

Looking at the data of table 1 it appears that, apart from Li, $|A(np)|$ amounts to only a very small fraction of $A(ns)$. Therefore, one would expect that for a given alkali metal the range of the usually measured positive h.f.s.c. will be much wider than the range of the negative h.f.s.c.

Furthermore it appears that only for Li $A(np)$ is distinctly negative. Therefore, one would expect that the possible occurrence of a negative h.f.s.c. would be the most pronounced for Li, and that for Rb no negative h.f.s.c. would be found at all.

Finally it is remarked that to explain the temperature dependence of the alkali h.f.s.c. in ion pairs in which a negative alkali h.f.s.c. was assumed to occur, it was argued that the alkali h.f.s.c. is the sum of a positive and a negative contribution. Because the former contribution is a zero order effect and the latter contribution a first order effect, one might assume that the positive contribution will show a much larger temperature coefficient than the latter contribution. Therefore one would expect that there would be in the plot of the metal h.f.s.c. versus the temperature a temperature region in which the plot would show a strong curvature, and a second region, at low temperatures, where the plot of the metal h.f.s.c. would level off to an approximately constant negative value.

It will be shown in sec. 5.1.2. that these expectations are not in accordance with the experimental results.

Therefore an M.O. description of the ion pair which takes into account only excitations in the „metallic" part $\Phi_1 \ldots\ldots \Phi_\kappa$ of the wavefunction ${}^2\Psi_N$ does not seem adequate to explain the occurrence of negative spin densities at the alkali nuclei.

Another possibility was mentioned by CORVAJA [38], who pointed out that excitations in the aromatic part $\Phi_1 \ldots\ldots \Phi_k$ of the wavefunction ${}^2\Psi_N$ have also to be taken into account in a C.I. calculation. Even if the admixture of the metal valence ns-A.O. φ_{ns} in the first antibonding π-M.O. Φ^0_{k+1} is forbidden because of symmetry reasons, lower and higher lying π-M.O.'s Φ^0_n and Φ^0_m may have the right symmetry to allow the admixture of φ_{ns}. Therefore, configurations ${}^2\Psi_i$ which represent the excitation of an electron from a doubly occupied bonding type M.O. Φ_n to an empty antibonding type M.O. Φ_m may produce a non-zero spin density in the ns-orbital of the alkali metal. If the alkali nucleus resides in a nodal plane of the M.O. Φ^0_{k+1} which is at the same time a symmetry plane of the

molecule, the spin density at the alkali nucleus might be determined in first order by these excited configurations.
The proposed mechanism is in fact the same by which the occurrence of negative spin densities at carbon atoms in π-radicals has been explained. It can be shown that, if the nodal plane in which the alkali ion resides passes through one or more carbon atoms of the aromatic π-system, the spin density at the alkali nucleus will be proportional approximately to the spin density at that carbon atom in the nodal plane which is the closest to the alkali nucleus.
One would expect that in general also this mechanism would produce a spin density of which the absolute value is an order of magnitude smaller than the commonly encountered positive spin densities, and that the plot of the alkali h.f.s.c. versus the temperature would show a strong curvature over a particular temperature region and would attain a more flat course at low temperatures. A preliminary calculation [38] for the case of an alkali naphthalene (Nl) ion pair showed that the proposed mechanism gives a nearly vanishing spin density at the alkali nucleus if the metal is placed in the nodal plane perpendicular to the plane of the Nl molecule of the first antibonding M.O. of Nl, and that this spin density bears a positive sign. Therefore, on theoretical grounds and on the basis of a comparison with the experiment (see sec. 5.1.2) it is thought that also this description is not appropriate to explain the occurrence of negative spin densities at alkali nuclei in radical ion pairs.

However, apart from the excitations considered up to here there are two other groups of excitations which should be taken into account.
The first group comprises excitations of electrons out of aromatic M.O.'s into metallic M.O.'s. One might think for instance of the excitation of an electron out of a doubly occupied bonding type M.O. Φ_n to the metallic valence M.O. Φ_{ns}.
The second group comprises excitations from metallic M.O.'s to aromatic M.O.'s. In this case one might think of the excitation of an electron out of the metallic core M.O. $\Phi_{(n-1)s}$ to an aromatic antibonding M.O. Φ_m.
Preliminary calculations [38] for the case of an alkali Nl ion pair have shown that these „cross-excitations" may produce spin densities at the metal nucleus of the right order of magnitude and of the right sign. Moreover it appeared from the calculation that for the occurrence of a negative sign of the spin density it is not strictly

necessary to place the nucleus in a nodal plane of the first antibonding π-M.O. Φ^0_{k+1}.

In summary the following four types of excitation can be discerned:

1 Excitations within the metallic part of the ground state wavefunction. By an excitation of this type an electron is excited from a metallic core M.O. Φ_ν into a metallic valence or higher metallic M.O. Φ_μ. Configurations corresponding with these excitations are mixed with the ground state wavefunction by the small amount of the metal valence *np*-A.O. which is mixed into the first antibonding M.O. of the aromatic molecule. In fact, taking into account these configurations results in a spin polarization of the metal core by the spin density in the *np*-A.O. of the metal.

2 Excitations within the aromatic part of the ground state wavefunction. By an excitation of this type an electron is excited from an aromatic bonding type M.O. Φ_n into an aromatic antibonding type M.O. Φ_m. Admixture of configurations representing this type of excitations produces a spin polarization of the aromatic M.O.'s. Because of the presence of slight amounts of metal A.O.'s in these aromatic M.O.'s it produces also an unbalanced spin density distribution over these metal A.O.'s and thus a possibly non-zero spin density at the metal nucleus.

3 Cross excitations by which an electron is excited out of an aromatic bonding type M.O. Φ_n into a metallic valence or higher metallic M.O. Φ_μ. These excitations in fact correspond with charge transfer configurations Ar*Me or Ar*Me* in which the aromatic molecule and possibly also the metal is in an excited state.

4 Cross excitations by which an electron is excited out of a metallic core M.O. Φ_ν into an aromatic antibonding M.O. Φ_m. These excitations correspond with charge transfer configurations $Ar^{=}$ Me^{++}.

Regarding the relative importance of these excitations the following comments are made.

It is remarked that the effect of the first type of excitations on the spin density at the metal nucleus is determined by the amount of admixture of the valence *np*-A.O. of the metal into the first antibonding M.O. of the aromatic molecule. For the other three types of excitation mainly the admixture of metal *s*-orbitals in the M.O.'s of the aromatic molecule is of importance. Looking at the admixture

of *s*-orbitals, it can be expected that the mixing coefficient of the valence *s*-orbital will be appreciably larger than the mixing coefficients of the lower lying *s*-orbitals in the core of the alkali metal. However, as the core *s*-orbitals have a much larger probability amplitude at the metal nucleus than the valence *ns*-orbital, the core *s*-orbitals cannot a priori be neglected in the construction of the L.C.A.O. M.O.'s. Regarding the admixture of metal A.O.'s other than *s*- or *p*-type orbitals, it is remarked that in some cases for instance a metal *d*-orbital may have a symmetry which is better adapted to the symmetry of the aromatic M.O. with which the metal orbital is to be mixed than an *s*- or *p*-type orbital. This will occur particularly for aromatic M.O.'s with a large number of nodes. However, generalizing the argument about the influence on the spin density at the metal nucleus, resulting from the admixture of the *np*-A.O. in the π-M.O.'s of the aromatic molecule, one expects that the mixing of non *s*-type metal A.O.'s with the π-M.O.'s of the aromatic molecule will probably have a negligeable influence on the spin density at the metal nucleus. Furthermore it is remarked that a second order perturbation calculation might admix doubly excited configurations into the ground state wavefunction. The mixing coefficients of these configurations will in general be an order of magnitude smaller than the coefficients of the singly excited configurations. The doubly excited states will give a non-zero spin density only in conjunction with the singly excited configurations. The total effect of doubly excited configurations on the metal spin density will therefore probably be negligeable and the effect of still higher orders of perturbation calculation can probably be neglected a forteriori.

From the foregoing it can be concluded that for the calculation of the spin density at the alkali nucleus in a radical ion pair it will be sufficient to perform a first order C.I. calculation, taking into account only configurations which represent cross excitations of electrons from aromatic to metallic M.O.'s or from metallic to aromatic M.O.'s. For the calculations probably only the mixing of *s*-type metal A.O.'s with aromatic π-M.O.'s will be of importance.

Finally it must be noted that the role of the solvent has been left out of consideration. It is not known whether the solvent molecules take part in the bonding within the complex and to what extent this influences the h.f.s.c.

(iii). Influence of temperature, solvent and concentration

In this paragraph a brief survey is given of the current theories which are used to explain the influence of temperature, solvent and concentration on the alkali metal h.f.s.c. In applying these theories for an analysis of the alkali NMR data it should be kept in mind that they were developed on the basis of experiments on very diluted solutions. It is not clear whether and in what way they have to be modified to be applicable also to the more concentrated ($\leqslant$ 1 M) solutions which were studied by NMR. For instance, the dissociation of ion pairs into free ions, which may be of considerable importance at low concentrations, probably does not play a role of any significance at high concentrations because of the usually small dissociation constants of these ion pairs [39-43].

Influence of the temperature

Three models have been proposed in the literature to describe the influence of the temperature on the metal h.f.s.c.

1 According to the first model, introduced by ATHERTON and WEISSMAN [10], the aromatic ion and its counterion are supposed to form a contact ion pair. The alkali ion vibrates around an equilibrium position and the mean value of the h.f.s.c. will depend upon the amplitude of the vibration and thus upon the temperature. It is expected that, when this model applies, a plot of the metal h.f.s.c. versus the temperature will show at most a slight curvature. If the metal h.f.s.c. changes sign this may be considered as an indication that one is dealing with contact ion pairs.

2 According to the second model, which was introduced by WINSTEIN et al. [44] and GRUNWALD [45] and elaborated by HIROTA and KREILICK [46] and HOGEN-ESCH and SMID [47], it is assumed that at a given temperature two kinds of ion pairs exist, in which the metal h.f.s.c. has different values, and which participate in a chemical exchange equilibrium. If the interconversion of the ion pairs is rapid, the observed h.f.s.c. is the weighted average of the h.f.s.c. in the two ion pairs. When the temperature is changed the equilibrium is shifted and the mean value of the h.f.s.c. changes. The equilibrium may be an equilibrium between two different kinds of contact ion pairs [46], between contact ion pairs and solvent separated or dissociated ion pairs [10, 46, 47],

or between periferally and intimately solvated ion pairs [44, 48].

3 According to the third model, which was elaborated by SZWARC et al. [42, 49] on the basis of the ideas of GRUNWALD [45], one assumes the potential well of the ion pair to be a function of the temperature. If the place of the minimum in the potential well changes with the temperature, it may occur that at high temperatures the metal ion is close to the aromatic ion, and that in lowering the temperature the distance between the ions increases, which enables the solvent molecules to occupy gradually a position in between them. In this way the character of the ion pair changes slowly from contact to solvent separated while nevertheless at each temperature only one single ion pair species exists.

In most cases the behaviour of the metal h.f.s.c., when the second model applies, will be the same as when the third model applies. Therefore, on the basis of the h.f.s.c. data alone it will not always be possible to make a distinction between the latter two models.
An asymptotic approach of the h.f.s.c. to zero at low temperatures indicates the formation of solvent separated or dissociated ion pairs. It excludes the possibility that model 1 is valid for that case.

Influence of the solvent

Usually the influence of the solvent on the magnitude of the alkali metal h.f.s.c. is assumed to be closely connected with the solvating power of the solvent [50]. This property depends on a. the dielectric constant of the solvent, b. the chelating sites in the solvent molecule and c. the steric conformation of the solvent molecules.

a. In general the solvating power of the solvent increases with increasing dielectric constant [11, 49-51].
b. In ethereal solvents the chelating sites consist of the oxygen atoms in the solvent molecule. In general the solvating power of the ether molecules increases with an increase of the amount of oxygen atoms per molecule [51].
c. The steric factors relate to the accessibility of the oxygen atoms for chelation with alkali ions. The low solvating power of 2-methyltetrahydrofuran (MTHF) compared with tetrahydrofuran for instance is explained by the steric hindrance of the methylgroup in the MTHF molecules [51]. Furthermore the chain length of

the solvent molecules and the distance between the oxygen atoms in the solvent molecules in relation to the radius of the alkali ion are of importance. For instance, the solvation of Li ions increases sharply in going from diglyme (Dg) to triglyme (Tg), probably because the Tg molecules, which are longer than the Dg molecules, fit better around the Li ion [52].

Influence of the concentration

It is clear that, if model 1 is used to describe the ion pair, the metal h.f.s.c. will be independent of the concentration.
Also for model 2 and model 3 the h.f.s.c. will be independent of the radical concentration as long as it is allowed to consider the concentration of the solvent to be independent of the total radical concentration. This will be the case for diluted solutions. However, if the radical concentration reaches values in the order of magnitude of 1 M the solvent concentration will depend on the radical concentration. In solutions with high radical concentrations dilution will increase the solvent concentration, so that the tendency will be enhanced to form solvent separated ion pairs. This may result in a decrease of the absolute value of the metal h.f.s.c.
Moreover, at high concentrations the formation of clusters of ion pairs may occur [39, 53, 54]. It is difficult to predict to what extent and in what manner this may influence the metal h.f.s.c. Comparing the NMR h.f.s.c. with the ESR h.f.s.c. of the alkali nuclei, one should be aware that, because of the difference in concentration at which the NMR and the ESR experiments are performed, it cannot be excluded *a priori* that large differences between the NMR and the ESR h.f.s.c. of the alkali nuclei may occur. This is in contrast with the expected behaviour of the NMR and the ESR h.f.s.c. of the aromatic protons, which were assumed to be less sensitive to variations in the radical concentration (see sec. 2.1.1).

2.2. THE LINEWIDTH

In the following sections first the derivation of general linewidth formulae will be discussed after which the applications will be considered in separate sections for the aromatic protons and the alkali nuclei.

(i). Introduction

The width of the resonance signal of the nucleus **I** will depend upon inter- and intramolecular interactions. For the ion pairs under consideration the intermolecular interactions are much smaller than the intramolecular interactions. Therefore, in the following only intramolecular interactions are considered.
An expression for the linewidth can be derived from eq. (1) by considering $\mathscr{H}_1(t)$ as a time-dependent perturbation on $\mathscr{H}_0$.
Looking at a transition between two energy levels, the width of the resonance signal will depend upon the magnitude of the perturbation, the energy difference $\hbar\omega$ between the two levels and the correlation time τ, which characterizes the random variation of the perturbation with the time [55, 56]. In general the linewidth will be proportional to the square of the matrixelement of the perturbation and to the value of the correlation spectrum $J(\omega, \tau)$, which is a measure for the intensity of the component with frequency ω in the Fourier-analysis of the time-dependence of the perturbation.

(ii). Linewidth formulae for the different interactions

For the present case $\mathscr{H}_1(t)$ consists of three parts viz. $\mathscr{H}_{Fc}(t)$, $\mathscr{H}_D(t)$ and $\mathscr{H}_Q(t)$, as is clear from eq. (14). Up to first order each part gives a contribution to the linewidth which is independent from the other parts. Therefore the linewidth can be found as the sum of these contributions. Formulae to calculate the individual contributions have been derived in the literature [57-60]. They are presented here without a derivation.

The Fermi contact interaction

The contribution to the linewidth from $\mathscr{H}_{Fc}(t)$ is denoted by $\left(\frac{1}{T_2}\right)_{Fc}$ and is given by [58, 59]

$$\left(\frac{1}{T_2}\right)_{Fc} = \frac{1}{3}\left(\frac{A}{\hbar}\right)^2 S(S+1)\left(\tau_e + \frac{\tau_e}{1+\omega_e^2\tau_e^2}\right) \tag{26}$$

in which τ_e is the correlation time characteristic for the variation of the orientation of $\mathbf{S}(t)$ with the time, and $\omega_e \equiv \gamma_e H$.

The anisotropic dipolar interaction

The contribution to the linewidth from $\mathscr{H}_D(t)$ is denoted by $\left(\frac{1}{T_2}\right)_D$. An explicit expression for $\left(\frac{1}{T_2}\right)_D$ has been derived for the case that **I** and **S** in eq. (13) are magnetic point dipoles separated by a distance r [57, 59]. In that case the tensor **T** is axially symmetric and has the principal values $-B$, $-B$ and $2B$, B being given by

$$B = \frac{\gamma_e \gamma_N \hbar^2}{r^3} \tag{27}$$

$\left(\frac{1}{T_2}\right)_D$ is given by

$$\left(\frac{1}{T_2}\right)_D = \frac{1}{15}\left(\frac{B}{\hbar}\right)^2 S(S+1)\left(7\tau_d + \frac{13\tau_d}{1+\omega_e^2\tau_d^2}\right) \tag{28}$$

in which τ_d is the dipolar correlation time. Because the time-dependence of $\mathscr{H}_D(t)$ is determined by the time-dependence of $\mathbf{T}(t)$ as well as of $\mathbf{S}(t)$, the dipolar correlation time depends on the correlation times of $\mathbf{T}(t)$ and $\mathbf{S}(t)$ and is given by

$$\frac{1}{\tau_d} = \frac{1}{\tau_r} + \frac{1}{\tau_e} \tag{29}$$

τ_r is the rotational correlation time, which characterizes the tumbling motion of the ion pair and therefore the variation of $\mathbf{T}(t)$ with the time.

In the case of an alkali radical ion pair, **I** is a hydrogen or an alkali nucleus and **S** is the unpaired electron, which is spread over the radical. As for the unpaired electron the point dipole approximation is no longer valid, the principal values of **T** cannot be calculated from a formula like eq. (27). In fact they have to be calculated from

eq. (8) by applying the appropriate expression for the spin density matrix of the unpaired electron. It can be anticipated that for a radical ion pair **T** will have in general no axial symmetry, so that its principal values cannot be characterized by one single parameter B. Also eq. (28), being derived for the case of an axially symmetric tensor **T**, will then be no longer valid. However, eq. (28) can still be used as an approximation by using an adapted value for the parameter B. It has been argued that for the anisotropic dipolar interaction the trace of the tensor (**T.T**) is closely connected with the relaxation rate of the nuclear species under consideration [61]. If **T** is axially symmetric it follows that

$$B^2 = \frac{1}{6} Tr\,(\mathbf{T}.\mathbf{T})$$

This expression for B will be used as the definition of the parameter B in eq. (28) for the case that **T** is not axially symmetric. Although the error made by this approximation has not yet been established, it is thought that the approximation will suffice for semiquantitative purposes.

The quadrupolar interaction

The contribution to the linewidth from $\mathscr{H}_Q(t)$ is denoted by $\left(\frac{1}{T_2}\right)_Q$ and is given by [60]

$$\left(\frac{1}{T_2}\right)_Q = \frac{3}{40}\,\frac{2I+3}{I^2(2I-1)}\left(\frac{e^2Qq}{\hbar}\right)^2\left(1+\frac{\eta^2}{3}\right)\tau_r \qquad (30)$$

in which $eq \equiv V_{zz}$, and $\eta \equiv \frac{V_{xx}-V_{yy}}{V_{zz}}$, V_{xx}, V_{yy} and V_{zz} being the principal values of **V**. The principal axes of **V** are denoted by x, y and z according to the convention $|V_{zz}| \geqslant |V_{yy}| \geqslant |V_{xx}|$, so that the asymmetry parameter η satisfies the condition

$$0 < \eta < 1$$

In order to simplify the application of eq. (30) it will be assumed

that $\mathbf{V}$ has axial symmetry, so that $\eta = 0$. This introduces an error of at most 25 % in the calculations.

It has still to be checked whether the conditions for which the eqs. (26), (28) and (30) were derived in the literature, are fulfilled under the present experimental conditions.
Eq. (26) has been derived under the condition $\omega_0 \ll \omega_e$, in which ω_0 is the nuclear resonance frequency, eq. (28) has been derived under the conditions $\omega_0 \ll \omega_e$, $\omega_0^2\tau_d^2 \ll 1$, and eq. (30) has been derived under the condition $\omega_0^2\tau_r^2 \ll 1$. Typical values for ω_0 and ω_e, encountered in the present study, are respectively 10^8 rad/s and 3×10^{11} rad/s. Typical values for τ_e, τ_d and τ_r are respectively 10^{-10}, 3×10^{-11} and 3×10^{-11} s. Therefore, the conditions under which the eqs. (26), (28) and (30) are valid are fulfilled for the solutions under investigation.

Conclusion

From the numerical values of ω_e and the correlation times, given above, it appears in addition that under the present experimental conditions in most cases $\omega_e^2\tau_e^2$, $\omega_e^2\tau_d^2 \gg 1$. Therefore the following simplified formulae can be derived from the eqs. (26), (28) and (30)

$$\left(\frac{1}{T_2}\right)_{Fc} = \frac{1}{4}\left(\frac{A}{\hbar}\right)^2 \tau_e \tag{31a}$$

$$\left(\frac{1}{T_2}\right)_{D} = \frac{7}{20}\left(\frac{B}{\hbar}\right)^2 \tau_d \tag{31b}$$

$$\left(\frac{1}{T_2}\right)_{Q} = \frac{3}{40} f(I) \left(\frac{W}{\hbar}\right)^2 \tau_r \tag{31c}$$

in which

$$B \equiv \left\{\frac{Tr\,(\mathbf{T}\,.\,\mathbf{T})}{6}\right\}^{\frac{1}{2}} \tag{32a}$$

$$f(I) \equiv \frac{2I+3}{I^2(2I-1)} \tag{32b}$$

$$W \equiv |e^2Qq| \tag{32c}$$

and in which it has been assumed that the field gradient at the nucleus has axial symmetry. It is remarked that in the definition of W in eq. (32c) the Sternheimer corrections have not yet been applied [28]. In the final calculation of W and in the discussion of the experimentally determined values of W they have to be taken into account. This will be discussed in sec. 2.2.2.

The total linewidth can be given now by

$$\frac{1}{T_2} = \left(\frac{1}{T_2}\right)_{Fc} + \left(\frac{1}{T_2}\right)_D + \left(\frac{1}{T_2}\right)_Q \tag{33}$$

in which $\left(\frac{1}{T_2}\right)_{Fc}$, $\left(\frac{1}{T_2}\right)_D$ and $\left(\frac{1}{T_2}\right)_Q$ are given by the eqs. (31) and (32). Eq. (33) will be used henceforth in the discussion of the proton and the alkali linewidths.

(iii). Correlation times

The correlation times τ_e, τ_d and τ_r are a function of the radical concentration c, the absolute temperature T and the viscosity η, which in turn is a function of c and T itself.
According to the DEBIJE-EINSTEIN model [60, 61] the dependence of τ_r on η and T is given by the proportionality

$$\tau_r \sim \frac{\eta}{T} \tag{34a}$$

while according to the model of Pake and Tuttle [62] the dependence of τ_e on c, T and η is given by

$$\tau_e \sim \frac{\eta}{T} \cdot \frac{1}{c} \tag{34b}$$

Combining the eqs. (29), (34a) and (34b) one finds for τ_d

$$\tau_d \sim \frac{\eta}{T} \tag{34c}$$

From the eqs. (31), (33) and (34) it follows that

$$\frac{1}{T_2} \sim \frac{\eta}{T} \tag{35}$$

The dependence of η on the concentration c can be presented by [63]

$$\eta(c,T) = \eta_0(T)\,(1+\lambda_1\sqrt{c}+\lambda_2 c) \tag{36}$$

in which η_0 is the viscosity of the pure solvent and, λ_1 and λ_2 are numerical constants. Some evidence has been reported in the literature, which indicates that the term in brackets in eq. (36) varies only slightly with the temperature [63]. Under that condition the temperature dependence of η will nearly completely be determined by the temperature dependence of $\eta_0(T)$. Combining the eqs. (35) and (36) it follows that the temperature dependence of the total linewidth, apart from a possible variation of the interaction parameters A, B and W (see the eqs. (31)), can be presented by

$$\frac{1}{T_2} \sim \frac{\eta_0(T)}{T} \tag{37}$$

Eq. (37) will be used in the analysis of the temperature dependence of the linewidth data. To check its applicability experiments were performed on solutions of a number of diamagnetic salts. The results are reported and discussed in chapter 3.

Regarding the influence of the concentration on the correlation times it is clear from eqs. (34) and (36) that τ_r will increase with an increase in c, that τ_e will only slightly be affected by a change in c and that τ_d will increase more or less, depending upon whether τ_r or τ_e dominates τ_d. Therefore, an increase in c will cause increase of $\left(\frac{1}{T_2}\right)_Q$, while the effect on $\left(\frac{1}{T_2}\right)_{Fc}$ and $\left(\frac{1}{T_2}\right)_D$ is more difficult to predict.

(i). Introduction

The analysis of the proton linewidths is facilitated by the circumstance that the quadrupole moment of a proton is zero, so that the quadrupolar relaxation is absent.
As the Fermi contact interaction parameter A can be determined by an ESR or an NMR experiment, only the anisotropic dipolar interaction has to be considered in detail.

(ii). The anisotropic dipolar interaction

It was pointed out in sec. 2.2.0 that the elements of $\mathbf{T}$ for the case of a delocalized electron have to be calculated from eq. (8). Furthermore it was pointed out that the set of A.O.'s needed for the calculation of the elements $\mathbf{T}_{ba}$ of eq. (9), could be divided into a set $\{\varphi_i\}$ of Slater $2p_z$-A.O.'s of the aromatic carbon atoms and a set $\{\varphi_\nu\}$ of alkali metal A.O.'s. In the calculation of the tensors $\mathbf{T}$ of the aromatic protons it will be assumed that the overlap between A.O.'s of the set $\{\varphi_i\}$ and A.O.'s of the set $\{\varphi_\nu\}$ can be neglected. Eq. (8) then reduces to

$$\mathbf{T} = \sum_{i\,j} \varrho_{ij}\,\mathbf{T}_{ji} + \sum_{\nu,\mu} \varrho_{\nu\mu}\,\mathbf{T}_{\mu\nu} \tag{38}$$

Next the following approximations are made:

1 The sum $\sum_{\nu,\mu} \varrho_{\nu\mu}\,\mathbf{T}_{\mu\nu}$ in eq. (38) is neglected. This appears to be justified if one takes into account that the total amount of spin density in the metal orbitals will be small, and that the aromatic protons will in general be much closer to the spin densities on the aromatic carbon atoms than to the spin density on the alkali metal.

2 It is assumed that

$$\varrho_{ij}\,\mathbf{T}_{ji} = \varrho_{ii}\,\mathbf{T}_{ii}\,\delta_{ij} \tag{39}$$

which is equivalent to the assumption that there is zero overlap between every two A.O.'s φ_i and φ_j.

Omitting one index from ϱ_{ii}, eq. (38) becomes with these approximations

$$\mathbf{T} = \sum_i \varrho_i \, T_{ii} \tag{40}$$

in which ϱ_i is the spin density in the $2p_z$-orbital of the carbon atom i.

A method to calculate the tensor $\mathbf{T}_{ii}$ has been indicated by McConnell and Strathdee [26]. They have calculated the elements of the anisotropic dipolar tensor of the proton in a *CH*-radical as function of the *C-H* distance. For this particular case two of the principal axes of the tensor are given respectively by the *Z*-axis of the $2p_z$-orbital, occupied by the unpaired electron, and the axis through the *C*- and the *H*-atom which is perpendicular to the former one. Derbyshire [64] has extended these formulae for the more general case of a *CH*-radical in which the axis through the *C*- and the *H*-atom is no longer perpendicular to the axis of the carbon $2p_z$-orbital.

Using the equations of McConnell and Strathdee or those of Derbyshire the tensors $\mathbf{T}_{ii}$ of eq. (40) can be calculated. Furthermore, the spin densities ϱ_i in eq. (40) can be derived from the experimental proton h.f.s.c. by using the McConnell-Weissman relation (see eq. (24)), or they can be found from a McLachlan calculation or a combined S.C.F. and C.I. procedure (see sec. 2.1.1). As the principal axis systems of the tensors $\mathbf{T}_{ii}$ are not the same, the summation over i in eq. (40) has to be performed by calculating the tensors $\mathbf{T}_{ii}$ in their own principal axis systems, multiplying them by their respective coefficients ϱ_i, transforming them to the same molecular axis system and summing them.

After the calculation of $\mathbf{T}$ according to eq. (40), B can be calculated according to the definition of eq. (32a). Details of the procedure will be given in sec. 5.2.1.

(iii). Correlation times

The parameters which remain unknown in eq. (33) are the correlation times τ_e and τ_d. By measuring in the NMR spectrum of the radical the linewidths of two inequivalent protons, two equations (33) are found from which τ_e and τ_d can be solved. From eq. (29) then τ_r can be calculated.

(i). Introduction

For the alkali isotopes used in the present study the quadrupole moment differs from zero, so that it will now not be allowed to neglect the quadrupolar interaction. As the Fermi contact parameter A can be determined directly from the experiment, only the anisotropic dipolar interaction and the quadrupolar interaction need to be discussed. This will be done for the two interactions respectively in the next two paragraphs, after which the application of the linewidth formulae will be taken into consideration in the fourth paragraph. Finally the relationship between ion pair model and the temperature dependence of the alkali linewidth will be considered in the last paragraph of this section.

(ii). The anisotropic dipolar interaction

The calculation of the elements of the tensor $\mathbf{T}$ of an alkali nucleus in a radical ion pair, the nucleus being at a given position with respect to the radical, proceeds in the same way as the calculation of the tensors $\mathbf{T}$ of the aromatic protons.
Starting again with eq. (38) the following approximations are made:

1 Just as in the case of the aromatic protons it is assumed that (see eq. (39))

$$\varrho_{ji}\,\mathbf{T}_{ij} = \varrho_{ii}\,\mathbf{T}_{ii}\,\delta_{ij}$$

2 The tensors $\mathbf{T}_{\mu\nu}$ of which μ or ν denotes an orbital with a higher principal or orbital quantum number than a valence *ns*- or *np*-orbital, are neglected. It is thought that this is justified partly in view of the fact that for higher quantum numbers the metal orbitals become to extended to give large tensor elements, partly because of the fact that the coefficients $\varrho_{\mu\nu}$ will become small for these orbitals. Therefore, only the tensors $\mathbf{T}_{ns\,ns}$, $\mathbf{T}_{ns\,np}$, $\mathbf{T}_{np\,ns}$ and $\mathbf{T}_{np\,np}$ have to be taken into account. As the former three tensors are zero, only the latter one, $\mathbf{T}_{np\,np}$, is of importance.

Applying these approximations and omitting the second index of the spin densities ϱ_{ii} and $\varrho_{\mu\mu}$, one finds from eq. (38)

$$\mathbf{T} = \mathbf{T}_{Ar} + \mathbf{T}_{Me} \tag{41}$$

in which $\mathbf{T}_{Ar}$ and $\mathbf{T}_{Me}$ are defined by

$$\mathbf{T}_{Ar} \equiv \sum_i \varrho_i \mathbf{T}_{ii} \tag{42a}$$

$$\mathbf{T}_{Me} \equiv \varrho_{np} \mathbf{T}_{np\,np} \tag{42b}$$

In these definitions ϱ_i and ϱ_{np} represent respectively the spin density in the $2p_z$-A.O. of carbon atom i and the spin density in the valence np-A.O. of the alkali metal. $\mathbf{T}_{Ar}$ characterizes the anisotropic dipolar interaction of the nucleus with the spin density on the radical, while $\mathbf{T}_{Me}$ characterizes the anisotropic dipolar interaction of the nucleus with the spin density present in metal A.O.'s.

If the position of the alkali nucleus with respect to the radical is known, $\mathbf{T}_{Ar}$ can be calculated by the same method by which the calculation of the anisotropic dipolar tensors of the aromatic protons was performed. The only difference is, that instead of the formulae of McConnel and Strathdee the more general formulae of Derbyshire have to be used to calculate the elements of $\mathbf{T}_{ii}$ (see sec. 2.2.1). After multiplying the tensors $\mathbf{T}_{ii}$ by their respective coefficients ϱ_i and transforming them from their individual principal axis systems to the same molecular framework, the summation over i in eq. (42a) can be performed.

The tensor $\mathbf{T}_{np\,np}$ is axially symmetric. Its principal values will be denoted by $-B(np)$, $-B(np)$ and $2B(np)$. Values for $B(np)$ can be derived for the different alkali metals from the positions of the spectral terms in the n^2P state of the respective free atoms. Therefore, if a particular value is assumed for ϱ_{np}, $\mathbf{T}_{Me}$ can be calculated too, according to eq. (42b).

Having calculated $\mathbf{T}_{Ar}$ and $\mathbf{T}_{Me}$ one would be able to calculate $\mathbf{T}$ by transforming $\mathbf{T}_{Ar}$ and $\mathbf{T}_{Me}$ to the same axis system and summing them according to eq. (41). However, for our purposes the anisotropic dipolar interaction is more conveniently characterized by two parameters B_{Ar} and B_{Me}, which, in analogy with the definition of eq. (32a), are defined by

$$B_{Ar} \equiv \left\{ \frac{Tr(\mathbf{T}_{Ar} \cdot \mathbf{T}_{Ar})}{6} \right\}^{\frac{1}{2}} \tag{43a}$$

$$B_{Me} \equiv \left\{ \frac{Tr(\mathbf{T}_{Me} \cdot \mathbf{T}_{Me})}{6} \right\}^{\frac{1}{2}} =$$

$$= \left| \varrho_{np} \, B(np) \right| \qquad (43b)$$

Further details of the calculation are given in sec. 5.2.2.

(iii). The quadrupolar interaction

For the calculation of the quadrupolar interaction parameter W a distinction must be made between the field gradient $\mathbf{V}_{out}$ caused by charges outside the alkali ion, and the field gradient $\mathbf{V}_{Me}$ caused by charge densities in A.O.'s of the alkali atom. This distinction is required because for the two types of field gradient different Sternheimer corrections must be applied [28, 65, 66].

In theory for the calculation of W a procedure might be followed by which $\mathbf{V}_{out}$ and $\mathbf{V}_{Me}$ are calculated separately, corrected by the appropriate Sternheimer corrections, transformed to the same axis system and summed, to find the total tensor $\mathbf{V}$, after which the parameter W might be calculated according to the definition of eq. (32c). However, for the present case a less detailed procedure will be adopted.

For the calculation of $\mathbf{V}_{out}$ it will be assumed that $\mathbf{V}_{out}$ has axial symmetry, so that this field gradient tensor can be characterized by the principal value eq_{out} along the Z-axis of its principal axis system. The magnitude of eq_{out} is determined by the charge density on the aromatic ion and by the number and the orientation of the electric dipole moments of the solvent molecules in the solvent shell around the alkali ion. Because an a priori calculation of eq_{out} would be rather time-consuming, no method will be indicated to calculate eq_{out} in detail. Instead it is sufficient for our purposes to define, in analogy with the definition of eq. (32c), a parameter W_{out} according to

$$W_{out} \equiv \left| e^2 Q q_{out} (1 - \gamma_\infty) \right| \qquad (44a)$$

in which γ_∞ is the Sternheimer shielding parameter.

For the calculation of the field gradient $\mathbf{V}_{Me}$, caused by the charge densities in the metal A.O.'s, the filled electron shells in the core of the alkali metal can be left out of consideration, because they have a spherically symmetric charge distribution and therefore do not give rise to a field gradient at the nucleus. Therefore, $\mathbf{V}_{Me}$ will be determined by the amount of charge density present in the valence A.O.'s and possibly even higher A.O.'s of the metal. For the same reasons as in the calculation of the anisotropic dipolar tensor $\mathbf{T}_{Me}$, only the charge density in the *np*-orbital needs to be taken into account. As charge density in a *p*-orbital gives always rise to an axially symmetric field gradient at the nucleus, $\mathbf{V}_{Me}$ will have axial symmetry. Assuming that, apart from the sign, the charge density and the spin density in the *np*-orbital are the same, the principal value of $\mathbf{V}_{Me}$ along the *Z*-axis can be given by $|\varrho_{np}|\, eq_{np}$, in which eq_{np} represents the field gradient caused by a full *np*-electron at the nucleus. Analogous to the definition of eq. (32c) a parameter W_{Me} can now be defined by

$$W_{Me} \equiv |\varrho_{np}|\, W(np) \tag{44b}$$

in which $W(np)$ is defined by

$$W(np) \equiv |e^2 Q q_{np} (1-R)| \tag{45}$$

R is the Sternheimer shielding factor which corresponds with eq_{np}.

The parameters W_{out} and W_{Me} characterize the quadrupolar interaction in a manner sufficiently detailed for our purposes. W_{out} is characteristic for the interaction of the nuclear quadrupole moment with the field gradient caused by charges outside the metal ion, W_{Me} is characteristic for the interaction of the nuclear quadrupole moment with the field gradient caused by charge densities in A.O.'s of the metal.

(iv). Experimental determination of B and W

After having defined for theoretical purposes the parameters B_{Ar} and B_{Me}, which characterize the anisotropic dipolar interaction, and the parameters W_{out} and W_{Me}, which characterize the quadrupolar

interaction, it is necessary to look what knowledge about the ion pair structure is needed for an *a priori* calculation of these parameters.

For the calculation of B_{Ar} one needs according to eq. (43a) the elements of the tensor $\mathbf{T}_{Ar}$. This tensor can be calculated, once a definite position for the alkali nucleus with respect to the radical ion has been assumed.
To calculate B_{Me} one needs according to eq. (43b) values for ϱ_{np} and $B(np)$. While $B(np)$ can be determined from the positions of the spectral terms in the n^2P state of the free atom, a value for ϱ_{np} has to be adopted more or less arbitrarily.
W_{out} can be calculated according to eq. (44a) if γ_∞ and eq_{out} are known. For γ_∞ theoretical estimates are available. To calculate eq_{out} detailed knowledge of the ion pair structure and of the structure of the solvent shell of the alkali ion is needed. However, even when this knowledge would be available, a detailed procedure to calculate eq_{out} would still have to be worked out.
Finally for W_{Me}, defined by eq. (44b), the same remarks apply as for B_{Me}: $W(np)$ can be determined from the positions of the spectral terms in the n^2P state of the free alkali atom and ϱ_{np} has to be guessed more or less.
So, an *a priori* calculation of the interaction parameters is possible on the basis of certain assumptions about 1⁰ the wavefunction of the ion pair, particularly about the magnitude of ϱ_{np}, and 2⁰ the structure of the ion pair.

Another way to obtain information about the magnitude of the anisotropic dipolar and the quadrupolar interaction is to determine the parameters B and W, defined by the eqs. (32a) and (32c), from the experiment.
Experimental values of B and W can be found by the use of eq. (31b) and (31c) by substituting for $\left(\frac{1}{T_2}\right)_D$ and $\left(\frac{1}{T_2}\right)_Q$ the experimentally determined quantities and for the correlation times the values determined from the proton experiments (see sec. 2.2.1).
However, the only experimentally measurable quantity is the total linewidth. Therefore, before the equations (31b) and (31c) can be applied, a separation must be accomplished between the three component parts of the total linewidth viz. $\left(\frac{1}{T_2}\right)_{Fc}$, $\left(\frac{1}{T_2}\right)_D$ and $\left(\frac{1}{T_2}\right)_Q$.

This separation can be performed in a number of ways.

1 The linewidth contribution from the Fermi contact interaction can always be estimated from the measured values of A and τ_e.

2 In some cases it is clear beforehand that one of the contributions to the linewidth can be neglected. For instance for ^{6}Li and ^{133}Cs the value of eQ is very small, so that for these nuclei the contributions of the quadrupolar interaction to the linewidth in most cases can be neglected.

3 If the linewidths of two isotopes A and B of the same alkali metal, $\left(\frac{1}{T_2}\right)_A$ and $\left(\frac{1}{T_2}\right)_B$, are measured in the same solution, it is possible to separate the sum $\left(\frac{1}{T_2}\right)_{Fc} + \left(\frac{1}{T_2}\right)_D$ from $\left(\frac{1}{T_2}\right)_Q$ for both isotopes [21].

This can be accomplished by writing eq. (33) for the two isotopes as

$$\left(\frac{1}{T_2}\right)_A = c_1 \gamma_A^2 + c_2 f(I_A)\,(eQ_A)^2 \tag{46a}$$

$$\left(\frac{1}{T_2}\right)_B = c_1 \gamma_B^2 + c_2 f(I_B)\,(eQ_B)^2 \tag{46b}$$

The first term in the right hand side of the eqs. (46) represents $\left(\frac{1}{T_2}\right)_{Fc} + \left(\frac{1}{T_2}\right)_D$ while the second one represents $\left(\frac{1}{T_2}\right)_Q$. Explicit expressions for c_1 and c_2 can be found by comparing the eqs. (46) with the eqs. (31) and (33). $f(I_A)$ and $f(I_B)$ can be found by substituting in the definition equation of $f(I)$ (eq. (32b)) the values of the nuclear quantum numbers I_A and I_B of the respective isotopes. If the gyromagnetic constants and the quadrupole moments of the two isotopes are known, it suffices to measure $\left(\frac{1}{T_2}\right)_A$ and $\left(\frac{1}{T_2}\right)_B$ in order to be able to solve the equations (46) for c_1 and c_2 and to make the separation between $\left(\frac{1}{T_2}\right)_{Fc} + \left(\frac{1}{T_2}\right)_D$ and $\left(\frac{1}{T_2}\right)_Q$.

It is pointed out that the method works as well for the case that

only the ratios of the gyromagnetic constants and the quadrupole moments are known.

When a separation of the different contributions is impossible the influence of the temperature, the concentration and the degree of reduction on the linewidth can be examined. In this way it will sometimes be possible to see whether the linewidth is dominated by one particular interaction, and how the magnitude of this interaction changes with the temperature.
The following cases can be descerned.

4 If the linewidth, plotted as a function of η_0/T, deviates markedly from a straight plot through the origin, this indicates a noticeable variation in the magnitude of one or more interaction parameters with the temperature.

5 An increase in the radical concentration will probably increase τ_r and perhaps decrease τ_e. This will cause an increase of $\left(\frac{1}{T_2}\right)_Q$ and in some cases also of $\left(\frac{1}{T_2}\right)_D$, while on the other hand it might cause a decrease of $\left(\frac{1}{T_2}\right)_{Fc}$.

6 Finally in partially reduced solutions an increase of f_p in general will result in an increase of τ_r and a decrease of τ_e. Thus $\left(\frac{1}{T_2}\right)_{Fc}$ will decrease, $\left(\frac{1}{T_2}\right)_Q$ will increase and $\left(\frac{1}{T_2}\right)_D$ may increase or decrease depending on whether τ_d is dominated by τ_r or by τ_e.

It is remarked that by comparing the experimentally determined values of B and W with the values of B_{Ar}, B_{Me}, W_{out} and W_{Me} calculated on the basis of certain assumptions about the ion pair structure, information can be obtained about the real ion pair structure.

(v). Ion pair models and linewidth

Finally it has to be discussed how the alkali linewidth will depend on the temperature for the various ion pair models which can be

applied in the analysis of the temperature behaviour of the metal h.f.s.c. and which were discussed in sec. 2.1.2.
For this purpose the implications for the linewidth predictable on the basis of the model of WINSTEIN, and HIROTA and KREILICK, which will be denoted by „model 2" or the „equilibrium model", and the implications predictable on the basis of the model of GRUNWALD and SZWARC, which will be denoted by „model 3" or the „static model", will be compared with each other.

Equilibrium model

According to the equilibrium model, over a range of temperatures two ion pair species exist in solution, which are involved in an equilibrium, that may shift with the temperature. For convenience the two species are designated by solvent separated and contact ion pairs, but the formulae to be derived can be applied to any two ion pair species which participate in an equilibrium.

The intramolecular interactions will in general be characterized by values of A, B and W which will be different for the two ion pair species. These values will be denoted by A_s, B_s and W_s for the solvent separated ion pairs and by A_c, B_c and W_c for the contact ion pairs.
Suppose that no interconversion between the ion pairs occurs and that the alkali nuclei in the two ion pair species show clearly separated NMR signals at values of the magnetic field of respectively H_s and H_c. The linewidths $\left(\frac{1}{T_2}\right)_s$ of the solvent separated species and $\left(\frac{1}{T_2}\right)_c$ of the contact species can be presented according to eq. (33) by

$$\left(\frac{1}{T_2}\right)_s = \sum_{x=Fc,\,D,\,Q} \left(\frac{1}{T_2}\right)_{x,s} \tag{47a}$$

$$\left(\frac{1}{T_2}\right)_c = \sum_{x=Fc,\,D,\,Q} \left(\frac{1}{T_2}\right)_{x,c} \tag{47b}$$

in which $\left(\frac{1}{T_2}\right)_{Fc,s}$ denotes the contribution from the Fermi contact

interaction in the solvent separated ion pairs to the linewidth of the solvent separated ion pairs and so on.
Now suppose that interconversion occurs between the two ion pair species and that the lifetimes τ_s and τ_c of respectively the solvent separated and the contact ion pairs satisfy the condition

$$\tau_s, \tau_c \gg \tau_e, \tau_d, \tau_r \tag{48}$$

which for typical experimental circumstances means that the lifetimes of the two ion pair species are much longer than $\cong 3 \times 10^{-11}$ s. The condition (48) implies that the relaxation processes for the alkali nuclei in each separate species have a much shorter time scale than the interconversion process itself. Under that condition it is still allowed to speak of two ion pair species with characteristic inverse relaxation times $\left(\frac{1}{T_2}\right)_c$ and $\left(\frac{1}{T_2}\right)_s$ for the alkali nuclei, as indicated by eq. (47). Therefore the shape of the NMR spectrum can be calculated with the usual linewidth formulae for the two site exchange problem [67]: in the „slow exchange" limit two NMR signals are observed whose linewidths equal approximately the linewidths in the case of no exchange, and whose resonance positions are approximately the same as the resonance positions for the case of no exchange, in the „rapid exchange" limit only one collapsed signal is observed of which the linewidth as well as the resonance position are weighted mean averages of the widths and resonance positions measured in the case of no exchange.

For the purpose of this study only the rapid exchange limit is of interest. This limiting case is encountered when the condition

$$\tau_s, \tau_c \ll \left|\gamma_N(H_c - H_s)\right|^{-1}$$

is fulfilled. Typical values for $\left|\gamma_N(H_c - H_s)\right|^{-1}$ are $10^{-4} - 10^{-5}$ s. If the fractions of solvent separated and contact ion pairs are denoted by respectively $(1 - f_c)$ and f_c, the total linewidth is presented in the rapid exchange limit by

$$\frac{1}{T_2} = (1 - f_c)\left(\frac{1}{T_2}\right)_s + f_c\left(\frac{1}{T_2}\right)_c \tag{49}$$

Substituting the expressions (47) in (49) one finds

$$\frac{1}{T_2} = \sum_{x = Fc, D, Q} \left(\overline{\frac{1}{T_2}}\right)_x \tag{50}$$

in which $\left(\overline{\frac{1}{T_2}}\right)_x$ is defined according to

$$\left(\overline{\frac{1}{T_2}}\right)_x \equiv (1-f_c)\left(\frac{1}{T_2}\right)_{x,s} + f_c\left(\frac{1}{T_2}\right)_{x,c} \tag{51}$$

The temperature behaviour of $\left(\overline{\frac{1}{T_2}}\right)_x$ depends on the temperature behaviour of $\left(\frac{1}{T_2}\right)_{x,s}$, $\left(\frac{1}{T_2}\right)_{x,c}$ and f_c. For the temperature dependence of $\left(\frac{1}{T_2}\right)_{x,s}$ one finds from eqs. (31), (34) and (36)

$$\left(\frac{1}{T_2}\right)_{x,s} \sim \frac{\eta_0}{T} X_s^2 \tag{52a}$$

in which X_s denotes one of the parameters A_s, B_s or W_s depending on whether x denotes respectively the Fermi contact, the anisotropic dipolar or the quadrupolar interaction.

In the same way one finds for $\left(\frac{1}{T_2}\right)_{x,c}$

$$\left(\frac{1}{T_2}\right)_{x,c} \sim \frac{\eta_0}{T} X_c^2 \tag{52b}$$

in which X_c is defined in a similar way as X_s.

For both proportionalities (52) the same proportionality constant applies. Therefore substitution of (52a) and (52b) in (51) gives

$$\left(\overline{\frac{1}{T_2}}\right)_x \sim \{(1-f_c) X_s^2 + f_c X_c^2\} \frac{\eta_0}{T} \tag{53}$$

Defining a parameter $\overline{X}$ by

$$\overline{X} \equiv (1-f_c)\,X_s + f_c X_c, \tag{54}$$

solving this identity for f_c and substituting the result for f_c in eq. (53) one finds

$$\left(\overline{\frac{1}{T_2}}\right)_x \sim \{\overline{X}(X_c + X_s) - X_c X_s\}\frac{\eta_0}{T} \tag{55}$$

Eqs. (50) and (55) now describe the temperature dependence of the total linewidth for the case that two ion pair species exist in solution, which are involved in an exchange equilibrium in the limit of rapid exchange.

Static model

According to the static model at each temperature only one ion pair species is present. Therefore, at a given temperature the parameters A, B and W are unequivocally determined and at each temperature the linewidth contributions of the different relaxation mechanisms are correctly presented by the eqs. (31). Thus the temperature dependence of the different linewidth contributions $\left(\frac{1}{T_2}\right)_{Fc}$, $\left(\frac{1}{T_2}\right)_D$ and $\left(\frac{1}{T_2}\right)_Q$ is, apart from the temperature dependence of η_0/T, given directly by the temperature dependence of the parameters A^2, B^2 and W^2.

Application

An example of the application of the formulae derived in this paragraph can be given if one considers an alkali radical salt in which the Fermi contact interaction provides the main relaxation mechanism of the alkali nucleus. Suppose that the ion pairs in a solution of this salt have to be described by the equilibrium model and that the interconversion of the solvent separated and contact ion pairs takes place in the rapid exchange limit.

As the condition $\left(\overline{\frac{1}{T_2}}\right)_D, \left(\overline{\frac{1}{T_2}}\right)_Q \ll \left(\overline{\frac{1}{T_2}}\right)_{Fc}$ is fulfilled in this case, it follows from the eqs. (50) and (55) that

$$\left(\frac{1}{T_2}\right) = \overline{\left(\frac{1}{T_2}\right)_{Fc}} \sim \{\overline{A}(A_c + A_s) - A_c A_s\}\frac{\eta_0}{T} \tag{56}$$

According to the definition of $\overline{A}$ of eq. (54), $\overline{A}$ is infact equal to the Fermi contact interaction constant A of the alkali nucleus, as measured from the ESR or the alkali NMR spectrum of the solution. Assuming for A_s the usual value of zero* one finds from eq. (56)

$$\frac{1}{T_2} \sim A A_c \frac{\eta_0}{T} \tag{57}$$

On the other hand, if the alkali radical ion pair under consideration would have to be described by the static model, one would find from the eqs. (31), (33), (34) and (36)

$$\frac{1}{T_2} = \left(\frac{1}{T_2}\right)_{Fc} \sim A^2 \frac{\eta_0}{T} \tag{58}$$

Eqs. (57) and (58) show that, when the Fermi contact interaction determines the alkali metal linewidth, the equilibrium model predicts this linewidth to be proportional to $A.A_c$, while the static model predicts a proportionality with A^2.
Therefore, if the analysis of the temperature behaviour of the metal h.f.s.c. does not give conclusive evidence about whether the ion pairs should be described by the static or by the dynamic model, a study of the temperature dependence of the linewidth may provide this evidence. The only assumption which is needed for the performance of a linewidth analysis as described above, is an estimate of A_c at different temperatures.

---

*) It is pointed out that the assumption $A_s = 0$ is in contradiction with the assumption that the Fermi contact interaction determines the linewidth of the alkali nuclei in the solvent separated ion pairs. However, when $A_s = 0$, in most cases the condition $\left(\frac{1}{T_2}\right)_s \ll \left(\frac{1}{T_2}\right)_{Fc,c}$ will be satisfied. Therefore, unless $f_c \cong 0$, the term $(1-f_c)\left(\frac{1}{T_2}\right)_s$ in eq. (49) may be neglected, which again leads to eq. (57).

PERFORMANCE OF THE EXPERIMENTS

In the following sections, the apparatus, the preparation of the samples and the experimental procedure are described. At the end a discussion of the experimental procedure is given.

3.1. APPARATUS

The NMR experiments have been performed on a Varian DP 60 EL spectrometer equipped with a V 4311 60 Mc/s, a V 4311 15 Mc/s and a V 4210 variable frequency transmitter, and the matching probes V 4331 B, V 4331 A and V 4230. The frequency of the V 4210 transmitter could be stabilized at different values by crystal stabilizers. The transmitter frequency was measured during the experiments with a HP 5245 L frequency counter. The resonance fields and frequencies which have been used to measure the resonance signals of the different nuclei are given in table 2.

	^{1}H	^{6}Li	^{7}Li	^{23}Na	^{39}K	^{85}Rb	^{87}Rb	^{133}Cs
ν_r, Mc/s	60.0	9.1	15.1	15.1	2.9	5.9	15.1	8.0
H_0, kgauss	14.1	14.6	9.1	13.4	14.3	14.3	10.8	14.2

Table 2. Resonance frequencies and magnetic fields used for the NMR experiments on different nuclei.

Apart from the standard probe inserts a home made 13 mm i.d. variable temperature insert for the V 4331 A probe was used for experiments at 15 Mc/s.
The temperature of the sample was controlled by a V 4353 or a V 4330 unit.
Audio lock-in detection could be performed with a V 3521 A unit at 2, 4 or 8 kc, or with a combination of the units V 4240, V 4250 and V 4270. Operation of the V 3521 A unit at 4 and 8 kc was made possible by a slight modification of the circuits.

For proton experiments at 60 Mc the field could be stabilized with a Varian external lock (EL) device or with a V 3506 flux stabilizer. For experiments at other frequencies only the latter unit could be used for the stabilization of the field, while in rare cases a Fieldial was employed. The field was swept, depending upon the mode of field stabilization, respectively by moving the pen of the spectrometer recorder, by using a V 3507 slow sweep unit or by using the Fieldial. The spectra were calibrated by using precalibrated NMR chart paper, by employing the side band technique or by measuring the field with an AEG gaussmeter during the experiments.
ESR measurements were performed on a Varian V 4502 X-band spectrometer.

3.2. PREPARATION AND REDUCTION OF THE SAMPLES

For the preparation of the reference solutions $LiClO_4$ (BDH), NaCl (Merck, p.a.), KCl (Brocades, 98%), RbCl (Merck, p.a.) and CsCl (Merck, p.a.) were used directly from stock. ^{6}LiBr was prepared by dissolving ^{6}Li metal in aqua dest., neutralizing the solution with HBr (Merck, p.a.), evaporating the solvent and drying the precipitate in vacuo at 150°C for 2-3 days. $NaBH_4$ (Fluka, purum) and $NaB\Phi_4$ ($\Phi \equiv$ phenyl) (Baker, p.a.) were used directly from stock.
Biphenyl (≡Bp) (BDH) was recrystallized from 96% ethanol and sublimed in vacuo. Fluorenone (≡Fluon) (U.C.B., 98%) was recrystallized from benzene and petroleum ether and dried at 60-80°C. Naphtalene (≡Nl) (Riedel & de Haen) was recrystallized from 96% ethanol and sublimed in vacuo. Phenanthrene (Pht) (Fluka puriss.) was used directly from stock.
The solvents tetrahydropyran (≡THP) (Fluka), 2-methyltetrahydrofuran (≡MTHF) (Schuchardt), tetrahydrofuran (≡THF) (Riedel & de Haen) and 1,2-dimethoxyethane (≡DME) (Merck), were stored over $CaCl_2$, dried before use over calciumhydride or over a sodium dispersion, distilled on the vacuum line and stored over Na/K alloy. The solvents diglyme (≡Dg) (Fluka), triglyme (≡Tg) (Fluka, Schuchardt) and tetraglyme (≡Ttg) (Fluka, Schuchardt) were dried just before use over a Na mirror and distilled in vacuo. The composition of DME, Dg, Tg and Ttg is presented by the formula $CH_3[OCH_2CH_2]_n OCH_3$ in which n is equal respectively to 1, 2, 3 and 4.

For the preparation of the samples the alkali metals were used in their normal isotopic abundance except ^{6}Li, which was bought from Philips Duphar with an enrichment of 95.6%. ESR and NMR samples were prepared by standard techniques on the vacuum line. The NMR samples were provided with 10, 13 or 15 mm o.d. Wilmad sample tubes. The concentration of the aromatic compounds in the NMR samples amounted in most of the cases to a value between 0.7 and 1.3 M. After complete reduction of the sample the radical concentration as calculated from the solvent shift (see the secs. 3.3 and 3.4) usually varied between 0.4 and 1.1 M. No special care was taken to make the sample solutions all of the same concentration. The reduction of Bp in the systems Na Bp THP and Na Bp MTHF required special care, because at room temperature the equilibrium

$$Na + Bp \leftrightarrows Na^+Bp^-$$

is shifted far to the left in THP and MTHF [48, 50, 68]. Therefore in these two cases the solutions were allowed to come to equilibrium over the metal mirror at $-20°$C, decanted at $-20°$C and measured by starting the measurements at low temperatures.

3.3 EXPERIMENTAL PROCEDURE

According to the theory which has been dealt with in the foregoing chapter, the following quantities are of interest: the radical concentration c, the fraction f_p of paramagnetic particles in the solution, the contact shift δ_c, the linewidth $\frac{1}{T_2}$, the absolute temperature T and the viscosity of the pure solvent η_0. The different ways in which these quantities were determined are discussed below.

(i). Determination of the concentration c

When a solution of an aromatic compound (Ar) is reduced with an alkali metal, the susceptibility of the solution changes because of the increase in the concentration of paramagnetic particles (Ar^-) in the solution. When a non-spherically shaped sample is used this change in the susceptibility causes all the NMR peaks to be shifted with

respect to their positions in the unreduced solutions by an amount which is the same for all the peaks and which is proportional to the concentration [17, 69]. From the magnitude of the shift the concentration can be calculated. In the present study the radical concentration was determined by measuring the shift δ_s of the solvent peaks with respect to their positions in an unreduced reference solution, the spectrometer operating in the EL mode. For the case that cylindrical sample tubes are used δ_s is given by [17]

$$\delta_s = \frac{2}{3}\pi \times 10^3 \frac{N(\gamma_e \hbar)^2}{kT} c, \text{ ppm} \tag{59}$$

in which N is Avogadro's number, and the other symbols have their usual meaning. The concentration c is expressed in mol/l while the other quantities are expressed in cgs units.

(ii). Determination of f_p

It was assumed that the maximum value, δ_s^0, of the solvent shift, attained at the end of the reduction, corresponded with 100% reduction. Therefore f_p could be calculated, after finishing the experiment, from the solvent shifts δ_s measured during the experiment, by

$$f_p = \frac{\delta_s}{\delta_s^0} \tag{60}$$

(iii). Determination of the contact shift δ_c

According to the definition of eq. (20) the contact shift depends on the resonance field H_0 of the nucleus in the reference solution, the resonance field H_p of the nucleus in the sample solution and the term $H_0\sigma_0 - H_p\sigma_p \cong H_0(\sigma_0 - \sigma_p)$. As the magnitude of the latter term is difficult to determine either theoretically or experimentally, this term was neglected, so that in practice δ_c was found by taking the difference of H_0 and H_p. The neglect of the term $H_0(\sigma_0 - \sigma_p)$ introduced a systematic error in δ_c, which will be discussed in the next section.

In the proton experiments H_p was measured with respect to the peaks of the solvent, which was used as an internal reference (see the figs. 6-8, sec. 4.1.1). H_0 was determined by measuring the NMR spectrum at room temperature of an unreduced solution of the aromatic compound using again the solvent as an internal reference.

In the alkali NMR experiments the spectra were calibrated by measuring and recording the magnetic field with an AEG gaussmeter during the recording of the NMR spectra. For a particular alkali nucleus H_0 was determined by measuring the resonance position of this nucleus in a diamagnetic reference solution at room temperature (see fig. 12, sec. 4.1.2). As reference solutions were used a solution of 1 M $LiClO_4$ in THF and solutions of 1 M ^{6}LiBr, 1 M NaCl, 1 M KCl, 1.5 M RbCl and 2.4 M CsCl in H_2O.

On the experimentally determined contact shifts of the alkali nuclei the following corrections were applied:

1 A correction which took into account the difference in bulk susceptibility between sample and reference. For the cases investigated in this study the susceptibility difference depended mainly on the difference in the paramagnetic susceptibility between the reference and the sample. Neglecting therefore the diamagnetic contributions to the susceptibility difference the correction was directly given by the solvent shift, which at room temperature usually amounted to 1-2 ppm.

2 A correction which took into the account the difference in the concentration between the reference and the sample.
In some cases the radical concentration differed markedly from the concentration of the inorganic salt in the reference solution. Therefore a correction was applied to the position of the reference signal to obtain the position of the signal of a reference solution of the same concentration as the reduced solution. The corrections were calculated on the basis of literature data [70]. Only in the Rb and Cs experiments these corrections were not negligeably small. However, even in these cases the corrections usually did not amount to more than a few percent of the measured contact shift.

3 For the ^{6}Li and the ^{7}Li NMR experiments reference solutions of different composition were used, viz. a ^{6}LiBr/H_2O solution for the ^{6}Li experiments and a $LiClO_4$/THF solution for the ^{7}Li experiments. In order to make a comparison between the ^{6}Li and

the ^{7}Li data possible a correction was applied to the ^{6}Li data which accounted for the shift of the ^{6}Li signal from a 1 M $^6LiBr/H_2O$ solution with respect to the ^{6}Li signal from a 1 M $^6LiClO_4$/THF solution [71]. In this way both the ^{6}Li and the ^{7}Li signals were referred to the signal of a 1 M $LiClO_4$/THF solution.

(iv). Determination of the linewidth $\frac{1}{T_2}$.

In studying the NMR signals of the different nuclei either the absorption curve was measured in the centerband or the sideband mode, or the derivative curve. As it was assumed that the line shape was Lorentzian, in the former case the value of $\frac{1}{T_2}$ was found by multiplying the half width of the signal at half height, measured in Ørsted, by γ_N, in the latter case by multiplying the derivative peak-peak distance ΔH, measured in Ørsted, by $\frac{1}{2}\sqrt{3}.\gamma_N$ [72].
If the derivative curve was measured, corrections were applied for modulation broadening [73]. The modulation amplitude H_m was measured according to a method described by SHPORER *et al.* [74]. When the inhomogeneity of the field was expected to give a non-negligeable contribution to the linewidth the homogeneity of the field was adjusted before starting the experiment.

(v). Determination of the temperature T

The sample temperature T was determined by measuring the E.M.F. of a thermocouple inserted between the sample tube and the glass wall of the probe insert.

(vi). Determination of the viscosity η_0

For the viscosities of the pure solvents literature data were used. Values for η_0 at other temperatures than at those reported were found from interpolation and extrapolation.
The values used in this study are presented in table 3.

T,°C	THP	MTHF	THF	DME	Dg
110	0.277	0.236	0.235	0.211	0.454
100	0.305	0.251	0.250	0.226	0.475
90	0.337	0.268	0.268	0.244	0.500
80	0.375	0.288	0.287	0.263	0.540
70	0.420	0.309	0.310	0.286	0.585
60	0.472	0.334	0.335	0.311	0.625
50	0.536	0.363	0.364	0.342	0.699
40	0.614	0.396	0.399	0.377	0.773
30	0.708	0.436	0.439	0.418	0.874
20	0.826	0.481	0.486	0.468	1.02
10	0.973	0.536	0.542	0.527	1.24
0	1.159	0.601	0.609	0.599	1.57
−10	1.403	0.681	0.691	0.688	2.00
−20	1.72	0.778	0.791	0.799	2.65
−30	2.15	0.897	0.917	0.938	3.75
−40	2.73	1.052	1.075	1.118	5.55
−50	3.55	1.25	1.28	1.353	8.75
−60	—	1.50	1.55	1.67	15.5
−70	—	1.85	1.91	2.10	30.8
−80	—	2.31	2.41	2.70	69
−90	—	2.98	3.11	3.58	—

Data were taken from the following references:
THP [43]; MTHF [41, 43]; THF [40, 43]; DME [40]; Dg [75].

Table 3. Viscosities of different solvents in centipoises.

3.4. DISCUSSION OF THE EXPERIMENTAL PROCEDURE

The methods, described in the foregoing section, to determine the quantities c, f_p, δ_c, $\frac{1}{T_2}$, T and η_0 may give rise to systematic and random errors which are discussed below.

(i). The concentration c

According to eq. (59) systematic errors in the determination of c are made if other factors than the bulk susceptibility alone influence the solvent shift. According to discussions in the literature the procedure adopted here to determine c has proved to be reliable [17]. The neglect of the diamagnetic contribution to the difference in the bulk susceptibility causes an error which falls within the experimental accuracy. However, the observation that the radical concentration, calculated at the end of the reduction from the solvent shift, usually

appeared to be lower than the initial concentration of the aromatic compound weighed in at the preparation of the sample, might indicate that there is a systematic error inherent to the method of calculating c from the solvent shift, which may cause the calculated value of c to be too small by an amount of 10-50%.
The random error in the determination of δ_s is estimated to be $\pm$ 2.5 cps, which in most cases corresponds to an inaccuracy of less than $\pm$ 2.5% in the concentration c.

(ii). f_p

Just like the concentration, the fraction of paramagnetic particles f_p is calculated from the solvent shift according to eq. (60). Therefore, regarding the inaccuracies in the determination of f_p the same remarks apply as for the concentration. However, it is remarked that, if eq. (59) is invalid because other factors than the bulk susceptibility alone determine δ_s, eq. (60) nevertheless may be correct if only δ_s is proportional to c. The random error in f_p is estimated to be less than $\pm$ 2.5%.

(iii). The contact shift δ_c

Of the errors made in the determination of δ_c first the systematic errors and next the random errors will be discussed.

Systematic errors

The systematic errors in δ_c originate from the neglect of the term $H_0\sigma_0 - H_p\sigma_p \cong H_0(\sigma_0 - \sigma_p)$ in eq. (20).
For an aromatic proton σ_0 and σ_p refer to the screening constants of the proton in respectively the neutral aromatic molecule and the negative ion of the aromatic compound. If in the negative ion the excess electronic charge would be concentrated on one single carbon atom, $\sigma_0 - \sigma_p$ would have a maximum value for the proton attached to this carbon atom of approximately 10 ppm [76]. This effect is negligeable compared with the contact shift, which amounts for a proton attached to a carbon atom bearing a full unpaired electron to approximately 2×10^3 ppm at room tempera-

ture. Therefore, the systematic error made in the determination of the contact shift of the aromatic protons by neglecting the term $H_0(\sigma_0 - \sigma_p)$ is negligeable.

The situation is different for the alkali NMR experiments. In general the screening constant of the nucleus of an alkali ion in solution will depend on the composition of the solvent shell around the ion. The solvent shell will consist mainly of solvent molecules and anions. In the present study solvent and anion in the reference solution nearly always differed from those of the sample solution. Therefore in most cases $\sigma_0 - \sigma_p$ will have been different from zero and it is of importance to get an impression about the order of magnitude the term $\sigma_0 - \sigma_p$ may reach. More particularly it is of interest to know

1 to what extent chelation of the alkali ions by solvent molecules influences the resonance positions of the alkali nuclei,
2 to what extent the presence of ring currents in the aromatic anions influences the resonance positions of the alkali nuclei,
3 to what extent the magnitudes of these two effects vary with the temperature.

An *a priori* theoretical approach to these problems would fall outside the scope of this study. Therefore, a more practical approach was chosen by investigating how large the above mentioned effects might be for a number of special cases. For this purpose a series of Na NMR experiments was performed on solutions of $NaBH_4$ and $NaB\Phi_4$ in THF, DME, Dg, Tg and Ttg, and of $NaB\Phi_4$ in MTHF. In these experiments the shift of the Na signal with respect to the signal of a 1 M $NaCl/H_2O$ solution, measured at room temperature, was determined as a function of the temperature. The concentrations of the solutions varied between 0.1 and 0.8 M. The $NaBH_4$ solutions were approximately saturated at room temperature. The choice for these salts and these solvents was made for the following reasons.

1 The solvating power of the solvents varies appreciably going from MTHF to Ttg. Moreover it is known that, compared with the other solvents, Ttg is a strong chelating agent for Na ions [52, 77]. Therefore it was thought that a study of solutions of a Na salt in these solvents would show the possible influence of the solvation or the chelation of the Na ions on the resonance position of the alkali nuclei.

2 Comparison of the shifts of the Na signals of the $NaBH_4$ solutions with those of the corresponding $NaB\Phi_4$ solutions would probably give a good indication about the magnitude of the ring current effect: ring currents are completely absent in the $NaBH_4$ salt while in the $NaB\Phi_4$ salt there are four aromatic rings in which ring currents will be present.

The experimental results can be summarized as follows. The results of the measurements on the $NaBH_4$ solutions can be divided into two categories. The first category is characterized by the observation that the shift of the Na NMR signal is zero with respect to the signal of a 1 M $NaCl/H_2O$ solution and that the shift is approximately independent of the temperature. This was observed for the solutions of $NaBH_4$ in THF, DME and Dg. The second category has the feature that the shift varies slowly with the temperature and that the shift amounts to approximately 2-4 ppm. This was observed for the solutions of $NaBH_4$ in Tg and Ttg. Examples of the two categories are given in respectively fig. 2 and fig. 3 in which the Na shift is given as a function of the temperature for respectively the systems $NaBH_4$ in Dg and $NaBH_4$ in Ttg. The salt concentration amounted for both systems to 0.6 M.
For the $NaB\Phi_4$ solutions the same division in two groups of solvents could be made: in THF, DME and Dg the shift is independent of the temperature and amounts to approximately 6 ppm, while in Tg and Ttg the shift is again independent of the temperature and amounts to approximately 10 ppm. As examples the results obtained on solutions of $NaB\Phi_4$ in Dg and Ttg are presented also in respectively fig. 2 and fig. 3. The concentrations of the two solutions amounted to respectively 0.5 M and 0.3 M.
Finally a somewhat different behaviour of the Na shift with the temperature was found for $NaB\Phi_4$ in MTHF. The results are presented in fig. 4. The salt concentration amounted to 0.6 M.

The results described above can be interpreted as follows.
1 For solutions of $NaBH_4$ as well as of $NaB\Phi_4$ there is an increase of 2-4 ppm in the Na NMR shift when the solvent is changed from THF, DME or Dg to Tg or Ttg. This is ascribed to the difference in the chelation of the Na ions in the different solvents. The chelation is supposed to be strong in a solvent like Ttg and relatively small in the solvents THF, DME and Dg. Apparently

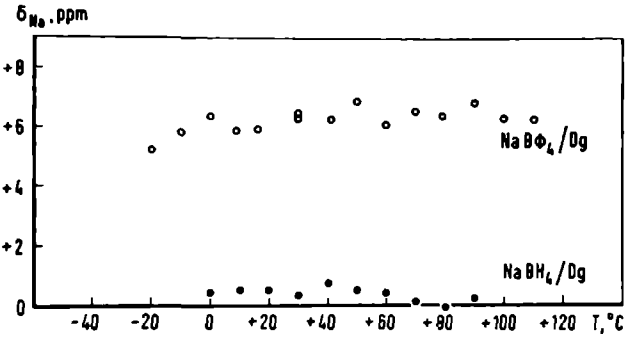

Fig. 2

Fig. 3

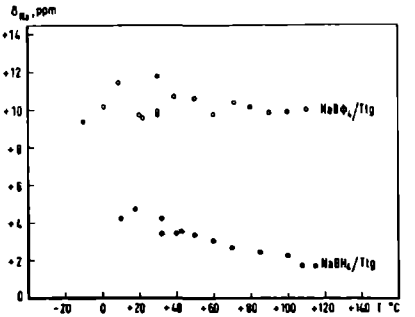

Fig. 4

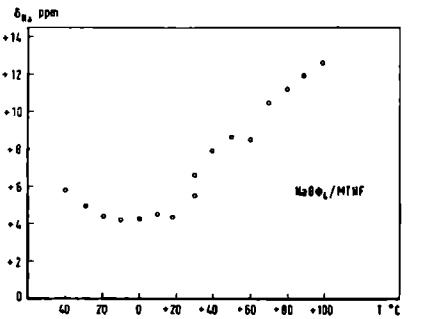

Figs. 2-4. Shifts of the ^{23}Na NMR signals, measured on solutions of some diamagnetic Na salts, *versus* temperature. Shifts were measured with respect to the Na signal of a 1 M $NaCl/H_2O$ solution at room temperature. A positive sign of δ corresponds with an upfield shift.

chelation of the sodium ions causes the Na NMR signal to be shifted upfield. It is of interest to note that in Tg the Na signal is shifted by the same amount as in Ttg. This may indicate that Tg is as good a chelating agent for Na ions as is Ttg.

2 Comparing solutions of $NaBH_4$ and $NaB\Phi_4$ in the same solvent the Na NMR signal of the $NaB\Phi_4$ solutions is always shifted 6-8 ppm to high field with respect to the signal of the $NaBH_4$ solutions. This is ascribed to the influence of ring currents, present in the $NaB\Phi_4$ salt, on the resonance position of the alkali ions in the $NaB\Phi_4$ solutions.

3 The influence of the temperature on the two effects described above is small except for the solution of $NaB\Phi_4$ in MTHF. This exception may correspond to the fact that $NaB\Phi_4$ forms contact ion pairs in MTHF, whereas it forms solvent separated ion pairs in the other ethers [43]. It may be supposed that in MTHF the Na ions

are close to the $B\Phi_4^-$ anions, so that a small change in the position of the Na ion in the ion pairs, caused by a change in the temperature, may result in a strong variation in the magnetic field exerted by the ring currents at the site of the alkali nucleus. According to this explanation the magnitude of this effect will depend strongly on the geometry of the ion pair.

From the above given interpretation of the experimental results it appears that the screening constant of a particular nucleus in a solution of an alkali radical salt may differ considerably from the screening constant of this nucleus in an aequeous solution of an alkali halide. Generalizing the experimental findings described above the following conclusions can be drawn about the influence of solvent, radical anion and temperature on the difference in screening constants.

1 The influence of the solvent on the shift of the alkali nucleus will be appreciable only if the solvent molecules are able to chelate the alkali ion strongly. For Na ions the effect is noticeable for the solvents Tg and Ttg, and its magnitude is for these cases equivalent to a Na h.f.s.c. of minus 7-15 milligauss.

2 Ring currents in the aromatic moiety of an ion pair may influence the position of the alkali resonance signal. The experiments indicate that this effect may be of the order of 6-8 ppm. For Na ions the magnitude of the effect is equivalent to a Na h.f.s.c. of minus 20-30 milligauss.

3 The influence of the temperature on the magnitude of the two effects described above is small in general. Therefore, if $H_0(\sigma_0 - \sigma_p)$ differs from zero the neglect of this term will cause in general a systematic error in the calculation of δ_c, which will be approximately independent of the temperature. As the alkali h.f.s.c. a is calculated from δ_c^0 by eq. (21), this means that a systematic error may be introduced in the determination of a, which is directly proportional to the temperature.

Random errors

The random errors made in the determination of the contact shift depended on 1. the short and long term stability of the magnetic field, 2. the accuracy of the gaussmeter and 3. the width of the NMR signal.

1. When regulated by the flux stabilizer, the short and long term

stability of the field amounted to approximately $\pm$ 1 : 10^7 respectively $\pm$ 1 : 10^6. When regulated by the Fieldial these values were $\pm$ 1 : 10^5 and $\pm$ 1 : 10^4.

2 The accuracy of the gaussmeter was approximately $\pm$ 3 milligauss for a single experiment.

3 The width of the NMR signal set a limit to the accuracy with which the position of the signal could be determined. It was estimated that the uncertainty in the determination of the position of the peak maximum amounted to $\pm$ 5 % of the linewidth.

As a result the absolute accuracy of the measurement of the shift for a single experiment amounted to $\pm$ 5 milligauss at best, while the relative accuracy in most cases was better than $\pm$ 5 %.

(iv). The linewidth $\frac{1}{T_2}$

As in most experiments not the exact value of $\frac{1}{T_2}$ but its variation with the temperature was of importance, it was not checked whether the resonance line shape was Lorentzian or not. In most cases no corrections on the linewidth were applied for the in homogeneity of the magnetic field and the broadening by intermolecular interactions. If needed the magnitude of these effects could be estimated respectively from the width of the corresponding reference signal and from the broadening of the solvent peak in the proton spectrum of the sample as follows. For a comparison of the magnitude of the field inhomogeneity with the linewidth of a given nucleus, expressed in s^{-1}, the value of the field inhomogeneity, expressed in gauss, should be multiplied by the gyromagnetic constant γ_N of the nucleus. For an estimate of the contribution from the intermolecular relaxation mechanisms to the linewidth of a given nucleus the amount of broadening of the solvent peak should be multiplied by γ_N^2/γ_H^2 in which γ_H is the gyromagnetic constant of the proton. If the homogeneity of the field was adjusted, the resultant inhomogeneity of the field over the sample volume amounted to approximately 2-4 milligauss. The broadening of the solvent peak in the proton spectrum of the solution amounted in most cases to 50-100 s^{-1}.

In some K and Rb measurements relatively high modulation amplitudes had to be used to obtain reasonable S/N ratios. This caused

an additional inaccuracy in the linewidth measurements, because for high modulation amplitudes the correction for modulation broadening becomes a steep function of the ratio $\Delta H/H_m$. Thus the correction itself becomes inaccurate.
The accuracy of the linewidth data for the proton experiments is estimated to be better than $\pm$ 5%, while for the alkali NMR experiments the accuracy is estimated to vary between $\pm$ 5 and $\pm$ 10%.

(v). The temperature T

The reliability of the method used to measure the temperature of the sample solution, was checked by inserting a sample tube filled with water in the probe and measuring with two thermocouples the temperature of the water in the sample tube and the temperature in the space between the sample tube and the glass wall of the insert. The two temperatures proved to be equal within the experimental error. Setting the temperature control for a temperature change of 10°C the two temperatures became again equal after 5-7 minutes.
The estimated accuracy of the temperature measurement is $\pm$ 1°C.

(vi). The viscosity η_0

The inaccuracies which were quoted in the literature for the viscosities used in this study, amounted in general to less than $\pm$ 2 percent, which was sufficiently small for our purposes.
It was pointed out in sec. 2.2.0 that the temperature dependence of the linewidth, the interaction parameters being constant, is given by a proportionality with η/T. It was argued that in this proportionality η could be replaced by the viscosity η_0 of the pure solvent provided the term in brackets in eq. (36) is temperature independent. Thus the proportionality of the linewidth with η_0/T presented by eq. (37) was obtained. In order to test the applicability of this equation the Na NMR linewidths were measured as a function of the temperature for a number of solutions of different concentration of $NaBH_4$ and $NaB\Phi_4$ in different ethers. The salts $NaBH_4$ and $NaB\Phi_4$ are diamagnetic and it is to be expected that in solutions of these salts the main relaxation mechanism of the Na nucleus will be provided by

the quadrupolar interaction [78]. It is known that the $NaB\Phi_4$ salts form solvent separated ion pairs over a large range of temperatures in most of the ethers used in this study [40, 43]. Therefore it can be expected that the structure of the solvent shell of the Na ions will not change markedly with the temperature, so that the magnitude of the quadrupolar interaction will also not change very much with the temperature. Thus the variation of the linewidth with the temperature will be determined for the $NaB\Phi_4$ and probably also for the $NaBH_4$ solutions by the variation in η/T alone and not by the variation in the magnitude of the interaction parameters. Therefore, these solutions probably constitute suitable testcases to check if it is allowed to present the temperature dependence of the linewidth by a proportionality with η_0 instead of η.

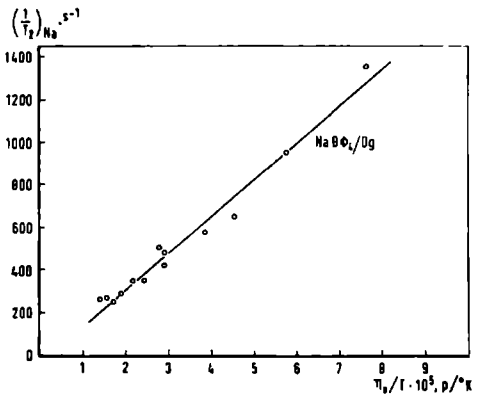

Fig. 5. ^{23}Na NMR linewidths, measured on a 0.5 M solution of $NaB\Phi_4$ in Dg, *versus* the viscosity of the pure solvent divided by the temperature.

It appeared that in plotting the width of the Na signal of these solutions versus η_0/T invariably a straight line through the origin was found. An example is shown in fig. 5. This was considered as a sufficient proof that the use of eq. (37) is allowed for a qualitative analysis of the temperature dependence of the linewidth.

EXPERIMENTAL RESULTS

The results of the measurements of the hyperfine splitting constants and the linewidths are presented in respectively sec. 4.1 and sec. 4.2. Unless otherwise stated the radical concentrations mentioned in the text or in the figures and the captions of the figures were calculated from the solvent shifts at the start of the experiments. Usually during the experiment the radical concentration diminished as a result of slight decomposition and sometimes partial precipitation of the alkali radical salts. In most cases this did not seem to influence the experimental results noticeably.

4.1. HYPERFINE SPLITTING CONSTANTS

Hyperfine splitting constants (h.f.s.c.'s) have been calculated from the experimentally measured contact shifts by using the eqs. (21) and (22). The results of the proton and the alkali measurements are presented in respectively sec. 4.1.1 and sec. 4.1.2.

4.1.1. PROTON H.F.S.C.

Spectra have been measured at room temperature of the negative ions of biphenyl (≡ Bp), fluorenone (≡ Fluon) and phenanthrene (≡ Pht). Examples are shown respectively in the figs. 6, 7 and 8. The spectra presented in these figures were obtained from solutions which were reduced with Na. The peaks in the different spectra were measured each with different *rf* power and audio modulation. The peaks of the solvents are denoted by *S* in the figures. In the unreduced solutions the signals of neutral Bp, Fluon and Pht lie respectively 250, 300 and 300 cps downfield from the peaks of the different solvents used in the experiments. The upper trace in fig. 8 was recorded in the EL mode. The peaks denoted by R are the peaks of neutral Pht in the unreduced solution. Peak no. 2, which is still visible in the upper trace of fig. 8, has shifted under the peaks of the solvent in the lower trace. The numbering of the peaks in fig. 8 does not correspond with a particular assignment of the peaks to the protons of Pht.

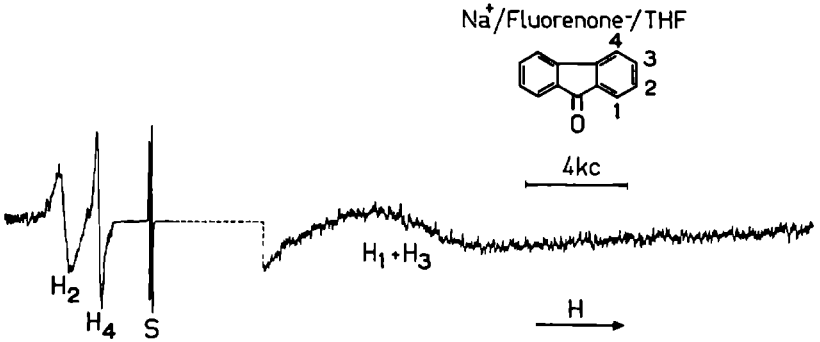

Fig. 7. Proton NMR spectrum at room temperature of a solution of Fluon in THF which was reduced by Na to a degree of reduction of 1.
The radical concentration amounted to 0.6 M.

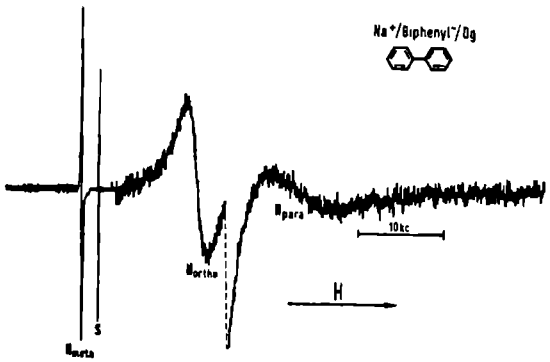

Fig. 6. Proton NMR spectrum at room temperature of a completely reduced solution of Bp in Dg. The radical concentration amounted to 0.9 M.

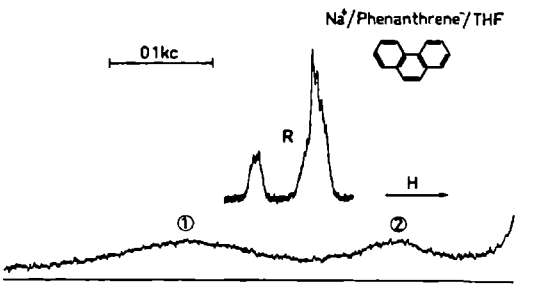

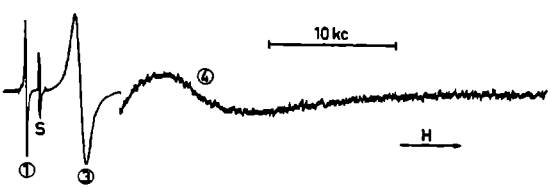

Fig. 8. Proton NMR spectra at room temperature of a partly reduced ($f_p = 0.15$, upper trace) and a completely reduced ($f_p = 1$, lower trace) solution of Pht in THF. The radical concentration in the latter solution amounted to 0.5 M. (See text for further explanation.)

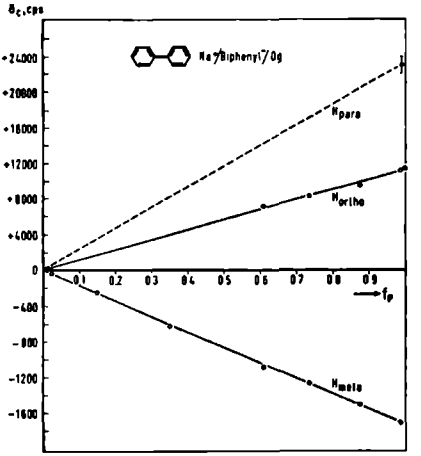

Fig. 9

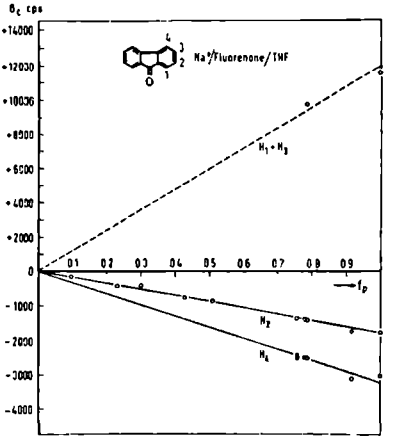

Fig. 10

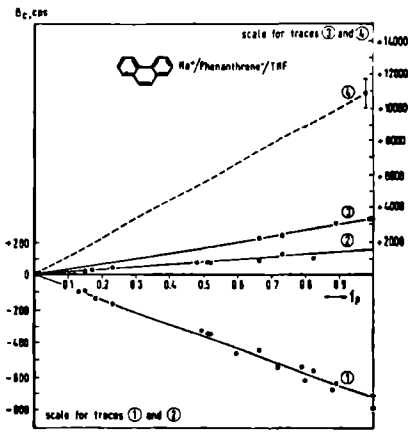

Fig. 11

Figs. 9-11. Contact shifts of the protons of Bp, Fluon and Pht at room temperature *versus* the degree of reduction of the respective solutions. N.B.: different vertical scales were used for different plots in the same figure.

The contact shifts δ_c of the protons have been plotted as a function of f_p in the figs. 9, 10 and 11 for respectively solutions of Bp in Dg, Fluon in THF and Pht in THF which were gradually reduced with Na. The radical concentrations at the end of the reduction amounted to 0.9 M for the system Na Bp Dg, 0.6 M and 0.9 M (two different samples) for the system Na Fluon THF, and 0.4, 0.7 and 0.8 M (three different samples) for the system Na Pht THF. As it was not always possible to resolve the NMR signals of protons with a large h.f.s.c. completely and to observe the resonance signals of these protons at all stages of the reduction, the contact shifts of these

protons could not be measured accurately. Therefore, for these protons the plots are presented by dashed lines in the figures.
Proton h.f.s.c. were determined from plots similar to the plots presented in the figs. 9-11 by using the eqs. (21) and (22). No influence of the temperature, the radical concentration or the degree of reduction on the proton h.f.s.c. was observed in the concentration range of 0.1-1.0 M.

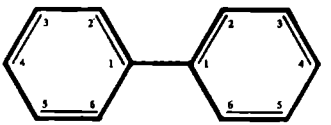

	1,1′	2,2′,6,6′	3,3′,5,5′	4,4′
NMR				
Li Bp Dg	—	—2.65	+0.38	—
Na Bp DME	—	—2.56	+0.40	—5.0
Na Bp Dg	—	—2.52	+0.40	—5.2
ESR				
Na Bp Dg	—	2.62	0.39	5.30
McLachlan [1])	—3.18	—2.54	+0.47	—5.10

[1]) Spin densities, multiplied by —25.
Table 4. Proton h.f.s.c. of Bp^- in gauss.

Numerical values of the proton h.f.s.c. are presented in the tables 4-6. For comparison also the ESR h.f.s.c. of the protons, obtained from the experiment or quoted from the literature, are entered in these tables, together with theoretically calculated values of the proton h.f.s.c. The latter values were found by multiplying the spin densities on the carbon atoms in the radical, calculated by the method of McLachlan [9], by a factor of —25 (see eq. (24)). In the M.O. calculations a value of 1 was used for the McLachlan parameter λ. For the calculation of the spin densities in the Fluon negative ion the Coulomb integral parameter of the oxygen atom was set equal to $\alpha + 2\beta$, and the resonance integral for the C-O bond was set equal to β [79], α and β being respectively the Coulomb and the exchange integral parameters for an aromatic carbon atom.
The results obtained from the experiments on Fluon and Pht need some further comments.

Fluorenone

The assignment of the h.f.s.c. of Fluon has been made according to DEHL and FRAENKEL [80].

In the analysis of the proton NMR spectrum of Na Fluon in THF (fig. 7) it was assumed that the observed high field peak consisted of the overlapping signals of the protons 1,8 and 3,6. The corresponding value of the NMR h.f.s.c. therefore probably presents the mean value of the h.f.s.c. of these protons.

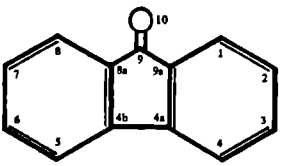

	1,8	2,7	3,6	4,5	9	10	4a,4b	8a,9a
NMR								
Li Fluon THF	—	+0.34	—	+0.65	—	—	—	—
Na Fluon THF	—2.6[1])	+0.41	—2.6[1])	+0.70	—	—	—	—
ESR								
Li Fluon THF	2.29	0.25	3.22	0.70	—	—	—	—
Na Fluon THF	2.09	0.12	3.18	0.67	—	—	—	—
Mg Fluon[2])	2.62	0.42	3.33	—	—	—	—	—
Ca Fluon[2])	2.53	0.35	3.25	0.73	—	—	—	—
McLachlan[3])	—2.10	+0.08	—2.30	+0.20	—10.2	—1.73	—2.53	+0.20

[1]) Mean value; see text.
[2]) Data of Hirota [81].
[3]) Spin densities, multiplied bij −25.

Table 5. Proton h.f.s.c. of Fluon$^-$ in gauss.

In solutions of Li Fluon in THF an extra diamagnetic proton signal was observed at the position of neutral Fluon. The signal doubled in intensity if MTHF was used as a solvent instead of THF. At the end of the reduction an additional weak paramagnetic signal at low field was observed.

Phenanthrene

The NMR h.f.s.c. of the protons of Pht differed strongly from the ESR and the theoretical values of the h.f.s.c. No assignment of the NMR h.f.s.c. could therefore be given. For the peaks designated by the numbers 1, 2, 3 and 4 in the figs. 8 and 11 the following values were respectively derived for the h.f.s.c.: +0.17, —0.036, —0.74 and —2.3 to —2.7 gauss.

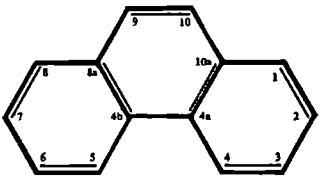

[1])	1,8	2,7	3,6	4,5	9,10	4a,4b	8a,10a
ESR Na Pht THF	3.71	0.48	2.89	0.61	4.47	—	—
McLachlan[2])	—3.83	+0.90	—3.05	—1.00	—4.85	—0.55	—0.15

[1]) The numbering of the carbon atoms does not correspond to the numbering of the proton peaks in the figures 8 and 11.

[2]) Spin densities, multiplied by —25.

Table 6. Proton h.f.s.c. of Pht^- in gauss.

It is pointed out that the numbering of the peaks in the figs. 8 and 11 does not correspond with the numbering of the protons in table 6. The peak in the NMR spectrum corresponding to the h.f.s.c. of —2.3 to —2.7 gauss is probably composed of the overlapping signals of two inequivalent groups of two protons. The assignment of the ESR h.f.s.c. presented in table 6 has been made according to COLPA and BOLTON [82].

4.1.2. ALKALI METAL H.F.S.C.

Alkali NMR spectra have been measured of the salts of Bp, Fluon and Naphthalene (Nl). In illustration some ^{133}Cs NMR spectra of solutions of CsBp in different ethers are reproduced in fig. 12. The experimentally determined values of the alkali NMR h.f.s.c. have been plotted as a function of the temperature in the figs. 13-38. In so far as the radical concentrations used in the NMR experiments are not indicated in the figures or in the captions of the figures they are mentioned below.

^{6}LiBp. Fig. 13: 0.4 M; fig. 14: 0.7 M; fig. 15: 0.8 and 0.9 M (two different samples).

^{7}LiBp. Fig. 13: 0.2, 0.4 and 0.7 M (three different samples); fig. 14: 0.3 M; fig. 15: 0.4 M; fig. 16: 0.8 M; fig. 17: 0.5 M; fig. 18: 0.5 M.

NaBp. Fig. 19: < 0.1 M (estimated value); fig. 20: 0.2 M; fig. 23: 1.0 M; fig. 24: 0.5 and 0.6 M (two different samples); fig. 25: 0.7 M.

RbBp. Fig. 27: 0.4, 0.4, 0.5 and 0.5 M (four different samples); fig. 28: 0.7 M; fig. 29: 0.5 M.

When they were available also ESR data were presented in the figures. The ESR data of the systems Na Bp THP and Rb Nl DME were taken respectively from ref. [14] and ref. [85]. ESR data of the system Na Bp THF were communicated by prof. T. R. TUTTLE, JR. The data of the following systems are shortly commented.

Biphenyl.

LiBp. The ratio of the ^{6}Li and the ^{7}Li h.f.s.c., measured in solutions of LiBp in THF, MTHF and THF (figs. 13-15), was found to be equal within the experimental error to $\gamma_{^6Li}/\gamma_{^7Li}$, in accordance with eq. (7).

NaBp. For the measurements on the systems Na Bp THF (fig. 21) and Na Bp DME (fig. 22) the concentration of the samples was varied by subsequent dilution of the solution. Concentrations were estimated from the width and the height of the Na signal.

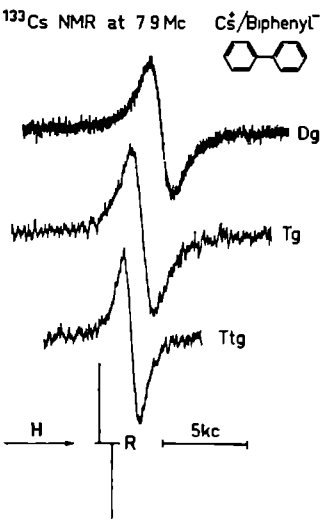

Fig. 12. ^{133}Cs NMR spectra of 0.4 M solutions of CsBp in Dg, Tg and Ttg, recorded at temperatures of respectively +50, +19 and +31° C. The trace designated by *R* is the spectrum of a 2.4 M CsCl solution in H_2O recorded at +30° C in the side band mode.

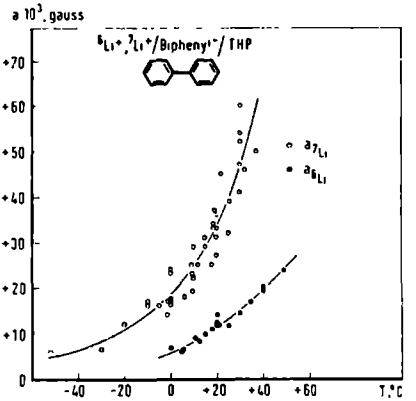

Fig. 13

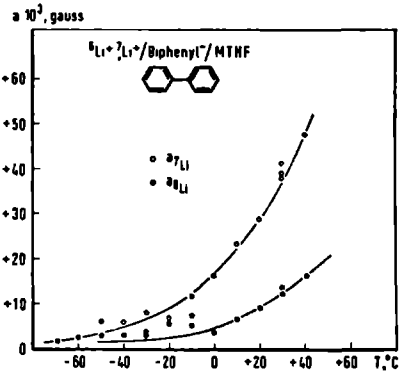

Fig. 14

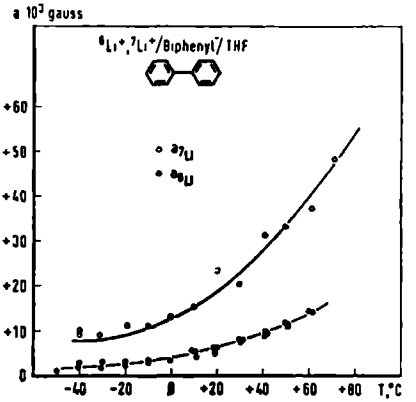

Fig. 15

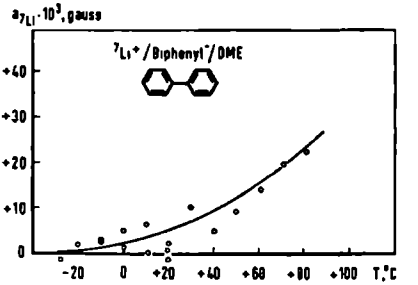

Fig. 16

Figs. 13-18. ^{6}Li and ^{7}Li NMR b.f.s.c. *versus* temperature for solutions of ^{6}LiBp and ^{7}LiBp in different ethers.

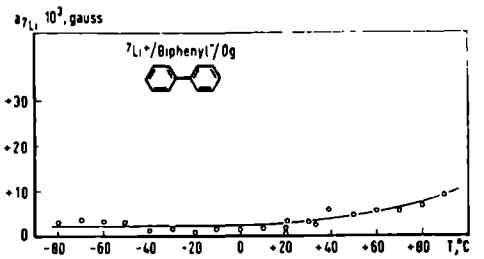

Fig. 17

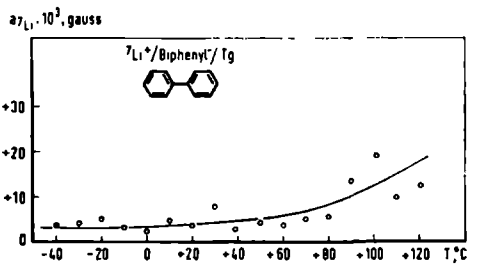

Fig. 18

RbBp. In the systems Rb Bp DME and Rb Bp Dg (figs. 27 and 28) the ratio of the ^{85}Rb and ^{87}Rb h.f.s.c. was found to be equal within the experimental error $\gamma_{^{85}Rb}/\gamma_{^{87}Rb}$, in accordance with the prediction of eq. (7).

Surveys. Surveys of the measurements of the h.f.s.c. in the Bp systems are presented in the figs. 30-36, in which for each metal the plots of the h.f.s.c., measured in different solvents, are combined in the same figure.

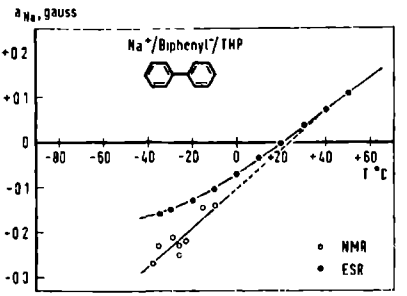

Fig. 19. ^{23}Na NMR and ESR h.f.s.c., measured on solutions of NaBp in THP, *versus* temperature. ESR data were taken from ref. [14].

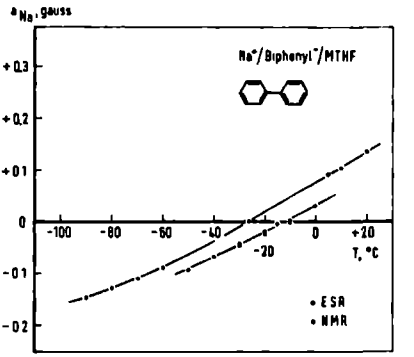

Fig. 20. ^{23}Na NMR and ESR h.f.s.c., measured on solutions of NaBp in MTHF, *versus* temperature.

Fluorenone.

The NMR data of fig. 37 can be compared with the ESR data of Hirota [15] and with the ESR results presented in fig. 1.
In the Li experiments, apart from a paramagnetic signal, a diamagnetic signal was observed of which the intensity doubled if MTHF was used as a solvent instead of THF. Also in the Cs spectra of solutions of Cs Fluon THF a weak diamagnetic signal was observed at low temperatures.

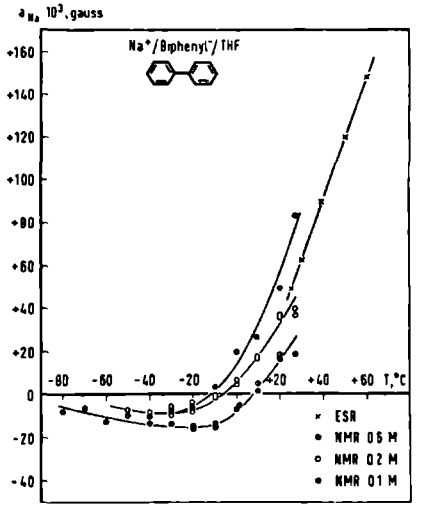

Fig. 21. ^{23}Na NMR and ESR h.f.s.c., measured on solutions of NaBp in THF, *versus* temperature. The radical concentration in the NMR experiments was varied by dilution of the solution. ESR data were communicated by prof. T. R. Tuttle, Jr.

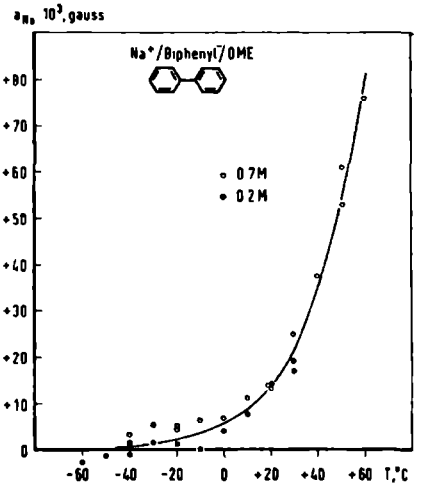

Fig. 22. ^{23}Na NMR h.f.s.c., measured on a solution of NaBp in DME at different dilutions, *versus* temperature.

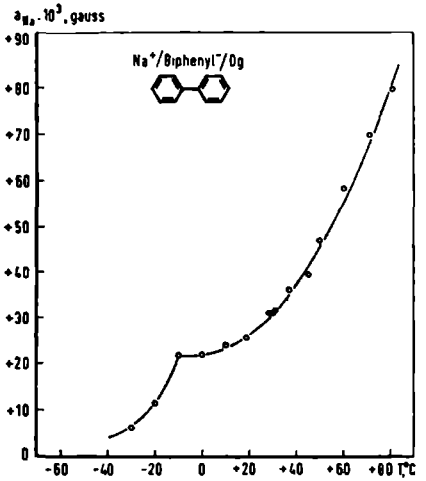

Fig. 23. ^{23}Na NMR h.f.s.c., measured on a solution of NaBp in Dg, *versus* temperature.

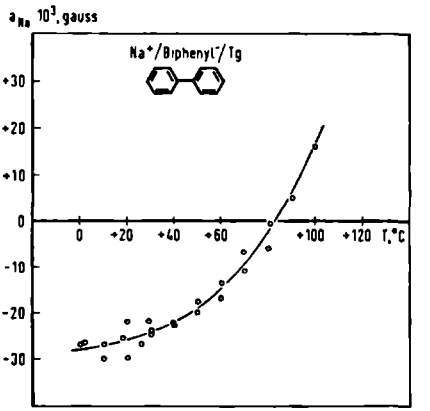

Fig. 24. ^{23}Na NMR h.f.s.c., measured on two different solutions of NaBp in Tg, *versus* temperature.

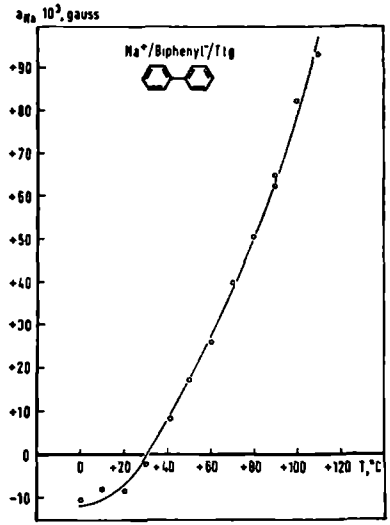

Fig. 25. ^{23}Na NMR h.f.s.c., measured on a solution of NaBp in Ttg, *versus* temperature.

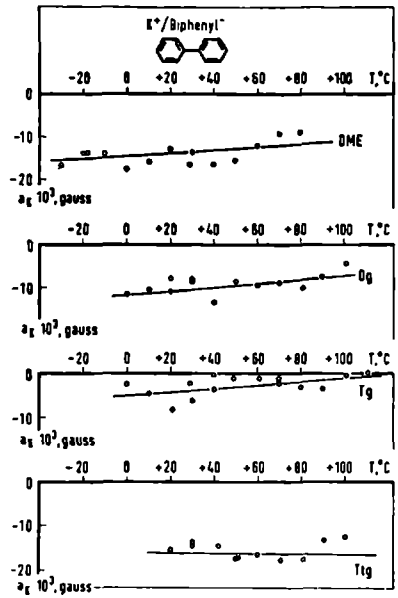

Fig. 26. ^{39}K NMR h.f.s.c., measured on solutions of KBp in the ethers DME, Dg, Tg and Ttg, *versus* temperature. The radical concentrations amounted to respectively 0.9, 0.6, 0.4 and 0.4 M.

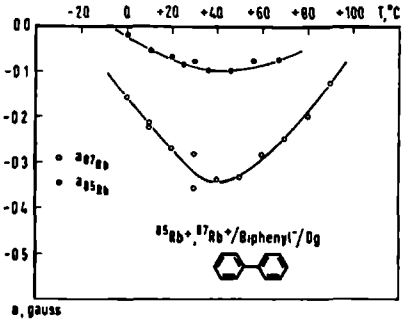

Fig. 28

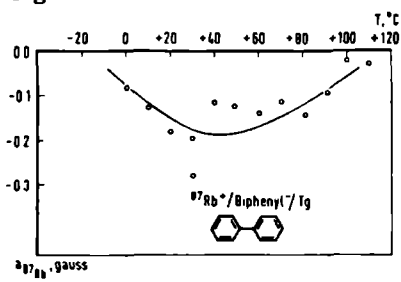

Fig. 29

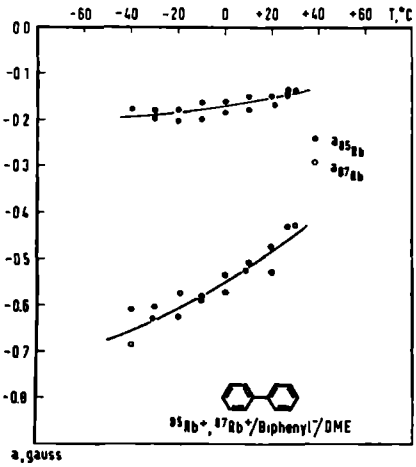

Fig. 27

Figs. 27-29. ^{85}Rb and ^{87}Rb NMR h.f.s.c., measured on solutions of RbBp in different ethers, *versus* temperature.

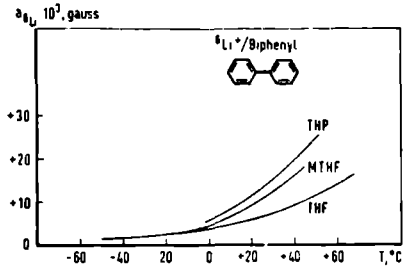

Fig. 30

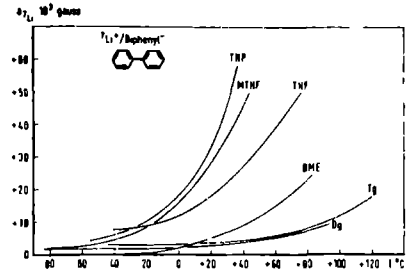

Fig. 31

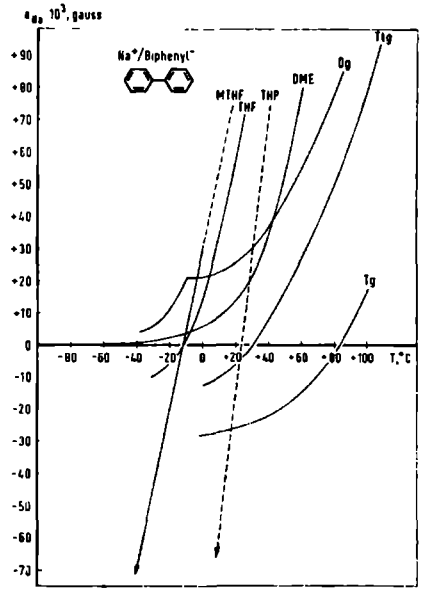

Fig. 32

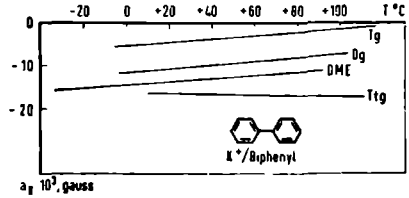

Fig. 33

Fig. 34

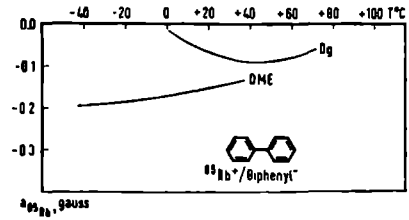

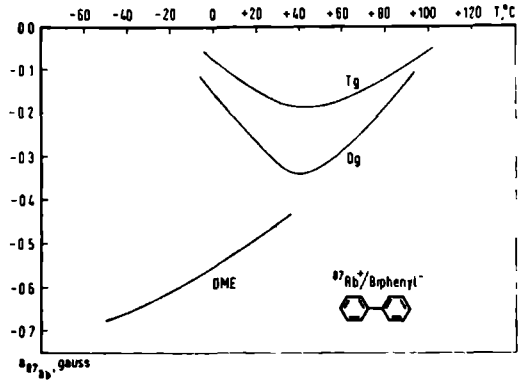

Figs. 30-35. Surveys of the plots of the alkali h.f.s.c. *versus* temperature, measured on solutions of a number of alkali Bp salts in different ethers. The plots were taken from the figs. 13-15 (^{6}Li), 13-18 (^{7}Li), 19-25 (^{23}Na), 26 (^{39}K), 27 and 28 (^{85}Rb), and 27-29 (^{87}Rb).

Fig. 35

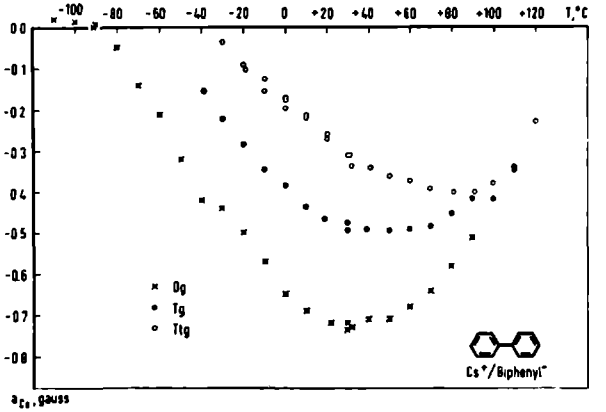

Fig. 36. ^{133}Cs NMR h.f.s.c., measured on 0.4 M solutions of CsBp in different ethers, *versus* temperature.

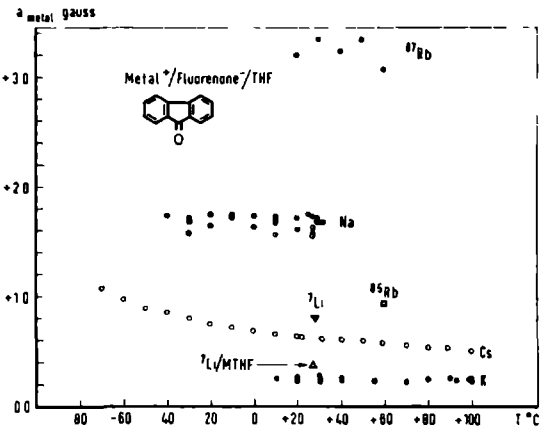

Fig. 37. Alkali NMR h.f.s.c., measured on solutions of different alkali Fluon salts, *versus* temperature. The radical concentrations in the different solutions varied from 0.4 to 0.7 M.

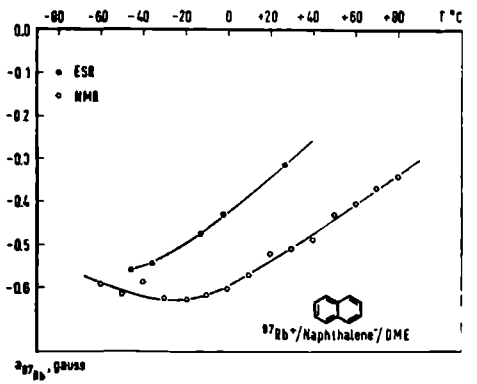

Fig. 38. ^{87}Rb NMR and ESR h.f.s.c., measured on solutions of RbNl in DME, *versus* temperature. The radical concentration used in the NMR experiments amounted to 0.7 M. ESR data were taken from ref. [85].

4.2. LINEWIDTHS

The results of the measurements on the proton and the alkali linewidths are presented in respectively sec. 4.2.1 and sec. 4.2.2.

4.2.1. PROTON LINEWIDTHS

The linewidths of the protons in the radical ions of Bp, Fluon and Pht have been measured in completely reduced solutions at room temperature. Values of the linewidths are presented in the tables 7-9.

	2,2′, 6,6′*	3,3′, 5,5′	4,4′
NMR h.f.s.c., gauss	−2.6 (1)	+0.39 (0.023)	−5.1 (3.85)
Linewidths, s^{-1}			
Li Bp Dg	31 000 (1)	1 030 (0.033)	—
Na Bp DME	11 000 (1)	420 (0.039)	38 000 (3.5)
Na Bp Dg	14 000 (1)	700 (0.05)	52 000 (3.7)

Table 7. Proton linewidths and NMR h.f.s.c. of Bp^- measured at room temperature.

Corrections on the linewidths were applied for broadening by intermolecular interactions and for inhomogeneity broadening (see sec. 3.3). In the tables also the values of the NMR h.f.s.c. are given, for which the mean values of the corresponding h.f.s.c. of the tables 4-6 were taken. The values in brackets represent the ratios of the linewidths and of the squares of the h.f.s.c. The data in the columns marked with an asterisk were used for the normalization of these ratios.

	1,8 & 3,6	2,7	4,5*
NMR h.f.s.c., gauss	−2.6[1]) (15)	+0.38 (0.31)	+0.68 (1)
Linewidths, s^{-1}			
Li Fluon THF	—	1 840 (0.56)	3 300 (1)
Na Fluon THF	27 000[1]) (12)	1 150 (0.50)	2 300 (1)

[1]) Mean value; see text.

Table 8. Proton linewidths and NMR h.f.s.c. of $Fluon^-$ measured at room temperature.

The signals of the protons 1,8 and 3,6 of Fluon⁻, mentioned in column two of table 8, were not observed separately (see fig. 7). The quoted values for the h.f.s.c. and the linewidth are probably the mean values of the h.f.s.c. and the linewidths of these two sets of protons.

NMR h.f.s.c., gauss	—0.036 (0.002)	+0.17 (0.05)	—0.74 (1)	—2.5[1]) (11.4)
Linewidths, s^{-1}				
Na Pht THF	160 (0.049)	510 (0.15)	3 300 (1)	45 000[1]) (13.6)

[1]) Mean value; see text.

Table 9. Proton linewidths and NMR h.f.s.c. of Pht⁻ measured at room temperature.

The data quoted in the last column of table 9 for Pht⁻ probably refer to the mean values of the h.f.s.c. and the linewidths of two inequivalent sets of two protons of which the signals could not be observed separately (see fig. 8).

4.2.2. ALKALI METAL LINEWIDTHS

Linewidths of various alkali nuclei have been measured at different temperatures on completely reduced solutions of the alkali salts of Bp, Fluon and Nl. The results are presented in the figs. 39-55, in which the linewidths are plotted as a function of η_0/T according to the methods outlined in sec. 2.2. In so far as the radical concentrations used in the experiments are not indicated in the figures or in the captions of the figures they are mentioned below.

^{6}LiBp. Fig. 39: 0.4 M; fig. 40: 0.6 M.
^{7}LiBp. Fig. 39: 0.4 M; fig. 40: 0.3 M; fig. 42: 0.3 M; fig. 43: 0.5 M.
NaBp. Fig. 44: 0.6 M.
RbBp. Fig. 47: 0.4 M; fig. 48: 0.7 M.
KBp. Fig. 53: 0.6 M for the DME as well as for the Dg solution.
KFluon. Fig. 53: 0.8 M.

^{6}Li linewidth data (figs. 39-41) were multiplied by $(\gamma_{^7Li}/\gamma_{^6Li})^2$ before plotting.

The linewidth data presented in the figures have not been corrected for inhomogeneity broadening and broadening by intermolecular interactions. However, these corrections will be applied in the quantitative analysis of the linewidth data, which will be given in sec. 5.2.2. No systematic study was made of the influence of the radical concentration on the linewidth. Only in a few cases the influence of the radical concentration (figs. 41, 45 and 46) and the degree of reduction (fig. 49) on the linewidth was studied.
The experimental data of the following systems are shortly commented.

Li Bp THP (fig. 39). In this system the Li linewidth broadened irreversibly upon aging of the solution. It is thought that this is caused by the growth of small particles in the solution, which slowly increase in magnitude on standing of the solution, and which probably consist of clusters of ion pairs. This can be related to the observation that LiBp forms easily supersaturated solutions in THP from which a crystalline precipitate is deposited upon standing.
Rb Fluon THF. Because of a low S/N ratio only a few reliable linewidth measurements could be performed on this system. At $T = +50°C$ values of 65 000 and 97 000 s^{-1} were measured respectively for the ^{85}Rb and the ^{87}Rb linewidth.
Surveys. In the figs. 51-55 surveys of the experimental data are given, in which for each metal the plots of the linewidths measured in different systems are combined in the same figure.

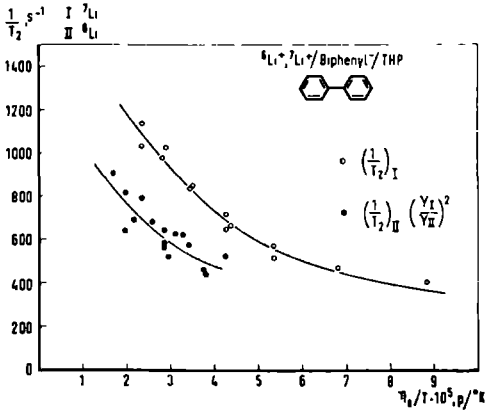

Fig. 39. ^{6}Li and ^{7}Li NMR linewidths, measured on solutions of ^{6}LiBp and ^{7}LiBp in THP, *versus* the viscosity of the pure solvent (η_0) divided by the absolute temperature (T).

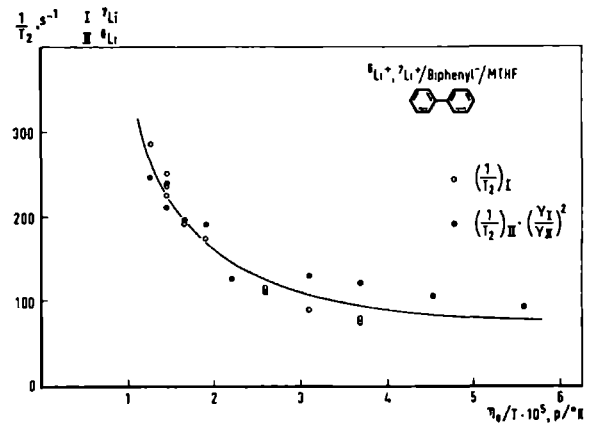

Fig. 40. ^{6}Li and ^{7}Li NMR linewidths, measured on solutions of ^{6}LiBp and ^{7}LiBp in MTHF, *versus* η_0/T.

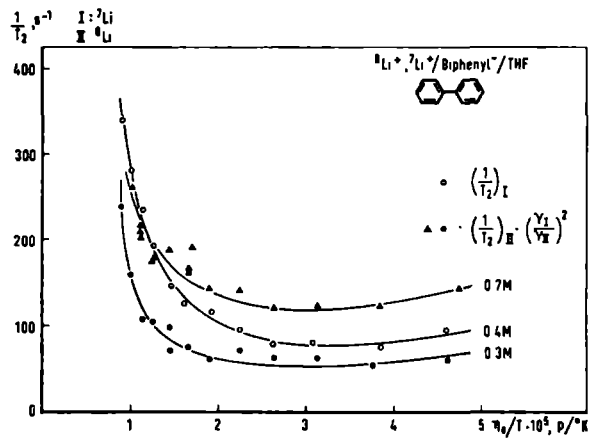

Fig. 41. ^{6}Li and ^{7}Li NMR linewidths, measured on solutions of ^{6}LiBp and ^{7}LiBp in THF, *versus* η_0/T.

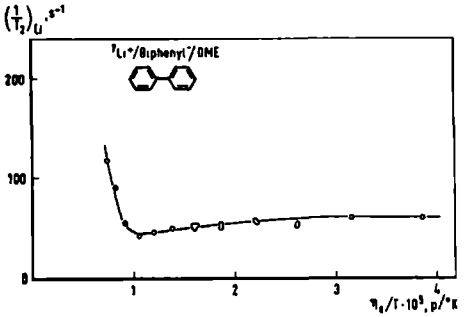

Fig. 42. ^{7}Li NMR linewidths, measured on a solution of LiBp in DME, *versus* η_0/T.

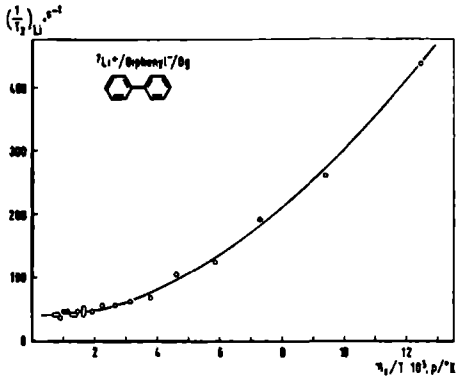

Fig. 43. ^{7}Li NMR linewidths, measured on a solution of LiBp in Dg, *versus* η_0/T.

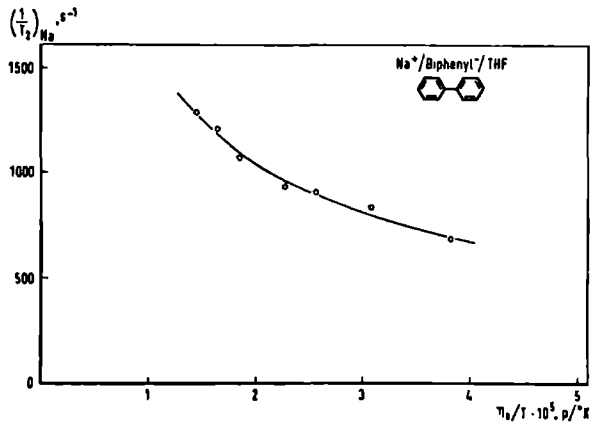

Fig. 44. ^{23}Na NMR linewidths, measured on a solution of NaBp in THF, *versus* η_0/T.

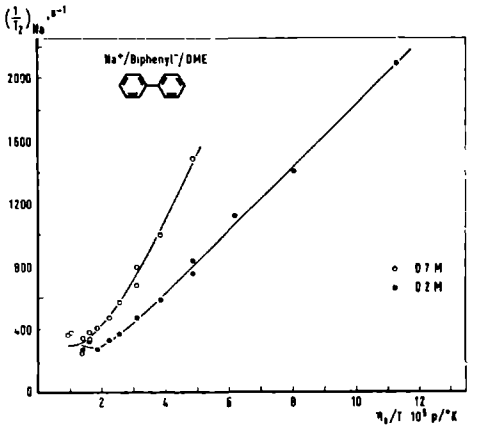

Fig. 45. ^{23}Na NMR linewidths, measured on a solution of NaBp in DME at different dilutions, *versus* η_0/T.

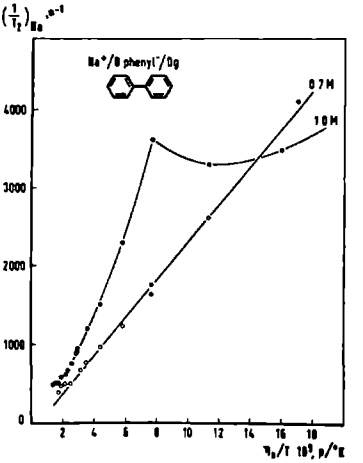

Fig. 46. ^{23}Na NMR linewidths, measured on a solution of NaBp in Dg at different dilutions, *versus* η_0/T.

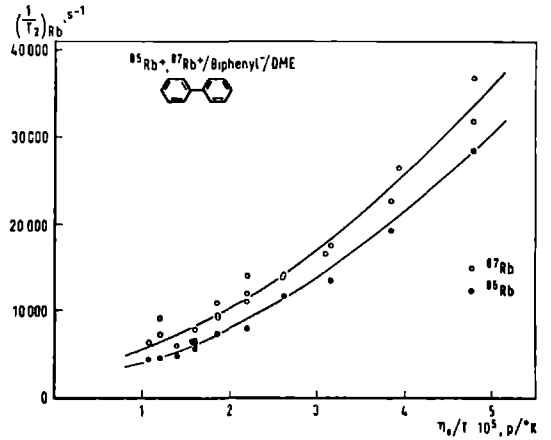

Fig. 47. ^{85}Rb and ^{87}Rb NMR linewidths, measured on a solution of RbBp in DME, *versus* η_0/T.

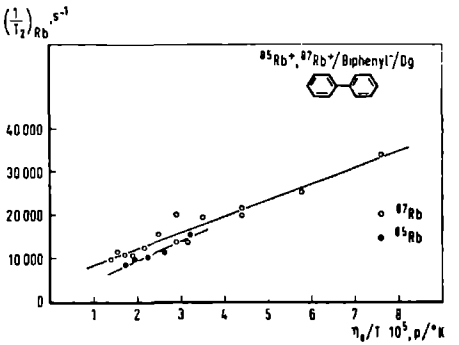

Fig. 48. ^{85}Rb and ^{87}Rb NMR linewidths, measured on a solution of RbBp in DME, *versus* η_0/T.

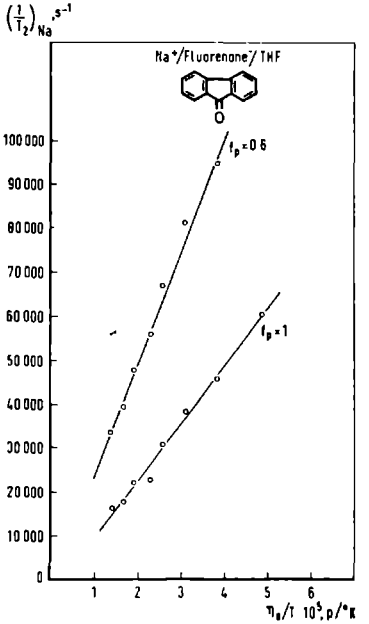

Fig. 49. ^{23}Na NMR linewidths, measured on a solution of Fluon in THF at different stages of the reduction ($f_p = 0.6$ and $f_p = 1$), *versus* η_0/T. The radical concentration at the end of the reduction amounted to 0.8 M.

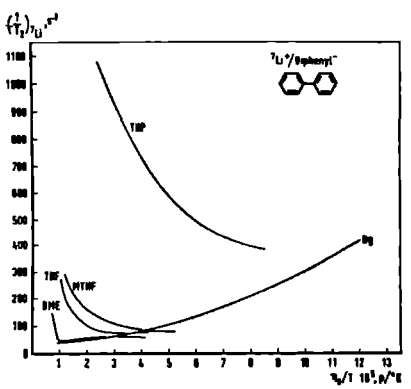

Fig. 51. Survey of the plots of the ^{7}Li NMR linewidths measured on solutions of LiBp in different ethers. The plots were taken from the figs. 39-43.

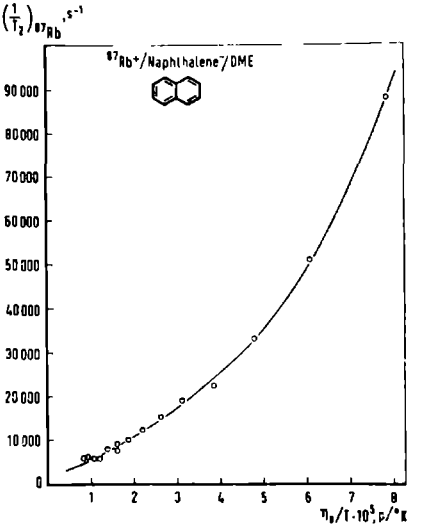

Fig. 50. ^{87}Rb NMR linewidths, measured on a 0.7 M solution of RbNl in DME, *versus* η_0/T.

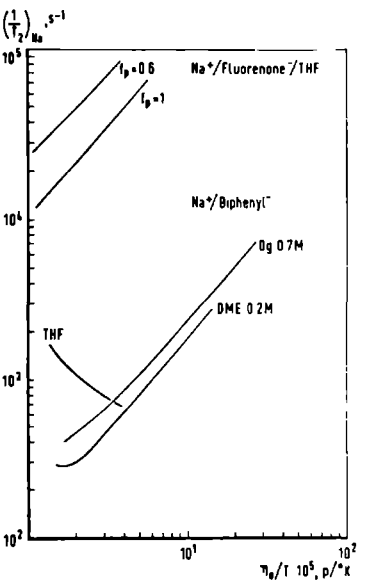

Fig. 52. Survey of the plots of the ^{23}Na NMR linewidths measured on solutions of NaBp and NaFluon in different ethers. The plots were taken from the figs. 44-46 and 49.

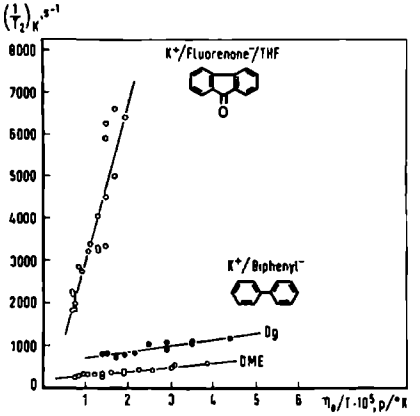

Fig. 53. ^{39}K NMR linewidths, measured on solutions of KBp and KFluon in different ethers, *versus* η_0 of the respective solvents divided by T.

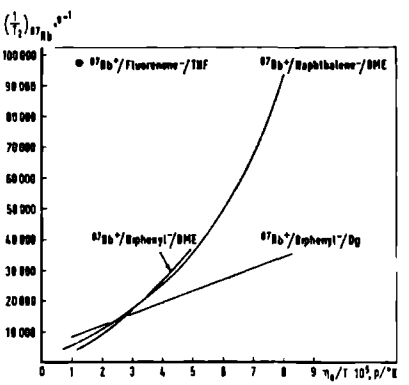

Fig. 54. Survey of the plots of the ^{87}Rb NMR linewidths measured on solutions of RbBp and RbNl in different ethers. The plots were taken from the figs. 47, 48 and 50. In addition the data of the ^{87}Rb linewidth measurements on a 0.7 M solution of RbFluon in THF are presented.

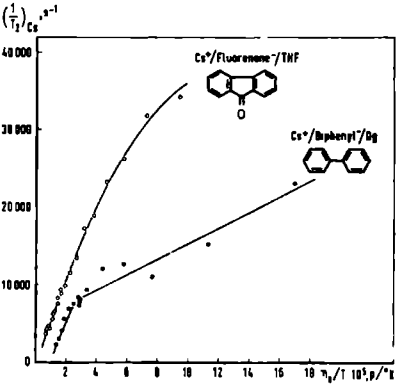

Fig. 55. ^{133}Cs NMR linewidths, measured on a 0.6 M solution of CsBp in Dg and a 0.4 M solution CsFluon in THF, *versus* η_0 of the respective solvents divided by T.

DISCUSSION

A discussion of the experimentally determined h.f.s.c. and linewidths is given in respectively sec. 5.1 and sec. 5.2.

5.1. HYPERFINE SPLITTING CONSTANTS

A discussion of the experimentally determined proton and alkali h.f.s.c. is given respectively in sec. 5.1.1 and sec. 5.1.2 on the basis of the theory presented in sec. 2.1. At the presentation of the experimental data it was remarked that the h.f.s.c. were calculated from the experimental contact shifts by using the eqs. (21) and (22). The application of these formulae included implicitly the assumption that the radicals are in a doublet ground state. This assumption is not necessarily correct for the case that one deals with concentrated radical solutions. Evidence has been reported in the literature, which indicates that in solutions of alkali radical salts ion pair dimers may be formed at concentrations above 0.01-0.1 M [53, 54]. If dimerization occurs the exchange interaction between the two unpaired electrons in the radical dimers may differ from zero. If the exchange interaction is small compared with the magnitude of the h.f.s.c., the dimers may still be considered as clusters of two separate doublet radicals each with quantum number $S = \frac{1}{2}$. However, if the exchange interaction is large the dimer has to be described as one single radical with $S = 1$ [83]. In the following it will be assumed, unless otherwise stated, that, supposed ion pair clusters are formed, the exchange interactions in the clusters are so small that the radicals may be considered as being in a doublet ground state.

5.1.1. PROTON H.F.S.C.

A discussion of the proton h.f.s.c. of Bp, Fluon and Pht is given on the basis of the data presented in sec. 4.1.1 in the tables 4-6.

Biphenyl. From the data of table 4 it appears that for Bp^- sign and

magnitude of the NMR h.f.s.c. agree with the results of the ESR measurements and the M.O. calculations. The small differences between the NMR h.f.s.c. of a particular proton, measured in different systems, are probably not significant.

Fluorenone. From the data of table 5 it appears in the first place that the magnitude of the proton h.f.s.c. varies considerably if the counterion changes. This is in accordance with the reported sensitivity of the proton h.f.s.c. of polar radicals like Fluon$^-$ towards the polarizing influence of the counterion [81].
In the second place the data of table 5 enable a comparison of the NMR h.f.s.c. with the ESR and theoretical h.f.s.c. It is recalled that in the NMR experiments only the mean value of the h.f.s.c. of the protons 1,8 and 3,6 could be determined. Therefore, in a comparison the mean values of the ESR and the theoretically calculated h.f.s.c. of the protons 1,8 and 3,6 have to be used. Performing the comparison in this way for the NMR and the ESR h.f.s.c. quoted in table 5, it appears that there is except for the protons 2,7 a reasonable agreement between the NMR h.f.s.c. and the ESR h.f.s.c. measured for Li and Na Fluon in THF, but that the agreement between the NMR h.f.s.c. of Li and Na Fluon and the ESR h.f.s.c. of Mg and Ca Fluon is better. A possible explanation of this observation can be given by assuming that the Mg and Ca salts of Fluon in solution consist of ion triples built up of two Fluon radicals centered around one doubly charged positive cation. A more or less similar configuration of the Fluon radicals can be expected to occur for the Na and Li Fluon salts at high concentrations. This is substantiated by a study of HIROTA and WEISSMAN, who reported that alkali Fluon salts form dimers at concentrations between 0.01 to 0.1 M [54]. The agreement between the NMR h.f.s.c. of Li and Na Fluon, and the ESR h.f.s.c. of Mg and Ca Fluon probably indicates that the for these cases reported values of the h.f.s.c. are characteristic for dimers instead of monomers of Fluon$^-$.
Finally we remark that the appearance of extra diamagnetic and paramagnetic signals in the proton as well as in the alkali NMR spectra of solutions of the Fluon salts indicates the existence of more than one ion pair species in these solutions. The fact that the diamagnetic proton and alkali signals increase in intensity if the less polar solvent MTHF is used instead of the more polar THF might be an indication that the diamagnetic signals originate from pinacol

dimers [54]. The formation of these diamagnetic dimers might have taken place according to the following reaction scheme [54, 81].

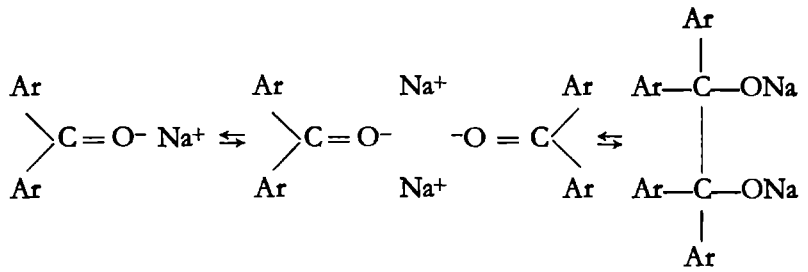

Phenanthrene. The only agreement between the NMR h.f.s.c. of Pht^- and the data of table 6 consists of the number of positive and negative signs of the h.f.s.c.: if it is assumed that the NMR h.f.s.c. of -2.3 to -2.7 gauss is the mean value of the h.f.s.c. of two inequivalent protons, it appears that four NMR h.f.s.c. have a negative sign and one has a positive sign, which is in agreement with the theoretical predictions. The reason for the large difference between the NMR and the ESR h.f.s.c. is still unknown. It is remarked that, if the NMR h.f.s.c. of -2.3 to -2.7 gauss is counted twice, the sum of the NMR h.f.s.c. equals about half the sum of the ESR h.f.s.c. This might indicate that in concentrated solutions Pht^- forms dimers in which the exchange interaction between electrons on different radicals is not small anymore.

5.1.2. ALKALI METAL H.F.S.C.

For a discussion of the alkali h.f.s.c. the data presented in the figs. 13-38 are used.
The influence of the temperature, the solvent and the radical concentration on the h.f.s.c. is treated in the first paragraph of this section, the second paragraph deals with the sign of the alkali metal h.f.s.c. and in the third and last paragraph a comparison is made between the NMR and the ESR h.f.s.c.

(i). Influence of temperature, solvent and concentration

Influence of the temperature

It was pointed out in sec. 2.1.2 that three models have been proposed

in the literature to describe the influence of the temperature on the metal h.f.s.c. The first model only deals with contact ion pairs in which the metal h.f.s.c. depends on the amplitude of the vibration of the metal ion in the potential energy well of the ion pair. The second and third model describe how the transition from contact into solvent separated or dissociated ion pairs may occur under the influence of a lowering of the temperature. According to the second model ("dynamic model" or "equilibrium model") this transition occurs as a result of a shift in the dynamical equilibrium in which the solvent separated and the contact ion pairs are assumed to participate, while according to the third model ("static model") the transition takes place as a result of a slow and continuous change in the structure of the ion pairs with the temperature. The experimental data are analysed in terms of these models of which the features were described in sec. 2.1.2 in more detail.

Biphenyl. In a discussion of the temperature dependence of the alkali h.f.s.c. the KBp systems are left out of consideration because the relatively large spread in the data of these systems makes it difficult to discern a particular trend in the temperature dependence of the K h.f.s.c. However, in the remaining systems the temperature dependence of the alkali h.f.s.c. is clearly visible. An analysis of the experimental data can be given in the following way.
The plot of the h.f.s.c. for Na Bp THP (fig. 19) and Na Bp MTHF (fig. 20) shows only a small curvature and in both systems the spin density at the nucleus changes sign with a change of the temperature. Therefore it is assumed (see sec. 2.1.2) that in these systems contact ion pairs exist within the temperature range investigated. For RbBp in DME (fig. 27) the metal h.f.s.c. as a function of the temperature is presented by a fairly straight line and the plot does not bend off to zero at low temperatures. Therefore it is assumed that also for this system contact ion pairs exist within the temperature range investigated.
On the other hand in a number of other systems the plot of the h.f.s.c. is approaching zero at low temperatures. It is thought that in these systems solvent separated ion pairs exist at low temperatures and that contact ion pairs are formed at high temperatures. This behaviour is observed for the LiBp solutions, the remaining NaBp and RbBp solutions, and the CsBp solutions (see the figs. 30-32 and 34-36).

Whether the transition of contact into solvent separated ion pairs and vice versa has to be described by the static or by the dynamic model, cannot be decided on the basis of the plots of the alkali h.f.s.c. It will be shown in sec. 5.2.2 that for Cs Bp Dg (fig. 36) the variation of the Cs linewidth with the temperature strongly indicates that for this system the static model applies [22]. Because of the similarity of the plots of the Cs h.f.s.c. for CsBp in Dg, Tg and Ttg (fig. 36) it will be assumed that not only in Dg but also in Tg and Ttg the static model applies for the CsBp ion pairs. Moreover, comparing fig. 35 with fig. 36 the similarity in the shape of the Rb h.f.s.c. plots and the Cs h.f.s.c. plots for the Dg and Tg solutions is striking. It may therefore be assumed that also in the RbBp systems the ion pairs must be described by the static model. In fact not any of the plots in the figs. 30-38 has a shape which is characteristic for the existence of an equilibrium between solvent separated and contact ion pairs viz. a graph consisting of a flat part at low temperatures, corresponding to a value of the metal h.f.s.c. of zero, a second relatively flat part at high temperatures, corresponding to a non-zero value of the metal h.f.s.c., and a third part with a relatively large slope, which connects the two plateaux. The absence of such plots for the cases investigated up till now, leads us to the assertion that for a description of concentrated solutions of radical ion pairs in ether solvents the static model may be more appropriate than the equilibrium model. *Assuming for the present the correctness of this statement the analysis of the alkali h.f.s.c. and the alkali linewidths will henceforth be performed on the basis of the static model.*

Fluorenone. It was pointed out in sec. 5.1.1 that at the concentrations used in the NMR experiments the Fluon salts form dimers. From the small curvatures and the small slopes of the plots of the alkali h.f.s.c. measured for the Fluon salts (fig. 37) it is concluded that the alkali ions form contact ion pairs with the Fluon radicals in the dimers. That the metal h.f.s.c. have relatively large values is considered as an indication that the alkali ions are close to a site in the radical with a high spin density and probably also a high charge density. Judging from the small influence of the temperature on the alkali h.f.s.c. the cations are attracted strongly enough by the radical to prevent complete solvation of the alkali ions at low temperatures.

Naphthalene. From the results presented in fig. 38 it is concluded

that RbNl forms contact ion pairs in DME down to a temperature of $-20°C$ and that at still lower temperatures the formation of solvent separated ion pairs starts.

Influence of the solvent

The influence of the solvent on the metal h.f.s.c. may become apparent by comparing the metal h.f.s.c. measured for a particular alkali Bp salt in different solvents. It was pointed out in sec. 2.1.2 that in general this influence is related to the solvating power of the solvent. According to the references cited in sec. 2.1.2 the solvating power of the solvents used in the experiments increases in the order THP, MTHF, THF, DME, Dg, Tg and Ttg. It should therefore be expected that for a given alkali radical salt the tendency to form solvent separated ion pairs in these ethers would increase if the solvent is changed from THP to Ttg in the above-given order. From the data presented in the figs. 30-36 it appears that in general this expectation is borne out by the experiments. Closer inspection of each individual system will confirm this more clearly.

LiBp. Looking at the Li h.f.s.c. in fig. 31 at for instance $+20$ or $+30°C$, one observes, going from THP to Tg, a decrease in the Li h.f.s.c., which can be accounted for by a progressive solvation of the Li ions. That there is nearly no difference between the Li h.f.s.c. in Dg and Tg is probably because in both solvents the LiBp ion pairs are likely to form completely solvent separated ion pairs, so that the h.f.s.c. should be equal to zero in both solvents. That in fact a very small non-zero Li h.f.s.c. is measured in these solvents is probably due to the neglect of the term $H_0\sigma_0 - H_p\sigma_p$ in eq. (20) in the determination of the contact shift (see sec. 3.4).

NaBp. For the NaBp solutions the behaviour of the metal h.f.s.c. is more complicated as appears from fig. 32, but also here a trend is observable in the behaviour of the Na h.f.s.c. as a function of the solvent: only contact ion pairs exist in the poor solvating agents THP and MTHF, in THF the formation of solvent separated ion pairs starts at temperatures below $-10°C$ and in DME and Dg this process begins already at temperatures between $+20$ and $+40°C$. (The singularity in the plot of the Na h.f.s.c. in the system Na Bp Dg corresponds with partial precipitation of the NaBp salt and will be discussed later on.) Finally the Na h.f.s.c. in Tg and Ttg shows an anomalous behaviour: judging from the shape of the Na h.f.s.c.

plots, solvent separated ion pairs are formed in these solvents at low temperatures, but instead of levelling off to zero the h.f.s.c. becomes negative at low temperatures. It is thought that these anomalies are caused by ring currents in the aromatic ion and by chelation of the Na ions by solvent molecules. Regarding the magnitude of the effect this explanation is consistent with the results of the Na NMR experiments performed on solutions of $NaBH_4$ and $NaB\Phi_4$, which were reported and discussed in sec. 3.4. That the effect is particularly large in the system Na Bp Tg corresponds with the observation that NaBp forms easily large single crystals with Tg. Apparently Tg molecules have a stereometric favourable conformation to form stable complexes with NaBp ion pairs.

KBp. For the KBp solutions (fig. 33) it appears that at a given temperature the K h.f.s.c. approaches zero if the solvent is changed from DME to Tg. This can be explained again by an increase of the solvation of the K ions. Extrapolating these results one would expect that in Ttg the K h.f.s.c. would be practically zero which is in contrast with the experimental findings. This anomaly is similar to the anomalies observed for the Na h.f.s.c. in the NaBp solutions in Tg and Ttg and it may be assumed that also in this case it is caused by the chelation of the metal ions by the solvent and possibly also by the influence of aromatic ring currents on the resonance position of the metal nuclei. Also in this case the anomaly corresponds with the observation that KBp forms easily single crystals with Ttg.

RbBp & CsBp. Finally for the RbBp and the CsBp solutions (figs. 34, 35 and 36) the influence of the solvent on the metal h.f.s.c. can be explained again by taking into account the solvating properties of the solvents: no solvent separated ion pairs are formed by RbBp in DME, which is a relatively poor solvating agent for Rb ions, but in Dg and Tg the solvation of the Rb ions becomes apparent from the curvature in the plot of the Rb h.f.s.c. versus the temperature. Moreover, at a given temperature the Rb h.f.s.c. in Tg is always closer to zero than in Dg which is again an indication of the better solvating properties of Tg compared with Dg. A similar sequence is observed for the Cs h.f.s.c. measured on CsBp solutions in Dg, Tg and Ttg, which can be explained in the same way.

The influence of the solvent on the alkali h.f.s.c. becomes apparent also in another way as follows. One expects that in a given solvent the alkali Bp salts form more easily solvent separated ion pairs as the

radius of the cation decreases. This expectation is in accordance with the experimental findings. For example, it appears that LiBp and NaBp form solvent separated ion pairs in DME at low temperatures whereas RbBp forms only contact ion pairs in this solvent.

Finally we like to point out another feature of the plots in the figs. 30-36. From fig. 36 it appears that at high temperatures the Cs h.f.s.c., measured in different solvents, tend to converge to the same values. A similar behaviour is observed for the Rb h.f.s.c. in fig. 34 and 35. (This will come out even more pronounced if the plot of the Rb h.f.s.c. in DME is extrapolated along a straight line to higher temperatures. Decomposition prevented the measurement of the Rb h.f.s.c. in DME at high temperatures.) Apparently the structure of the RbBp and the CsBp ion pairs is at high temperatures not very much dependent anymore upon the nature of the solvent. A similar behaviour is observed for the Na h.f.s.c. measured in the NaBp solutions in THP up to and including DME. At high temperatures the plots of the h.f.s.c. more or less converge to the same values. However, for a second group of solvents, consisting of Dg, Tg and Ttg the Na h.f.s.c. do not seem to converge to the same plot. A similar phenomenon is found for the LiBp solutions. Here the first group of solvents comprises only THP and MTHF and the second group consists of the solvents THF up to and including Tg. It may therefore be concluded that the larger the cation the less important are the differences in the solvating power of the solvents with respect to the structure of the ion pairs at high temperatures.

Influence of the concentration

The influence of the concentration on the alkali h.f.s.c. can be inferred from the results obtained on the systems Na Bp DME (fig. 22) and Na Bp THF (fig. 21). In the former system the h.f.s.c. appeared to be independent of the radical concentration. In the latter system the influence of the concentration on the Na h.f.s.c. is clearly visible as appears from fig. 21. It was argued in sec. 2.1.2, that in concentrated solutions a change in the radical concentration will often cause a non-negligeable change in the concentration of the solvent, which in turn may result in the formation of more solvent separated-like or more contact-like ion pairs. It is possible that this effect is responsible for the change in the Na h.f.s.c. with the concentration observed for

Na Bp THF. On the other hand, the presence of ion pair clusters, of which the concentration may vary upon dilution, may have played also a role. However, a detailed explanation cannot yet be offered.
Finally we remark that the singularity in the plot of the Na h.f.s.c. in the system Na Bp Dg (fig. 23) at $-10°C$ is probably caused by a change in the ion pair concentration brought about by the partial precipitation of the salt at a temperature between -10 and $-20°C$. Also in this case cluster formation may have influenced the alkali metal h.f.s.c.

(ii). Sign of the alkali h.f.s.c.

Regarding the sign of the metal h.f.s.c. the results of the measurements on Bp and Fluon can be summarized as follows.
Biphenyl. In LiBp the Li h.f.s.c. is positive in all solvents.
In NaBp the metal h.f.s.c. may be positive as well as negative depending upon solvent and temperature. A sign reversal, occurring at a change in the temperature, was observed for Na Bp MTHF (fig. 20). It is not certain whether the sign reversal observed for Na Bp THF (fig. 21) is real. The effect is not pronounced enough to rule out completely the possibility that it is caused by ring currents in the aromatic ion or shielding of the Na nucleus by solvent molecules in the solvent shell of the metal ion. The sign reversal of the metal h.f.s.c. in Na Bp Tg and Na Bp Ttg (figs. 24 and 25) was discussed in the foregoing paragraph and probably does not correspond with a real sign reversal of the spin density at the metal nucleus.
Finally in the K, Rb and CsBp salts the metal h.f.s.c. shows a negative sign.
Fluorenone. In the Li, Na, K, Rb and Cs salts of Fluon the metal h.f.s.c. has a positive sign.

From these data it can be concluded in the first place that for each alkali nucleus the sign of the h.f.s.c. may be positive as well as negative, except for Li, for which up until now only positive h.f.s.c. were measured by NMR. In the second place it is concluded that a sign reversal of the metal h.f.s.c. at a change of the temperature can take place. This has been ascertained for at least one system viz. Na Bp MTHF (fig. 20). These two conclusions show that for a number of cases the hypothesis of DE BOER about the sign of the

spin density at alkali nuclei in radical ion pairs, which was mentioned in sec. 2.1.2, is correct.
A third conclusion which can be drawn from the experimental data is that an increase of the radius of the alkali ion seems to be correlated with a tendency of the metal h.f.s.c. to become negative. This is in agreement with observations of HIROTA [84] and DODSON and REDDOCH [85], which show that there is a correlation between the ionic radius and the magnitude of the alkali h.f.s.c. Apparently the distance between radical and counterion determines in part sign and magnitude of the alkali h.f.s.c. The same conclusion may be drawn from the observation that in Na Bp MTHF the Na h.f.s.c. becomes negative at low temperatures, which may be connected with an increase in the distance between radical and counterion, caused by a slight increase of the solvation of the Na ions at lower temperatures.

It was argued in sec. 2.1.2, by using an M.O. description for an alkali radical ion pair, that in a zero order approximation the spin density at the metal nucleus would be always non-negative and that it would be determined mainly by the admixture of *s*-orbitals φ_s of the alkali metal into the first antibonding M.O. Φ^0_{k+1} of the free aromatic molecule. When the admixture of φ_s is small the first order correction to the spin density might become important. The magnitude of this correction could be found by calculating the effect on the spin density resulting from the admixture of singly excited configurations in the zero order ground state wavefunction.
It was shown that, if configurations which represent excitations in the *metallic* part of the wavefunction would play a major role in producing spin densities at the metal nuclei, one would expect to find negative h.f.s.c. for Li and positive h.f.s.c. for Rb. The experimental results discussed above are clearly not in accordance with these expectations. Therefore it was argued in sec. 2.1.2 that other excitations, of which probably the „cross excitations" are the most important, must be responsible for the occurrence of negative alkali h.f.s.c. Moreover it was shown in sec. 2.1.2 that, while the magnitude of the zero-order contribution to the spin density at the metal nucleus would depend on the admixture of *s*-A.O.'s of the metal in the first *anti-bonding* M.O. Φ_{k+1} of the aromatic compound, the effect of the cross excitations on the spin density at the metal would be determined by the admixture of *s*-A.O.'s in the *bonding* M.O.'s of the aromatic molecule. This can be elaborated in more detail as follows.

The admixture of an s-A.O. φ_s into the *anti-bonding* M.O. Φ^0_{k+1} will depend on the overlap of these two orbitals. If the distance between the alkali ion and the aromatic molecule is large and if the dimension of φ_s is large compared with the dimensions of the aromatic molecule, the overlap will be determined by the overlap of φ_s with all the constituent $2p_z$-A.O.'s of the M.O. Φ^0_{k+1}. Usually the first antibonding π-M.O. of an aromatic molecule is characterized by the presence of a number of nodes in the wavefunction. Therefore, the overlap of φ_s with the different $2p_z$-A.O.'s of Φ^0_{k+1} will cancel partly and thus the admixture of φ_s with Φ^0_{k+1} will be small irrespective whether the alkali ion is in a nodal plane of Φ^0_{k+1} or not. On the other hand, if the distance between alkali ion and aromatic ion is small and if the dimension of φ_s is small compared with the dimensions of the aromatic molecule, the overlap between φ_s and Φ^0_{k+1} will depend on the overlap between φ_s and the $2p_z$-A.O. of the carbon atom in the aromatic molecule, which is closest to the alkali ion. This means that the overlap between φ_s and Φ^0_{k+1} may be large, irrespective of the number of nodes in Φ^0_{k+1}, unless the alkali ion resides very close to a nodal plane of Φ^0_{k+1}. To estimate the admixture of φ_s in the *bonding* M.O.'s of the aromatic molecule this reasoning cannot be followed because these M.O.'s usually have a higher symmetry than the first antibonding M.O. In general the bonding M.O.'s will have less nodal planes than the anti-bonding M.O.'s. Therefore, the admixture of metal s-orbitals into the bonding M.O.'s of the aromatic molecule will be less sensitive to variations in the interionic distance and the dimensions of the s-orbitals than the admixture of these orbitals into the first anti-bonding M.O. of the aromatic molecule.

We conclude that, as the distance between the alkali ion and the aromatic ion increases or as the dimensions of the orbitals φ_s increase, the admixture of s-orbitals of the metal in the bonding M.O.'s will become relatively more important compared with the admixture of these metal A.O.'s in the first antibonding M.O. of the aromatic molecule. This means that an increase in the interionic distance or, more in general, an increase in the atomic number of the alkali metal will cause the first order (possibly negative) contribution to the spin density to become more important compared with the zero order spin density at the metal nucleus, which may explain why the metal h.f.s.c. shows a tendency to become negative with an increase in the interionic distance or an increase in the atomic number of the alkali metal.

(iii). Comparison with ESR h.f.s.c.

A comparison between the NMR and the ESR h.f.s.c. of the alkali metals can be performed on the basis of the results obtained on the systems Na Bp THP, Na Bp MTHF, Na Bp THF (figs. 19-21), Rb Nl DME (fig. 38) and the systems of the alkali Fluon salts in THF (figs. 37 and 1; see also ref. [15]).
For the Fluon salts the difference between the NMR and the ESR h.f.s.c. is large. This is probably connected with the fact that in the ESR experiments monomers of the Fluon salts have been studied whereas in the NMR experiments dimers. This was already discussed in sec. 5.1.1 and in the first paragraph of this section. If the alkali ions occupy different positions with respect to the radical in respectively the monomer and the dimer, this may result in different spin densities at the metal nuclei.
In the other systems the variation with the temperature is not very different for the NMR and the ESR h.f.s.c. Furthermore, at a given temperature the difference between the ESR and the NMR h.f.s.c. is much smaller than for the Fluon systems. These small differences probably result from the neglect of the term $H_0\sigma_0 - H_p\sigma_p$ in eq. (20), from which the contact shift was calculated. This was discussed in sec. 3.4. Ring currents in the aromatic ion, shielding of the alkali nucleus by solvent molecules in the solvent shell of the alkali ion and clustering of the radical ion pairs may have contributed to the difference in shielding constants of the nucleus in the reference and in the sample solution.

5.2. LINEWIDTHS

An analysis of the proton and the alkali linewidths will be given in respectively sec. 5.2.1 and sec. 5.2.2 on the basis of the theory presented in sec. 2.2.
For the purpose of such an analysis a theoretical calculation or a theoretical estimate of the interaction parameters of the aromatic protons as well as of the alkali nuclei will be made. For the case of the aromatic protons these values will be used to calculate values of the correlation times from the experimental linewidth data. For the case of the alkali nuclei the theoretical values will be used for a comparison with the experimental values, which will be derived

from the alkali linewidth data on the basis of the correlation times calculated from the proton linewidths.
Finally also the influence of the temperature, the solvent and the concentration on the alkali linewidths will be discussed.

5.2.1. PROTON LINEWIDTHS

(i). Introduction

It was pointed out in sec. 2.2.1 that the proton linewidths are determined by the Fermi contact and the anisotropic dipolar interaction. The former interaction is characterized by the experimentally determinable parameter A, given by the eqs. (5) and (6). The contribution from this interaction to the linewidth is given by eq. (31a). The latter interaction is characterized by the anisotropic dipolar tensor $\mathbf{T}$, defined according to the eqs. (8)-(10), and the parameter B, defined according to eq. (32a). Its contribution to the linewidth is given by eq. (31b).
In the following a detailed analysis of the linewidths of the aromatic protons of Bp^- is given together with a semi-quantitative analysis of the proton linewidths measured for the Fluon and the Pht radical ions. For that purpose in the second paragraph of this section the parameters A and B of the protons in the Bp radical ion will be calculated. In the third paragraph a discussion of the calculated values will be given in connection with the experimental data and in the fourth and last paragraph the theory will be applied for a calculation of the correlation times on the basis of the experimentally determined proton linewidths (sec. 4.2.1, tables 7-9).

(ii). Numerical analysis: calculation of the parameters A and B for the protons of Bp^-

The parameters A of the three inequivalent protons of Bp^- were calculated from eq. (6) by using the experimentally determined values of the NMR h.f.s.c. presented in table 7.
To calculate the parameters B the tensors $\mathbf{T}$ had to be calculated. This was done according to the procedure described in sec. 2.2.1. For the calculation it was assumed that the Bp^- radical is planar.

Furthermore the lengths of the *C-H* bonds in the Bp negative ion were set equal to 1.08 Å, the two aromatic rings were assumed to be regular hexagons with sides of 1.39 Å and the length of the *C-C* bond connecting the two rings was set equal to 1.51 Å [86]. For each proton the tensor **T** was calculated by applying eq. (40). The tensors $\mathbf{T}_{ii}$, occurring in this equation, were calculated according to the formulae of DERBYSHIRE with one exception: the principal values of a tensor $\mathbf{T}_{ii}$ for which the index i denoted the carbon atom adjacent to the proton under consideration, were set equal to the experimentally determined values of the anisotropic dipolar tensor of the proton in a *C-H* radical fragment, which amount to 31.3, —3 1.2 and —0.2 Mc [26]. Apart from ϱ_1 and $\varrho_{1'}$, the spin densities ϱ_i on the carbon atoms in the Bp radical ion, which occur in eq. (40), were calculated from the proton h.f.s.c. of table 7 by using eq. (24), substituting for Q a value of —25. ϱ_1 and $\varrho_{1'}$, were obtained from a McLachlan M.O. calculation. (The numbering of the *C* atoms in the Bp molecule has been indicated at table 4). The values obtained for ϱ_1, ϱ_2, ϱ_3 and ϱ_4 are respectively 0.127, 0.104, —0.0156 and 0.204. The other spin densities can be derived from these values by symmetry arguments. For the complete calculation a computer program DIPDIP was written by which the tensor **T** of a nucleus at a given arbitrary position with respect to a planar π-radical could be calculated. For this program the more general formulae of DERBYSHIRE were used instead of the formulae of MCCONNELL and STATHDEE (see sec. 2.2.1). After the calculation of the tensors **T** of the ortho, meta and para protons of the Bp^- radical, the parameters B were calculated according to eq. (32a). Values of a, A^2 and B^2 are presented in table 10.

	a, gauss	$(A.h^{-1})^2$, Mc^2/s^2	$(B.h^{-1})^2$, Mc^2/s^2	$(B_0.h^{-1})^2$, Mc^2/s^2
ortho	+2.6	53	4.8	3.5
meta	—0.39	1.20	1.77	0.08
para	+5.1	204	17.3	13.6

Table 10. Interaction parameters and h.f.s.c. of the protons in the Bp negative ion.

In addition a calculation of the latter parameter was performed in which only the spin density on the carbon atom adjacent to the

proton under consideration was taken into account in the calculation of $\mathbf{T}$. For that case eq. (40) becomes

$$\mathbf{T} = \varrho_{adj}\, \mathbf{T}_{adj\ adj} \tag{61}$$

in which the index *adj* denotes the carbon atom adjacent to the proton under consideration, and in which the principal values of $\mathbf{T}_{adj\ adj}$ are given by the above-mentioned principal values of the proton tensor in a *C-H* radical. The value of the anisotropic dipolar interaction parameter calculated in this way is denoted by B_0. Values of B_0^2 are presented in table 10.

(iii). Numerical analysis: discussion

By combining the eqs. (6) and (24), using a numerical value of -25 for the parameter Q in eq. (24) and expressing A, h and γ_e in cgs units, the following numerical relationship between A/h and ϱ_{adj} can be established

$$\left(\frac{A}{h}\right)^2 = 4.91 \times 10^3\, \varrho_{adj}^2\ ,\ Mc^2/s^2 \tag{62}$$

In a similar way a numerical relationship between B_0 and ϱ_{adj} can be established by combining the eqs. (32a) and (61) and using for the principal values of $\mathbf{T}_{adj\ adj}$ the numerical data indicated in the foregoing paragraph. In this way one finds

$$\left(\frac{B_0}{h}\right)^2 = 3.25 \times 10^2\, \varrho^2_{adj}\ ,\ Mc^2/s^2 \tag{63}$$

From the eqs. (62) and (63) it follows that for a given proton

$$\left(\frac{A}{h}\right)^2 \gg \left(\frac{B_0}{h}\right)^2 \tag{64}$$

The values of A and B_0 quoted in table 10, are in accordance with this inequality.

Looking at the parameters A and B one can distinguish three cases:

1 $A^2 \gg B^2$
This situation will occur mainly when $|\varrho_{adj}|$ is large, so that the contributions to B from spin densities other than ϱ_{adj} are small. In that case B will be approximately equal to B_0 and from eq. (64) then the above-given inequality follows. Moreover it follows from eq. (63) that, if $B \cong B_0$, not only A^2 but also B^2 will in a good approximation be proportional to ϱ^2_{adj}.
For Bp^- the para and the ortho protons fall in this category, as appears from the data in table 10.

2 $A^2 \cong B^2$
If this situation is encountered, it follows from eq. (64) that $B^2 \gg B_0{}^2$, so that B^2 is no longer proportional to ϱ^2_{adj}.
From the data of table 10 it appears that the meta protons of Bp^- are in this category.

3 $A^2 \ll B^2$
This case will be encountered mainly for protons with a very small absolute value of the h.f.s.c. It is estimated that this case occurs when $|a| < 0.1$ gauss. However, the geometrical structure of the radical and the spin distribution of the unpaired electron over the radical also determine to a certain extent whether the sub 3 given inequality is fulfilled or not.

To predict the relative magnitude of the linewidth contributions $(T_2^{-1})_{Fc}$ and $(T_2^{-1})_D$ not only the interaction parameters A and B, but also the respective correlation times τ_e and τ_d must be taken into consideration according to the eqs. (31a) and (31b).
Regarding the magnitudes of τ_e and τ_d it follows from eq. (29) that τ_e will always be larger than τ_d. However, as will appear later on, in concentrated radical solutions τ_e and τ_d have the same order of magnitude, so that for that case

$$\tau_e \geqslant \tau_d \tag{65}$$

On the other hand, for diluted solutions τ_e will become large and

τ_d will become equal to the rotational correlation time. Therefore, for diluted solutions the following inequality holds

$$\tau_e \gg \tau_d \tag{66}$$

Distinguishing in the following discussion between diluted and concentrated solutions the three cases dealt with in the comparison of the interaction parameters can be considered on the basis of the eqs. (31a) and (31b):

1 $A^2 \gg B^2$

It is clear that in this case, because of the inequalities (65) and (66), always the inequality $(T_2^{-1})_{Fc} \gg (T_2^{-1})_D$ holds, irrespective whether one deals with a concentrated or a diluted solution. Moreover, both linewidth contributions will be proportional to ϱ^2_{adj} or to a^2, which is the same. Therefore the total linewidth of a proton of this category will be proportional to a^2.

This comes out nicely in table 7 for the protons 2,2', 6,6' and 4,4' of Bp^-, in table 8 for the protons 1,8 & 3,6 and 4,5 of $Fluon^-$ and in table 9 for the protons of Pht^- mentioned in the last two columns of table 9. The ratios of the linewidths and of the squares of the h.f.s.c. are presented in these tables in parentheses behind the quoted values of the linewidths and the h.f.s.c.

It is remarked that in diluted solutions τ_e may become so large that the signals of the protons in this category become too broad to be observable.

2 $A^2 \cong B^2$

In this case $(T_2^{-1})_{Fc}$ will be approximately equal to $(T_2^{-1})_D$ if one deals with concentrated solutions. On the other hand, in diluted solutions the inequality $(T_2^{-1})_{Fc} \gg (T_2^{-1})_D$ will be valid.

It was pointed out that if $A^2 \cong B^2$, B^2 is no longer proportional to ϱ^2_{adj} or a^2. This means that also $(T_2^{-1})_D$ is no longer proportional to a^2. Therefore, in concentrated solutions, in which $(T_2^{-1})_D$ constitutes a considerable part of the total linewidth, the total linewidth will no longer be proportional to a^2. In fact the linewidth will appear to be larger than would be expected on the basis of a proportionality with a^2.

These expectations are borne out nicely by the results gathered in the tables 7-9. The linewidths of the protons 3,3', 5,5' of Bp^-, the protons 2,7 of $Fluon^-$ and the protons of Pht^- mentioned in column 3 of table 9 are all larger than would be expected on the basis of a proportionality with a^2.

3 $A^2 \ll B^2$

In this case the inequality $(T_2^{-1})_{Fc} \ll (T_2^{-1})_D$ is valid if one deals with a concentrated solution. In that case the total linewidth will be much larger than would be expected on the basis of a proportionality with a^2.

This is again in agreement with the experiment, as appears from the data in column 2 of table 9 for Pht^-. It is pointed out that for protons in this category the contributions from intermolecular relaxation processes to the total linewidth may become appreciable.

For diluted solutions the relative magnitudes of $(T_2^{-1})_{Fc}$ and $(T_2^{-1})_D$ will depend on the particular case under consideration, so for diluted solutions this category cannot be treated in a general way like the foregoing categories.

(iv). Calculation of correlation times

The theory of the two foregoing paragraphs can be used for the calculation of the correlation times τ_e and τ_d from the experimental proton linewidths. In the following discussion only the case of a concentrated radical solution is considered.

If the parameters A and B have been calculated for a given proton, two parameters remain unknown in the expression (33) for the total linewidth viz. the correlation times τ_e and τ_d. Two methods to calculate τ_e and τ_d can be applied. The first method is to reduce the number of parameters by one by neglecting $(T_2^{-1})_D$ in eq. (33). In this way it is always possible to find an upper limit for τ_e. If one is dealing with a proton of the category 1, which means a proton with a large h.f.s.c., the calculated upper limit will in fact be a good approximation of τ_e, because for such a proton the total linewidth is approxi-

mately equal to $(T_2^{-1})_{Fc}$. Even if one deals with a proton of the second category the calculated value of τ_e will be too large by at most a factor of two.

The second method consists of measuring the linewidths of two inequivalent protons, writing down for each proton the complete expression (33) and solving the two in this way obtained equations for τ_e and τ_d. The linewidth of protons of the third category will in most cases not be useful for this purpose, because it will be difficult to determine an accurate value for the linewidths in view of the large corrections which have to be applied for broadening by intermolecular interactions. Also the linewidths of two protons of the first category cannot be used, because these linewidths are proportional to the squares of the respective h.f.s.c. and so the two equations for the linewidths become mutually dependent. Therefore the combination of the linewidth of a proton of the first category and the linewidth of a proton of the second category should be used for this method.

	$\tau_e \times 10^{11}$, s	$\tau_d \times 10^{11}$, s
Li Bp Dg	6	2
Na Bp DME	2	1
Na Bp Dg	2	2
Li Fluon THF	9	
Na Fluon THF	6	
Na Pht THF	8	

Table 11. Correlation times in solutions of different radical salts at room temperature. The radical concentrations, as calculated from the solvent shifts at the end of the reduction, varied from approximately 0.4 to 0.9 M.

The first method has been applied for the calculation of τ_e in the Fluon$^-$ and Pht$^-$ radical solutions by using the data quoted in the starred columns of the tables 8 and 9.

The second method has been applied for the calculation of τ_e and τ_d in the Bp$^-$ radical solutions by using the linewidth data of the ortho and meta protons mentioned in table 7 and the interaction parameters mentioned in table 10.

The results are presented in table 11. The accuracy of the calculated correlation times is estimated to amount to $\pm$ 25%.

From table 11 it appears that the values of τ_e and τ_d lie in the range of 2×10^{-10} to 2×10^{-11} s. The values which can be calculated for the rotational correlation time by substituting the values of τ_e and τ_d in eq. (29) are not very accurate because of the inaccuracies in τ_e and τ_d; they appear to have the same order of magnitude as τ_e and τ_d. It is not clear whether the observed influence of the cation on the magnitude of τ_e in the Bp^- and the $Fluon^-$ radical solutions is real or accidental.

5.2.2. ALKALI METAL LINEWIDTHS

(i). Introduction

It was pointed out in sec. 2.2.2 that the alkali linewidths are determined by the Fermi contact, the anisotropic dipolar and the quadrupolar interaction. These interactions are characterized respectively by the parameters A, B and W, which are defined respectively by the eqs. (5), (32a) and (32c), while the linewidth contributions from these interactions are given respectively by the eqs. (31a), (31b) and (31c).
A numerical analysis of the linewidth data will be performed in the next three paragraphs of this section. For that purpose theoretical calculations on the anisotropic dipolar and the quadrupolar interaction parameters B and W will be performed in the second paragraph of this section. In the third paragraph experimental values for the parameters A, B and W together with experimental values for the correlation time τ_e will be derived from the measured alkali h.f.s.c. and alkali linewidths. In the fourth paragraph these data will be discussed on the basis of a comparison with the theoretical values. In the fifth and last paragraph of this section the influence of the temperature, the solvent and the radical concentration on the alkali linewidths will be analysed.
It was pointed out in sec. 5.1.2, in the discussion of the temperature dependence of the alkali h.f.s.c., that the static model of the ion pair gave the best fit with the experimental data. Therefore, the analysis of the linewidth data will be performed on the basis of this model.

This will mean that for a given alkali radical ion pair at a given temperature the parameters A, B and W each have an unambiguously defined value.

(ii). Numerical analysis: theoretical values for B and W

In sec. 2.2.2 we pointed out that for the interpretation of the experimental data the parameters B and W are not very useful from a theoretical point of view, as long as the structure of the ion pairs is not known. Therefore we introduced the parameters B_{Ar}, B_{Me}, W_{out} and W_{Me}. Here we will outline in which way reasonable numerical values can be obtained for them.

Calculation of B_{Ar} and B_{Me}

According to eq. (43a) we need for a calculation of B_{Ar} the tensor $\mathbf{T}_{Ar}$ (see eq. (42a)). $\mathbf{T}_{Ar}$ can be calculated by the same computer program DIPDIP by which the tensors $\mathbf{T}$ for the aromatic protons of Bp^- were calculated. A detailed calculation was performed for the case of an alkail Bp ion pair. The alkali nucleus was placed successively at a great number of intersection points of a regular network, drawn parallel to and at a distance d from the plane of the Bp molecule. After calculating the value of B_{Ar} in each point, contour curves could be drawn connecting points of equal B_{Ar}. In this way a clear picture was obtained of the variation in B_{Ar} as the nucleus moves in a plane parallel to the Bp ion. The procedure was repeated for several values of d.

From the calculations it appeared that there is no unequivocal correspondence between d and B_{Ar}: for a given value of d, B_{Ar} may pass through a whole series of values as the alkali ion moves parallel to the plane of the Bp molecule. In order to establish nevertheless a rough correspondence between B_{Ar} and d, the following procedure was used. For a given value of d the values of B_{Ar} were averadged over the area of a circle with a radius of 1Å, drawn in a plane parallel to and at a distance d from the plane of the Bp ion, the circle having its center right above the center of one of the aromatic rings of the Bp molecule. The averadge values of B_{Ar} calculated in this way for a given value of d, are presented in table 12 as a function of the parameter $\varkappa$ and are denoted by $\overline{B}_{Ar}$. $\varkappa$ is defined by $\varkappa + r^+ \equiv d$, in which r^+ is the ionic radius of the alkali metal.

According to the definition of eq. (43b) values of ϱ_{np} and $B(np)$ are needed for the calculation of B_{Me}. Values of $B(np) \cdot h^{-1}$ for different alkali metals have been gathered from the literature. They are presented in table 12. No literature data were available from which $B(np) \cdot h^{-1}$ could be calculated for ^{133}Cs. The estimated value amounts to 40 Mc/s.

An estimate of ϱ_{np} is based on the following reasoning. It was argued in sec. 5.1.2 that the alkali metal h.f.s.c. would be determined by the spin densities present in the *s*-orbitals of the metal. Of these the spin density in the valence *ns*-orbital will probably be the most important. Therefore, dividing the experimentally found Fermi contact parameters A by the respective Fermi contact interaction constants $A(ns)$ measured for the free atoms in the n^2S ground state (see table 1), one gets an estimate of the spin density in the *ns*-orbital of the metal in the ion pair. This amount of spin density has been calculated in this way for a large number of radical ion pairs on the basis of literature data for the alkali h.f.s.c. It appears that the absolute value of this spin density is nearly always smaller than 0.01. Generalizing this result it will be assumed that the absolute value of the spin density present in the valence *s*- and *p*-orbitals of the alkali ions in alkali-radical ion pairs is less than 0.01. The quoted values for $B_{Ar} \cdot h^{-1}$ in table 12 are based on a value of 0.01for $|\varrho_{np}|$ and are therefore upper limits. For comparison also the values of the parameter $0.01 \times A(ns) \cdot h^{-1}$ for the different alkali metals are given in this table.

Calculation of W_{out} and W_{Me}

According to the definition of eq. (44a) one needs for the calculation of W_{out} values for γ_∞, eQ and eq_{out}. Values of γ_∞, for which theoretical estimates are available, and values of eQ were taken from the literature. The data are presented in table 13. It was pointed out in the third paragraph of sec. 2.2.2 that the calculation of eq_{out} is impossible as long as detailed information about structure and wavefunction of the ion pair is lacking. Therefore, for the present case such a calculation must be omitted. This means that a calculation of W_{out} cannot be performed. However, the values of γ_∞ and eQ quoted in table 13 allow a mutual comparison of the values of W_{out} for the various alkali ions in the following way. It appears from literature data that the quadrupolar interaction constants of ^{7}Li, ^{23}Na and ^{39}K in different

	$\gamma_N/2\pi$, Hz/gauss	r^+, Å	$B(np).h^{-1}$, Mc/s	$0.01 \times A(ns).h^{-1}$, Mc/s	$\bar{B}_{Ar}.h^{-1}$, Mc/s [3] $x =$ 0.5 Å	1.0 Å	1.5 Å	2.0 Å	2.5 Å	3.0 Å	$B_{Me}.h^{-1}$, [2] Mc/s
^{6}Li	626.5	0.60	2.0	1.52	0.92	0.53	0.33	0.22	0.15	0.11	0.02
^{7}Li	1654.6	0.60	5.3	4.02	2.43	1.39	0.86	0.58	0.40	0.30	0.05
^{23}Na	1126.2	0.95	14.1	8.86	1.09	0.68	0.44	0.30	0.22	0.17	0.14
^{39}K	198.7	1.33	4.3	2.31	0.13	0.09	0.06	0.04	0.03	0.03	0.04
^{85}Rb	411.1	1.48	18.2	10.1	0.23	0.16	0.11	0.09	0.06	0.05	0.18
^{87}Rb	1393.1	1.48	61.7	34.2	0.79	0.53	0.36	0.26	0.20	0.17	0.62
^{133}Cs	558.5	1.69	40 [1]	22.9	0.27	0.18	0.13	0.09	0.08	0.06	0.4 [1]

[1]) Estimated value.
[2]) The quoted values are assumed upper limits.
[3]) The quoted values were calculated for the special case of an alkali Bp ion pair.

Values of $\gamma_N/2\pi$ were taken from the Varian isotope table 1967.
Values of r^+ were taken from ref. [87].
Values of $B(np)$ were derived from the following references:
Li [33]; Na [34]; K [35]; Rb [36, 37].
Values of $A(ns)$ were taken from table 1.

Table 12. Value of the parameters needed for the calculation of the magnetic dipolar interaction constants of the alkali nuclei.

ionic compounds usually fall in the range of respectively 0.01-0.1 Mc/s, 0.5-2.0 Mc/s and 1.0-2.0 Mc/s [28]. Substituting these values, multiplied by the constant of Planck, in eq. (44a) for W_{out} one obtains a rough estimate of the range in which the field gradient $|eq_{out}|$ in alkali radical ion pairs may fall. In this way one calculates for eq_{out} values of respectively $(0.4\text{-}4.1) \times 10^7$, $(1.0\text{-}4.1) \times 10^7$ and $(0.8\text{-}1.7) \times 10^7$ esu/cm^3. Taking the mean value of the upper limits and the mean value of the lower limits of these ranges one finds an averadge range of $(0.8\text{-}3.3) \times 10^7$ esu/cm^3 for $|eq_{out}|$. Substituting these values of $|eq_{out}|$ in eq. (44a) and using the values of eQ and γ_∞ quoted in table 13 for ^{85}Rb, ^{87}Rb and ^{133}Cs, one expects for these metals $W_{out}.h^{-1}$ to fall in the range of respectively 8-34, 4-16 and 0.2-0.8 Mc/s. These estimated values are given in table 13 together with the above-quoted values for ^{7}Li, ^{23}Na and ^{39}K.

	I	$f(I)$	$eQ \times 10^{24}$, e, cm^2	γ_∞	$W(np).h^{-1}$, Mc/s	$W_{out}.h^{-1}$, [1] Mc/s		$W_{Me}.h^{-1}$, [2] Mc/s
^{6}Li	1	5.0	—0.0008	+ 0.26	0.006	2×10^{-4}	-2×10^{-5}	6×10^{-5}
^{7}Li	3/2	1.33	—0.045	+ 0.26	0.36	0.01	-0.1	0.004
^{23}Na	3/2	1.33	+0.12	— 4.56	5.7	0.5	-2	0.057
^{39}K	3/2	1.33	+0.09	— 17.3	5.6	1.0	-2	0.056
^{85}Rb	5/2	0.32	+0.29	— 47.2	52.0	8	-34	0.52
^{87}Rb	3/2	1.33	+0.14	— 47.2	25.2	4	-16	0.25
^{133}Cs	7/2	0.14	—0.003	—103	0.92	0.2	-0.8	0.009

[1]) Estimated values; see text.
[2]) The quoted values are assumed upper limits.

Values of eQ were taken from the following references:
Li [88]; Na [34]; K [35, 89]; Rb [36, 37, 90]; Cs [91, 92]. They were calculated from the experimental data with neglect of the Sternheimer correction factor (1—R).
Values of γ_∞ were taken from ref. [65].
Values of $W(np)$ were derived from the following references:
Li [33]; Na [34]; K [35]; Rb [37]; Cs [91].

Table 13. Values of the parameters needed for the calculation of the quadrupolar interaction constants of the alkali nuclei.

According to the definition of W_{Me} (see eq. (44b)) one needs for the calculation of W_{Me} values for the parameters ϱ_{np} and $W(np)$. Values of $W(np)$ can be calculated from the positions of the spectral terms of the free alkali atoms in the n^2P state. Literature values of $W(np).h^{-1}$ are given in table 13. Just as in the calculation of B_{Me}

for $|\varrho_{np}|$ a value of 0.01 is adopted in order to find an upper limit for W_{Me}. Values of $W_{Me}.\hbar^{-1}$, calculated from eq. (44b) on the basis of these data, are presented in table 13.

(iii). Numerical analysis: experimental values of τ_e, B and W

It was pointed out in sec. 2.2.2 that it is possible to derive values for the interaction parameters B and W of the alkali nuclei from the alkali linewidth data by using the eqs. (31) - (33) together with the values of the correlation times determined from the proton experiments.
For the alkali salts of Bp and Fluon such a calculation of B and W will be performed on the basis of the alkali linewidths measured at room temperature on the solutions of these salts. The values of the correlation times to be applied in the calculations are: an upper limit of 2×10^{-10} s for τ_e, and upper and lower limits of respectively 10^{-10} and 2×10^{-11} s for both τ_d and τ_r. The choice for these values of the correlation times has been made on the basis of the data presented in table 10.

The calculation of the linewidth contribution $(T_2^{-1})_{Fc}$, the correlation time τ_e, the anisotropic dipolar interaction constant B and the quadrupolar interaction constant W will be performed as follows.

$(T_2^{-1})_{Fc}$ or τ_e:
When it is clear either on theoretical grounds or on the basis of the experimental results, that $(T_2^{-1})_D$, $(T_2^{-1})_Q \ll (T_2^{-1})_{Fc}$, a value of τ_e can be calculated from the experimentally determined linewidth by neglecting in the expression (33) the terms $(T_2^{-1})_D$ and $(T_2^{-1})_Q$ and inserting in the resulting equation for the parameter A the experimentally measured value.
In all other cases an upper limit for $(T_2^{-1})_{Fc}$ will be calculated by inserting in eq. (31a) the above-mentioned upper limit of 2×10^{-10} s for τ_e together with the experimentally determined value of A.

B: Provided it has proved possible to establish a value for $(T_2^{-1})_D$ from the experiment, upper and lower limits for B will be calculated by inserting in eq. (31b) for $(T_2^{-1})_D$ the experimentally

determined value and for τ_d the above-mentioned lower and upper limits.

W: For the calculation of upper and lower limits of W the same procedure as in the calculation of B will be used, applying now eq. (31c) and using for τ_r the same values as for τ_d.

The linewidth data used in the calculations were, if necessary, corrected for inhomogeneity broadening and broadening by intermolecular interactions.

Biphenyl

LiBp.

The data measured on the system Li Bp MTHF are analysed as an example. The analysis of the data measured on the other LiBp systems proceeds in the same way.

At $T = +30$ °C one finds for the ^{7}Li linewidth and the ^{7}Li h.f.s.c. for Li Bp MTHF: $T_2^{-1} = 190$ s^{-1} and $a = 0.037$ g (figs. 40 and 14). For Li Bp MTHF the ^{6}Li as well as the ^{7}Li linewidths were measured. From fig. 40 it appears that the ratio of the ^{6}Li and the ^{7}Li linewidths is equal to the ratio of the squares of the respective magnetic moments. This indicates, according to the argument given in the discussion of the eqs. (46) in sec. 2.2.2, that $(T_2^{-1})_Q$ is negligeably small so that $(T_2^{-1})_{Fc} + (T_2^{-1})_D \cong T_2^{-1} = 190$ s^{-1}. From the reported value of the ^{7}Li h.f.s.c. an upper limit of 20 s^{-1} is calculated for $(T_2^{-1})_{Fc}$. Therefore, $(T_2^{-1})_D \geqslant 170$ s^{-1} from which a value of 0.35-0.8 Mc/s is calculated for $B.\hbar^{-1}$. Comparison with the data quoted for ^{7}Li in table 12 shows that B_{Me} is too small to account for this value of B, so that it is concluded that $\bar{B}_{Ar}.\hbar^{-1} \cong B.\hbar^{-1} = 0.35$-$0.8$ Mc/s. A comparison with the values of $\bar{B}_{Ar}.\hbar^{-1}$ quoted in table 12 learns that, supposed the ^{7}Li ion is above an aromatic ring of the Bp molecule, the distance d of the nucleus to the plane of the Bp molecule would amount to 2.2-3.4 Å.

NaBp.

The experimental data obtained for the systems Na Bp DME and Na Bp Dg are discussed first, after which the data obtained for the system Na Bp THF are discussed.

At $T = +20$°C the Na linewidth and the Na h.f.s.c. in the systems

Na Bp DME and Na Bp Dg amount to $T_2^{-1} = 400\text{-}600\ s^{-1}$ and $a = 0.015\text{-}0.025$ g (figs. 45, 46 and 22, 23).
Calculation of an upper limit of $(T_2^{-1})_{Fc}$ shows that $(T_2^{-1})_{Fc}$ is negligeably small so that $(T_2^{-1})_D + (T_2^{-1})_Q \leqq 500\ s^{-1}$.
As in solutions of diamagnetic salts like $NaBH_4$ and $NaB\Phi_4$ (fig. 5) approximately the same values for the Na linewidths are found as in the above-mentioned NaBp solutions, it is assumed that the Na linewidth in these cases is determined by the quadrupolar interaction, so that $(T_2^{-1})_Q \leqq 500\ s^{-1}$. From this value of $(T_2^{-1})_Q$ a value of 1.1-2.6 Mc/s is calculated for $W.h^{-1}$.

For NaBp in THF one finds at $T = +20°C$ for the Na linewidth: $T_2^{-1} = 1\,100\ s^{-1}$ (fig. 44). Using a value of 0.058 g for the Na h.f.s.c. (fig. 21), an upper limit of $50\ s^{-1}$ is calculated for $(T_2^{-1})_{Fc}$. Assuming that in this system $(T_2^{-1})_Q$ has approximately the same value as in the DME and the Dg solutions, which means that $(T_2^{-1})_Q$ is equal to approximately $500\ s^{-1}$, it follows that $(T_2^{-1})_D \leqq 550\ s^{-1}$, from which a value of 0.6-1.3 Mc/s is calculated for $B.h^{-1}$.
This value is too large to be accounted for by interaction with a spin density of $\pm$ 0.01 in the $3p$-orbital of the Na ion, so that interaction with the spin density on the radical must determine the anisotropic dipolar interaction. Comparison with the values of $\bar{B}_{Ar}.h^{-1}$ quoted in table 12 for Na learns that the distance d of the Na nucleus to the Bp plane has to be equal to 1.3-2.1 Å.

KBp.
Regarding the KBp systems, as an example the data found for K Bp DME are considered in detail.
At $T = +20°C$ one finds for the linewidth and the h.f.s.c. of K in the system K Bp DME: $T_2^{-1} = 350\ s^{-1}$ and $a = -0.015$ g (figs. 53 and 26).
Again $(T_2^{-1})_{Fc}$ appears to be negligeably small, so that $(T_2^{-1})_D + (T_2^{-1})_Q \leqq T_2^{-1} = 350\ s^{-1}$. If the anisotropic dipolar interaction would determine the linewidth, a value of 0.5-1.1 Mc/s would be calculated for $B.h^{-1}$, which is at least an order of magnitude too large to be accounted for by B_{Me} or by $\bar{B}_{Ar}$, or by both together (see table 12). It is concluded that the quadrupolar interaction determines the linewidth. From $(T_2^{-1})_Q \leqq 350\ s^{-1}$ a value of 0.9-2.1 Mc/s is calculated for $W.h^{-1}$.

RbBp.

Regarding the RbBp systems, as an example the data found for Rb Bp DME will be considered in detail.

At $T = +20°C$ one finds for the linewidth and the h.f.s.c. of respectively ^{85}Rb and ^{87}Rb: $T_2^{-1} = 6\,200\ s^{-1}$ and $a = -0.15$ g, and $T_2^{-1} = 8\,300\ s^{-1}$ and $a = -0.49$ g (figs. 47 and 27). Performing the analysis of the linewidths according to the method indicated at the discussion of the eqs. (46) one finds for ^{85}Rb: $(T_2^{-1})_Q = 6\,000\ s^{-1}$ and $(T_2^{-1})_{Fc} + (T_2^{-1})_D = 200\ s^{-1}$, and for ^{87}Rb: $(T_2^{-1})_Q = 6\,300\ s^{-1}$ and $(T_2^{-1})_{Fc} + (T_2^{-1})_D = 2\,000\ s^{-1}$. From the values of $(T_2^{-1})_Q$ one calculates for ^{87}Rb: $W.\hbar^{-1} = 8.0\text{-}17.9$ Mc/s and for ^{87}Rb: $W.\hbar^{-1} = 3.9\text{-}8.8$ Mc/s. Furthermore it appears that if $(T_2^{-1})_{Fc}$ would be negligeably small, $B.\hbar^{-1}$ would have values of 0.5-1.2 Mc/s and 1.2-2.7 Mc/s for respectively ^{85}Rb and ^{87}Rb. Comparison with the values of B_{Me} and B_{Ar} quoted for ^{85}Rb and ^{87}Rb in table 12 shows that these values of B are too large to be realistic. It is concluded that $(T_2^{-1})_D \ll (T_2^{-1})_{Fc}$, so that $(T_2^{-1})_{Fc} \cong 200\ s^{-1}$ for ^{85}Rb and $((T_2^{-1})_{Fc} \cong 2\,000\ s^{-1}$ for ^{87}Rb. Using the values of the h.f.s.c. mentioned above one calculates from these data a value of 1.1×10^{-10}s for τ_e.

CsBp.

Regarding the CsBp systems, as an example the data obtained from the experiments on the system Cs Bp Dg will be considered in detail.

At $T = +30°C$ the linewidth and the h.f.s.c. of Cs amount to $T_2^{-1} = 8\,100\ s^{-1}$ and $a = -0.72$ g (figs. 55 and 36).

If either the quadrupolar or the anisotropic dipolar interaction would determine the Cs linewidth completely one would calculate from the quoted value of the linewidth respectively $W.\hbar^{-1} = 14\text{-}32$ Mc/s or $B.\hbar^{-1} = 2.4\text{-}5.4$ Mc/s.

In both cases the calculated values are at least an order of magnitude too large to be realistic (see the tables 12 and 13). It is concluded that the Fermi contact interaction determines the Cs linewidth in Cs Bp Dg. From the reported values of the linewidth and the h.f.s.c. a value of 2.0×10^{-10}s is calculated for the correlation time τ_e.

Fluorenone

The analysis of the linewidth data obtained from the experiments on the alkali Fluon solutions proceeds in the same way as the analysis

of the linewidth data of the alkali Bp solutions. Therefore the calculations on the Fluon systems are not reproduced in detail and only the results are presented.

Na Fluon THF.
At $T = +30°C$ and at a degree of reduction of $f_p = 1.0$ the linewidth and the h.f.s.c. of Na in the system Na Fluon THF amount to $T_2^{-1} = 15\,000\ s^{-1}$ and $a = 1.65$ g (figs. 49 and 37). From the calculations it appears that the Fermi contact interaction determines the linewidth. From the reported values of the linewidth and the h.f.s.c. a value of 7×10^{-11} s is calculated for τ_e. At $f_p = 0.6$ one finds under the same circumstances $T_2^{-1} = 34\,500\ s^{-1}$, from which a value of 1.6×10^{-10} s is calculated for τ_e.

K Fluon THF.
At $T = +20°C$ the linewidth and the h.f.s.c. of K in the system K Fluon THF amount to $T_2^{-1} = 5\,500\ s^{-1}$ and $a = 0.24$ g (figs. 53 and 37). For $(T_2^{-1})_{Fe}$ an upper limit of $900\ s^{-1}$ is calculated. The remaining part of the linewidth appears to be determined by the quadrupolar interaction. A value of 3.4-7.7 Mc/s is calculated for $W.h^{-1}$.

	$\|A\|.h^{-1}$, Mc/s	$\tau_e \times 10^{11}$, s	$B.h^{-1}$, [1] Mc/s	d, Å	$W.h^{-1}$, [1] Mc/s	$\|eq_{out}\| \times 10^{-7}$, esu/cm³
Biphenyl						
^{6}Li MTHF	0.04 (10)	—	0.15 (90)	2.2-3.4	—	—
^{7}Li MTHF	0.11 (10)	—	0.35 (90)		—	—
^{23}Na THF	0.16 (0)	—	0.6 (50)	1.3-2.1	1.1 (50)	2.3
^{39}K DME	0.04 (0)	—	—	—	0.9 (100)	0.8
^{85}Rb DME	0.42 (5)	—	—	—	8.0 (95)	0.8
^{87}Rb DME	1.37 (25)	11	—	—	3.9 (75)	
^{133}Cs Dg	2.02 (100)	20	—	—	—	—
Fluorenone THF						
^{23}Na f_p=1	4.63 (100)	7	—	—	—	—
f_p=0.6	4.63 (100)	16	—	—	—	—
^{39}K	0.67 (15)	—	—	—	3.4 (85)	3.7
^{85}Rb	2.52 (5)	4	—	—	26 (95)	2.6
^{87}Rb	8.98 (35)		—	—	13 (65)	
^{133}Cs	1.80 (100)	25	—	—	—	—

[1]) The quoted values are the calculated lower limits of this parameter.

Table 14. Interaction parameters, correlation times, field gradients and interionic distances for a number of alkali radical ion pairs, calculated from the alkali linewidths measured at room temperature.

Rb Fluon THF.
At $T = +50°C$ the linewidth and the h.f.s.c. of ^{85}Rb and ^{87}Rb in Rb Fluon THF amount to respectively $T_2^{-1} = 65\,000\ s^{-1}$ and $a = 0.9$ g, and $T_2^{-1} = 97\,000\ s^{-1}$ and $a = 3.2$ g (figs. 54 and 37; see also sec. 4.2.2).
It is calculated that $(T_2^{-1})_D$ is negligeably small for both isotopes and that for ^{85}Rb $(T_2^{-1})_Q = 62\,000\ s^{-1}$ and $(T_2^{-1})_{Fc} = 3\,000\ s^{-1}$, while for ^{87}Rb $(T_2^{-1})_Q = 65\,000\ s^{-1}$ and $(T_2^{-1})_{Fc} = 32\,000\ s^{-1}$. The calculated values for $W.\hbar^{-1}$ are 26-50 Mc/s for ^{85}Rb and 13-29 Mc/s for ^{87}Rb. For the correlation time τ_e a value of 4×10^{-11}s is found.

Cs Fluon THF.
At $T = +30°C$ the linewidth and the h.f.s.c. of Cs amount to $T_2^{-1} = 7500\ s^{-1}$ and $a = 0.64$ g (figs. 55 and 37).
It appears that the Fermi contact interaction determines the linewidth completely. A value of 2.5×10^{-10}s is calculated for the correlation time τ_e.

The results of the foregoing calculations have been put together in table 14. For reasons of simplicity only the calculated *lower* limits of the parameters B and W are given, which correspond with an upper limit of 10^{-10}s for the correlation times τ_r and τ_d. The values of A in table 14 were calculated from the experimentally determined values of the alkali h.f.s.c. by using eq. (6). The numbers in parentheses behind the quoted values of the parameters indicate the percentages of the total linewidth, which were found to be determined by the corresponding interactions. The values of $|eq_{out}|$ quoted in table 14 have been calculated by setting the experimentally determined value of W equal to W_{out} and applying eq. (44a) using for γ_∞ and eQ the values given in table 13. This procedure will be discussed in the next paragraph in greater detail.

(iv). Numerical analysis: discussion

On account of the data presented in the tables 12, 13 and 14 the following comments are made.

The anisotropic dipolar interaction.
1 Regarding the anisotropic dipolar interaction it appears from the

data of table 12, that for Li the interaction with spin density on the aromatic molecule, symbolized by the parameter $\bar{B}_{Ar}$, is much larger than the interaction with spin density in orbitals of the metal, symbolized by the parameter B_{Me}. This relationship between $\bar{B}_{Ar}$ and B_{Me} reverses if one proceeds along the series of the alkali metals from Li to Cs, so that for Cs B_{Me} is relatively more important than $\bar{B}_{Ar}$.

This reversal is caused partly by the increase of the ionic radius from Li to Cs and the accompanying increase in the distance between aromatic ion and counterion. As $\bar{B}_{Ar}$ roughly varies with the inverse cube of this distance, $\bar{B}_{Ar}$ will show a relative decrease in magnitude along the series of the alkali metals from Li to Cs. On the other hand $B(np)$ increases with increasing atomic number as a result of the deeper penetration of the np-orbital in the metal core. Therefore, ϱ_{np} being constant, B_{Me} will show a relative increase in magnitude along the series of the alkali metals from Li to Cs.

2 From the data of table 12 and 13 it should be expected in the first place that in going along the series of the alkali metals from Li to Cs, the anisotropic dipolar interaction becomes less important for the relaxation of the alkali nuclei than the other two interactions, viz. the Fermi contact and the quadrupolar interaction. In the second place it should be expected in view of the argument presented under point 1 that the anisotropic dipolar interaction for the lighter alkali metals like Li and Na will be determined mainly by $\bar{B}_{Ar}$.

As appears from table 14 these expectations are borne out by the experiments. In the first place it appears that only in solutions of LiBp and NaBp the anisotropic dipolar interaction gives a notable contribution to the linewidth of the alkali nucleus, as may be clear from the linewidth percentages indicated in parentheses behind the values of the different interaction parameters. In the second place for these two salts the anisotropic dipolar interaction appears to be completely dominated by $\bar{B}_{Ar}$ as was argued at the calculation of B in the foregoing paragraph.

The interionic distance d

3 From the experimentally determined values of the parameter $\bar{B}_{Ar}$ of the alkali nuclei in the systems Li Bp MTHF and Na Bp THF values of respectively 2.2-3.4 Å and 1.3-2.1 Å were calculated

for the distance d of the alkali nucleus to the plane of the Bp molecule. Using averadge values for this distance of respectively 2.8 and 1.7 Å and assuming that in the ion pairs in these solutions the alkali ions and the radical ions are more or less in contact with each other, one can obtain a value for the "van der Waals radius" of the Bp ion by diminishing the above-mentioned averadge values of d by the respective ionic radii of the alkali metals. In this way one finds values for the "half thickness" of the Bp ion measured in a direction perpendicular to the plane of the molecule of respectively 2.1 Å and 0.8 Å.

This can be compared with estimated values of the "van der Waals radius" of an aromatic ion reported in the literature, which amount to 2-2.5 Å [42, 47, 93].

The value of 0.8 Å, calculated on the basis of the Na experiments on Na Bp THF, may be somewhat in error, since for these experiments high rf powers had to be used to obtain a satisfactory S/N ratio. This may have resulted in a partial saturation and a broadening of the Na signal which in turn may have given rise to too large a value for B and too small a value for the interionic distance d. Furthermore it should be kept in mind that the use of the parameter B in eq. (31b) is based on an approximation. This may introduce also an error in the calculation of the interionic distance d. However, allowing for these inaccuracies the values found from the present experiments for the "half thickness" of an aromatic ion nevertheless seem to be smaller by an amount of 0.5-1 Å than the values reported in the literature.

The quadrupolar interaction

4 Regarding the quadrupolar interaction it can be expected from the data of table 13 in the first place that for all the alkali isotopes dealt with in this study, the contribution of W_{Me} to the quadrupolar interaction constant will be negligeable compared with the contribution from W_{out}. In the second place it can be expected from a comparison of the estimated values of $W_{out}.h^{-1}$, reported in table 13, with the values of the other interaction parameters, reported in table 12, that the quadrupolar relaxation will be important only for ^{23}Na, ^{39}K, ^{85}Rb and ^{87}Rb. This is related to the relatively large quadrupole moments and large Sternheimer shielding factors of these nuclei.

The latter expectation is confirmed nicely by the experiment:

from the data of table 14 it appears that only for Na, K and Rb the quadrupolar relaxation gives an important contribution to the linewidth.

5 On the basis of the preceding argument the calculation of $|eq_{out}|$ was performed, as was indicated already at the end of the foregoing paragraph, by setting the experimentally determined value of W equal to W_{out}.

From the data of table 14 it apears that for the Bp salts $|eq_{out}|$ falls in the range of $(0.8\text{-}2.3) \times 10^7$ esu/cm^3 and that for the Fluon salts $|eq_{out}|$ falls in the range of $(2.6\text{-}3.7) \times 10^7$ esu/cm^3. These data show that there is a difference in magnitude between the field gradients in the Bp salts and those in the Fluon salts. Although the number of data is still too small to draw definite conclusions, it seems allowed to assume that this difference is not accidental. It has been argued already in sec. 5.1.2 in the discussion of the alkali metal h.f.s.c. of the Fluon salts, that the alkali ions are probably relatively strongly bonded in the alkali Fluon ion pairs and that they are probably close to a site in the radical which bears a large charge density. This charge density may produce a large field gradient at the metal nucleus, which may explain why the field gradient in the alkali Fluon ion pairs is larger than in the alkali Bp ion pairs.

Correlation times

6 It was pointed out in the third paragraph of this section that in the calculation of the parameter W from the alkali linewidths a value for the rotational correlation time τ_r had to be assumed. Although the calculated value of W depends on the square root of this correlation time and is therefore not very sensitive to changes in τ_r, the calculated values of W may serve nevertheless as a rough means to check whether the assumed value of τ_r was approximately correct.

Thus, comparing the theoretically estimated values of $W_{out}.h^{-1}$ reported in table 13, with the experimentally determined values of $W.h^{-1}$ reported in table 14, it appears that the latter values fall in the theoretically predicted range. This may indicate that the value of $10^{-10}s$ used for τ_r in the calculation of W is in fact not an upper limit but an approximately correct value for τ_r.

7 From the data reported in table 14 for the electron spin correlation time τ_e, it appears that in the system Na Fluon THF there is a

distinct influence of the degree of reduction on the magnitude of τ_e: when f_p increases from 0.6 to 1.0, τ_e decreases by more than a factor of two.

As was explained in sec. 2.2.2, this shortening of τ_e may be caused by the increase of the radical concentration which accompanies the increase of f_p. However, the effect is too large to be accounted for simply by this cause alone. An extra source of line broadening may be provided by the electron transfer process which occurs in a partly reduced solution of an aromatic compound. ADAM and WEISSMAN have shown that the electron transfer process may proceed via an alkali atom transfer process [94]. Similar observations were made later on by HIROTA and WEISSMAN [95]. One can imagine that during the atom transfer process the unpaired electron resides during a short time completely on the alkali atom and produces during this time-interval a spin density at the metal nucleus which exceeds the spin density present at the alkali nucleus during the rest of the time, by two or three orders of magnitude. Consequently the Fermi contact interaction will cause the alkali nucleus to experience a strong and short magnetic pulse during the atom transfer, which may enhance the relaxation of the alkali nucleus.

Thus the alkali atom transfer process may constitute a relaxation mechanism for the alkali nuclei which depends upon the degree of reduction and which may be responsible for the apparent strong dependence of τ_e on the degree of reduction.

This explanation has still to be checked by further experiments.

8 The values of the electron spin correlation times reported in table 14 fall in the range of $2 \times 10^{-10} - 2 \times 10^{-11}$ s except for the case of Cs Fluon THF. Apart from the latter exception it appears from a comparison with the data presented in table 11 that the values found for τ_e agree nicely with the values of τ_e calculated on the basis of the linewidths of the aromatic protons.

That for Cs Fluon THF an exceptionally large value for τ_e was found, may correspond with the circumstance that it proved impossible to reduce solutions of this system completely, so that the experiments had to be performed on a partly reduced solution. As was pointed out in the discussion under point 7, in a partly reduced solution the electron transfer reaction may cause an additional broadening of the alkali NMR signal which

may result in apparently too large a value for the electron spin correlation time.

Finally from the data given in the tables 12, 13 and 14 the following predictions can be made regarding the relative importance of the different intramolecular interactions for the relaxation of the alkali nuclei in radical ion pairs.

Li: The relaxation of ^{6}Li as well as of ^{7}Li nuclei will be determined in most cases by the Fermi contact interaction. However, if this interaction is very small the anisotropic dipolar interaction will determine the relaxation.

Na: The relaxation of ^{23}Na nuclei will be determined by the Fermi contact interaction only if the Na h.f.s.c. is large ($\geqslant 1$ gauss). Otherwise the quadrupolar interaction will determine the relaxation of the Na nuclei, while in some cases the anisotropic dipolar interaction may become equally important.

K: The relaxation of ^{39}K nuclei will nearly always be determined to an amount of 80-100% by the quadrupolar interaction.

Rb: For the relaxation of ^{85}Rb the same remarks apply as for the relaxation of ^{39}K.
The relaxation of ^{87}Rb will in most cases be determined for the larger part by the quadrupolar interaction, while the remaining part will be determined by the Fermi contact interaction.

Cs: The relaxation of ^{133}Cs will nearly always be completely determined by the Fermi contact interaction.

(v). Influence of the temperature, solvent, concentration and degree of reduction

Influence of the temperature

The variation of the alkali linewidths with the temperature will be analysed, according to the theory outlined in sec. 2.2.2, by considering the linewidth as a function of η_0/T. If the linewidth appears to be presented by a curved graph this will be considered as an indication that the interaction parameters change with the temperature.

The analysis will be performed for the linewidth data which were

obtained for solutions of the alkali salts of Bp, Fluon and Nl and which were presented in the figs. 39-55.

A. Biphenyl

LiBp.

In the discussion of the alkali linewidth data obtained for the LiBp systems the data of Li Bp Dg (fig. 43) are left out of consideration, because at high temperatures the linewidth corrections amount for this system to more than 50% of the linewidth.

It was shown in paragraph three of this section that in the system Li Bp MTHF the Li linewidth is determined by the anisotropic dipolar interaction. For the systems Li Bp THP and Li Bp THF the analysis of the Li linewidth data can be performed in the same way: from fig. 39 and fig. 41 it appears that in these systems the ratio of the ^{6}Li and the ^{7}Li linewidths is again approximately equal to the ratio of the squares of the respective magnetic moments, from which it can be concluded that also in these systems the quadrupolar relaxation of the Li nuclei is negligeable. Again it can be shown that $(T_2)^{-1}_{Fc}$ is negligeably small compared with the experimentally determined linewidth, which means that also for these systems the Li linewidth is nearly completely determined by the anisotropic dipolar interaction.

It is pointed out that the difference between the ^{6}Li and the ^{7}Li data in fig. 39 for Li Bp THP is accidental. As was remarked in sec. 4.2.2, in solutions of Li Bp THP the Li NMR signal broadens irreversibly upon ageing of the solution. As for the ^{6}Li and the ^{7}Li experiments different solutions were used, in which the broadening of the Li signal had not proceeded to the same level at the time of the experiments, this may explain the observed difference between the ^{6}Li and ^{7}Li data in fig. 39. However, it was checked that the temperature dependence of the Li linewidth was not influenced by the process of ageing of the solution.

As appears from the figs. 39-41 the temperature dependence of the Li linewidth in the systems Li Bp THP, Li Bp MTHF and Li Bp THF is not characterized by a proportionality with η_0/T, but instead by an increase of the linewidth with an increase of the temperature. Since it was argued that in these systems the anisotropic dipolar interaction determines the Li linewidth, it is concluded that this interaction

increases in magnitude upon an increase of the temperature, which is explained by assuming that the Li ion is coming closer to the Bp ion as the temperature is raised. This explanation is consistent with the explanation given in sec. 5.1.2 of the increase of the Li h.f.s.c. with the temperature in the systems Li Bp THP, Li Bp MTHF and Li Bp THF (figs. 13-15). There it was also assumed that the interionic distance in the ion pair decreases with an increase of the temperature.

A similar behaviour of the Li linewidth as a function of the temperature is found in the system Li Bp DME (fig. 42). Although for this system no ^{6}Li experiments were performed we believe that also in this case the alkali lnewidth is determined by the anisotropic dipolar interaction, at least at high temperatures. We conclude that also in this case a decrease in the distance between the Li and the Bp ions in the ion pairs and an accompanying increase of the anisotropic dipolar interaction causes the increase of the Li linewidth, observed at high temperatures.

NaBp.

The temperature dependence of the Na linewidth in the systems Na Bp THF, Na Bp DME and Na Bp Dg may become clear from the figs. 44-46.

It was argued in the third paragraph of this section that in the system Na Bp THF the Na linewidth is determined for a large part by the anisotropic dipolar interaction. Therefore, the increase of the alkali linewidth with the temperature observed for this system (fig. 44) is, just as in the case of the system Li Bp MTHF, explained by assuming that a decrease of the distance between the Na and the Bp ions occurs at higher temperatures with a corresponding increase of the anisotropic dipolar interaction. This decrease in the distance is also reflected in the increase of the Na h.f.s.c. (fig. 21) at higher temperatures, as was discussed in sec. 5.1.2.

Apart from the singularity in the plot of the Na linewidth, observed for the 1 M solution of NaBp in Dg (fig. 46), the Na linewidth in the systems Na Bp DME and Na Bp Dg appears in a good approximation to be proportional to η_0/T over a large range of temperatures. As it was assumed that for these systems the Na linewidth is completely determined by the quadrupolar interaction, the straight plots in the figs. 45 and 46 show that this interaction does not change markedly with the temperature. This is not in accordance with the

observed change in the magnitude of the Fermi contact interaction (figs. 22 and 23) from which it was concluded in sec. 5.1.2 that the NaBp ion pairs change their structure from solvent separated at low temperatures to contact ion pairs at high temperatures. Apparently this change in structure does not influence the magnitude of the quadrupolar interaction to a great extent. It is pointed out that, just as in the LiBp systems, at very high temperatures the influence of the anisotropic dipolar interaction becomes apparent in a curvature of the linewidth plots in the figs. 45 and 46.
The singularity in the Na linewidth plot observed in fig. 46 for the 1 M solution of NaBp in Dg corresponds with the singularity observed in the plot of the Na h.f.s.c. in fig. 23. As was pointed out already in sec. 5.1.2 this singularity is caused by a partial precipitation of the Na Bp salt. The precipitation caused a decrease in the viscosity η of the solution and an accompanying shortening of the rotational correlation time. This in turn resulted in the observed decrease of the Na linewidth.

KBp.
In paragraph three of this section the K linewidths measured in the KBp systems were shown to be determined completely by the quadrupolar interaction. Judging from the straight plots in fig. 53 this interaction does not change with the temperature.

RbBp.
It was shown in the third paragraph of this section that the ^{85}Rb as well as the ^{87}Rb linewidths in the RbBp systems are determined mainly by the quadrupolar interaction.
From the figs. 47 and 48 it is concluded that in the system Rb Bp DME this interaction increases with decreasing temperature, while this interaction stays constant with the temperature in Rb Bp Dg. These changes in the magnitude of the quadrupolar interaction do not run parallel with the observed changes in the magnitude of the Fermi contact interaction (figs. 27 and 28). From the change of the Rb h.f.s.c. with the temperature it was concluded in sec. 5.1.2 that RbBp forms contact ion pairs in both DME and Dg at high temperatures, but that at low temperatures the ion pair structure is different in the two solvents: in DME still contact ion pairs exist, but in Dg solvent separated ion pairs are formed. Apparently the

assumed large change in the ion pair structure with the temperature in the latter system is not reflected in a change in the quadrupolar interaction constant, while the assumed small change in the ion pair structure with the temperature in the former system seems to be accompanied by a notable change in the magnitude of the quadrupolar interaction.

CsBp.

From fig. 55 it appears that in the system Cs Bp Dg the linewidth is not proportional to η_0/T. In the two foregoing paragraphs it was shown that the Cs linewidth in this system is completely determined by the Fermi contact interaction. Therefore it is worth-while to check if the disproportionality between the Cs linewidth and η_0/T is related to the variation of the Cs h.f.s.c. with the temperature. Moreover this system may provide a test-case for the hypothesis put forward at the end of sec. 2.2.2, that an analysis of the temperature dependence of the alkali linewidth may reveal in some cases whether the static or the dynamic model of the ion pair has to be applied for an explanation of the temperature dependence of the alkali h.f.s.c.

According to the theory presented in the last paragraph of sec. 2.2.2 one expects that, if in Dg the Cs Bp ion pairs behave according to the static model, the Cs linewidth will be proportional to $a^2 . \eta_0/T$, in which a is the experimentally measured Cs h.f.s.c. On the other hand, if the Cs Bp ion pairs behave according to the equilibrium model, one expects the Cs linewidth to be proportional to $aa_c . \eta_0/T$, in which a_c is the value of the Cs h.f.s.c. in the contact ion pairs. In order to distinguish between these two possibilities an assumption has to be made about the possible magnitude of a_c at different temperatures. On the basis of the analysis of the temperature dependence of the Cs h.f.s.c. in Cs Bp Dg, which was given in sec. 5.1.2, it may be assumed that at high temperatures a_c equals the experimentally determined Cs h.f.s.c. (see fig. 36), and that the high temperature part of the curve of Cs Bp Dg in fig. 36 needs only to be extrapolated by a straight line to find the possible values of a_c at lower temperatures. Examples of such straight plots were encountered in other systems for which the existence of contact ion pairs over the complete range of temperature investigated was postulated, for instance in the system Rb Bp DME (fig. 27) and in the system Na Bp MTHF (fig. 20). The result of this extrapolation

is given in fig. 56. Using the values of a and a_c indicated in this figure, $T_2^{-1}.T/\eta_0$ has been plotted versus a^2 and versus aa_c in fig. 57. The results show clearly that the Cs linewidth is proportional to a^2 and not to aa_c. From this it is concluded that in a concentrated solution of CsBp in Dg the ion pairs have to be described by the static model [22]. This conclusion was anticipated in the analysis of the temperature dependence of the alkali h.f.s.c. in the first paragraph of sec. 5.1.2.

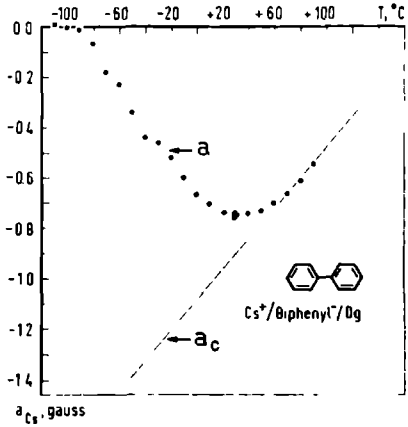

Fig. 56. ^{133}Cs NMR h.f.s.c. *versus* temperature for the system Cs Bp Dg. The points denoted by the symbol a represent the experimental data (see fig. 36). The straight plot denoted by the symbol a_c represents the ^{133}Cs h.f.s.c. in the possible contact ion pairs of CsBp (see text).

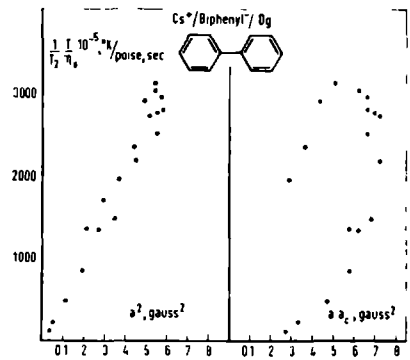

Fig. 57. ^{133}Cs linewidths multiplied by T/η_0 *versus* a^2 (static model) and aa_c (dynamic model) for the system Cs Bp Dg (see text).

B. Fluorenone

In sec. 5.1.2 the conclusion was put forward that in the alkali Fluon THF systems the change in the structure of the ion pairs in the dimers is small as the temperature is changed. It is therefore to be expected that the alkali interaction parameters do not change very much with the temperature and that the alkali linewidths will be

proportional to η_0/T. This is found indeed for the Na and K Fluon salts (figs. 49 and 53). For the Cs salt, however, there is a deviation from a straight line at low temperatures (fig. 55) which is not consistent with the slow increase of the Cs h.f.s.c. observed at low temperatures (fig. 37). It is possible that this anomaly is caused by the interference of the diamagnetic Cs Fluon species of which the signal was observed at low temperatures (see sec. 4.1.2). To provide a detailed explanation further experiments have to be performed.

C. Naphthalene

Assuming that in Rb Nl DME (fig. 50) the Rb linewidth is again determined mainly by the quadrupolar interaction, as it was the case in the system Rb Bp DME, the linewidth-plot of fig. 50 shows that this interaction increases with decreasing temperature. It seems as if there is again no correlation between the temperature-dependence of the alkali h.f.s.c. (fig. 38) and the temperature-dependence of the quadrupolar interaction: from the change in the Rb h.f.s.c. it was concluded that RbNl forms contact ion pairs above $T = -20°C$ and that below this temperature the formation of solvent separated ion pairs starts; on the other hand the change of the Rb linewidth with the temperature indicates that there is a steady and continuous increase of the quadrupolar interaction upon a decrease of the temperature.
It is remarked that the Rb linewidths in Rb Nl DME and Rb Bp DME are approximately equal and show a similar behaviour as a function of the temperature (fig. 54).

D. Conclusion

From the above-given analysis of the experimental data of the different alkali Bp, Fluon and Nl systems it is concluded that, when the alkali linewidth is determined by the Fermi contact or the anisotropic dipolar interaction, there is a good qualitative and sometimes a good quantitative correlation between the variation of the alkali linewidth and the variation of the alkali h.f.s.c. with the temperature. Such a correlation is lacking if the quadrupolar interaction determines the linewidth. A provisional conclusion may be 1. that in the alkali Bp ion pairs the field gradient at the alkali nucleus is mainly determined by the solvent molecules in the solvation shell of the

cation, 2. that this field gradient is relatively insensitive to changes in the position of the radical ion with respect to the alkali ion and 3. that, even if there is a change from contact into solvent separated ion pairs, the actual change in the solvation shell of the alkali ion is small. The observed similarity of the Rb linewidths in solutions of RbBp and RbNl in DME seems to confirm that the nature of the solvent and not the aromatic ion is specific for the magnitude of the quadrupolar interaction. On the other hand, if the alkali ion is relatively strongly bonded to the radical ion, as is probably the case in the Fluon dimers, the electronic charge on the radical ion itself may give an important contribution to the field gradient at the alkali nucleus. This was discussed already in the foregoing paragraph.

Influence of the solvent

The influence of the solvent on the interaction parameters will be analysed on the basis of the data of the Li Bp and the NaBp systems, which were presented respectively in the figs. 51 and 52.
From fig. 51 it appears that for a given value of η_0/T the Li linewidth increases as the solvent changes in the order DME, THF, MTHF, THP, which appears to be also the order of decreasing solvating power of these solvents. It was argued in the foregoing paragraph that the Li linewidth in these systems is determined by the anisotropic dipolar interaction, so that the observed increase in the Li linewidth may be interpreted as being caused by a decrease of the distance between the Li and the Bp ions in the ion pairs as the solvating power of the solvent decreases. This explanation agrees with the general theory outlined in sec. 2.2.2 about the correlation between ion pair structure and solvating properties of the solvent. Moreover, this explanation is consistent with the explanation offered in sec. 5.2.1 for the observation that the Li h.f.s.c. increases as the solvating power of the solvent decreases.
On the other hand the Li linewidth does not show an increase upon an increase of the temperature in the system Li Bp Dg. Apparently the solvation by the Dg molecules prevents the Li ions of coming close enough to the Bp radical ions in the ion pairs to make the influence of the anisotropic dipolar interaction perceptible. This is not surprising in view of the better solvating properties of Dg compared with DME.
Regarding the NaBp systems it was pointed out in the preceding

paragraph that the contribution of the anisotropic dipolar interaction to the Na linewidth is much larger in the THF than in the DME and Dg solutions. This indicates that the interionic distance in the NaBp ion pairs is smaller in THF than in DME or Dg, which is again consistent with the lower solvating power of THF compared with DME and Dg.

Influence of the concentration and the degree of reduction

The influence of the concentration on the alkali linewidth was measured in some detail in the systems Li Bp THF, Na Bp DME and Na Bp Dg (figs. 41, 45 and 46). The influence of the degree of reduction on the alkali linewidth was investigated for the system Na Fluon THF (fig. 49).

It was pointed out in sec. 2.2.2 that an increase of the radical concentration is expected to cause an increase of the rotational correlation time τ_r, so that in the systems in which the quadrupolar interaction determines the linewidth, the linewidth is expected to increase upon an increase of the radical concentration. This is observed indeed in the systems Na Bp DME and Na Bp Dg (figs. 45 and 46). It was pointed out already in this paragraph that the singularity in the Na linewidth plot of the 1 M solution of NaBp in Dg in fig. 46 was caused by a decrease in the ion pair concentration as a result of a partial precipitation of the NaBp salt and an accompanying decrease in the magnitude of the rotational correlation time τ_r.

On the other hand, it was argued in sec. 2.2.2 that it is difficult to predict the influence of the radical concentration on the dipolar correlation time τ_d. In the foregoing paragraph it was shown that in the system Li Bp THF the alkali linewidth is nearly completely determined by the anisotropic dipolar relaxation. This means according to eq. (31b) that the linewidth will be proportional to τ_d. The small increase of the Li linewidth observed when the radical concentration is increased (see fig. 41) might therefore indicate that the dipolar correlation time slowly increases with the concentration.

Regarding the influence of the degree of reduction on the Na linewidth in the system Na Fluon THF, the plots in fig. 49 show that this influence is appreciable. It was pointed out in the preceding paragraph that the decrease of the linewidth which occurs upon an increase of the degree of reduction is too large to be accounted for

only by a shortening of the electron spin correlation time τ_e. As a possible source of line broadening in partly reduced solutions the alkali atom transfer process was invoked. Since this process is a diffusion controlled process one would expect, assumed that it plays a role in the relaxation of the Na nuclei, that in a partly reduced solution the alkali linewidth would remain proportional to η_0/T. This is observed indeed in fig. 49. Therefore, the hypothesis that the dependence of the alkali linewidth upon the degree of reduction is related to the influence of the electron transfer reaction on the relaxation of the alkali nucleus, is for the present not in contradiction with the observed temperature dependence of the alkali linewidth in the system Na Fluon THF.

CONCLUSION

(i). Introduction

In the preceeding chapters it has been shown that the NMR method is suited to investigate concentrated solutions of alkali radical ion pairs. Information was obtained 1. about the sign and the magnitude of the proton and the alkali h.f.s.c., 2. about the intramolecular interactions which determine the relaxation of the different nuclei in radical ion pairs and the correlation times corresponding with these interactions, and 3. about the structure of alkali radical ion pairs. The information obtained in this study regarding these three subjects will be summarized successively in the next three paragraphs, after which in the last paragraph of this chapter a number of features will be dealt with concerning the application of the NMR method to the study of concentrated solutions of radical ion pairs.

(ii). Sign and magnitude of the h.f.s.c.

Regarding the aromatic protons, sign and magnitude of the h.f.s.c. proved in most cases to be in agreement with the results of ESR experiments and M.O. calculations.
Regarding the alkali nuclei, the determination of the sign of the h.f.s.c. is of particular importance because there has been speculation about this subject in the literature. It was shown that the sign of the alkali h.f.s.c. may in general be positive as well as negative and that in some cases the alkali h.f.s.c. as a function of the temperature may change its sign. These observations meant the experimental proof of DE BOER's hypothesis, put forward in 1965, about the occurrence of different signs for the alkali h.f.s.c. in radical ion pairs and about the possibility of a sign reversal of the alkali h.f.s.c. with the temperature.
It was shown in chapter 2 that for a theoretical description of sign and magnitude of the spin density at the metal nuclei in alkali radical ion pairs it is probably sufficient to perform a zero order M.O. calculation refined by a first order C.I. calculation. The configurations

which probably give important contributions to the spin density at the metal nucleus and which are probably also responsible for the possible occurrence of a negative sign of the metal h.f.s.c. are those which represent structures like Ar^*Me, in which the aromatic molecule is in an excited state, and Ar^-Me^{++}, in which the aromatic molecule and the metal atom bear respectively a doubly negative and a doubly positive charge. These configurations can be obtained from the ground state configuration Ar^-Me^+ by so-called cross excitations of an electron respectively out of an "aromatic" M.O. into a "metallic" M.O. or out of a "metallic" M.O. into an "aromatic" M.O.

The proposed mechanism also explains in a natural way the observed tendency of the spin density at the metal nucleus to decrease and to become negative if one proceeds along the series of the alkali salts of a given radical ion from Li to Cs. The explanation is based on the theoretically predicted correlation between sign and magnitude of the spin density at the metal nucleus on the one hand and the distance between alkali ion and radical ion and the dimensions of the metal *s*-orbitals on the other hand.

(iii). Intramolecular interactions and correlation times

In general three types of intramolecular interactions are of importance for the relaxation of the various nuclei in radical ion pairs, namely the Fermi contact interaction, the anisotropic dipolar interaction and the quadrupolar interaction.

The relaxation of the aromatic protons in a radical is determined by the former two interactions. The magnitudes of these two interactions can be calculated in detail, either by simple calculus or by a computer procedure, from a knowledge of the electron spin distribution over the radical.

On the other hand all three above-mentioned interactions may play a role in the relaxation of an alkali nucleus in a radical ion pair. Of these the Fermi contact interaction appears to be the most sensitive for changes in the ion pair structure. The anisotropic dipolar interaction will in general be important only in special cases. Its magnitude is mainly determined by the interaction of the nucleus with spin density on the radical and depends markedly on the distance between the radical and the alkali nucleus. Finally the quadrupolar interaction

often plays an important role in the relaxation of a number of alkali nuclei. The magnitude of this interaction seems to depend not as much on the distance of the alkali nucleus to the radical as on the structure of the solvation shell of the alkali ion, unless the alkali ion is bonded to a polar radical like fluorenone$^-$ to form a stable contact ion pair with it.

The study of the linewidths of the protons in an aromatic radical provides an excellent means to determine the magnitude of the electron spin correlation time τ_e. Also values for the rotational correlation time τ_r, though in general somewhat less accurate, can be found from such a study. The values for τ_e and τ_r measured at room temperature on solutions with radical concentrations in the order of magnitude of 1 M, varied between 2×10^{-10} s and 2×10^{-11} s.
In some cases also the study of the alkali linewidths may provide information about the magnitude of the electron spin correlation time, particularly when the alkali h.f.s.c. is large. In this way the apparent influence of the degree of reduction on the electron spin correlation time could be established. As was pointed out in sec. 5.2.2 the observed effect is possibly connected with the influence of the electron transfer reaction on the relaxation of the alkali nuclei.

(iv). Ion pair structure

Regarding the structure of alkali radical ion pairs there has been discussion in the literature how close the ions in a contact ion pair may approach each other. Defining a „van der Waals radius" of an aromatic radical as the distance of closest approach measured in a direction perpendicular to the plane of an aromatic ring of the radical, the values found in this study for this Van der Waals radius varied between approximately 1 and 2 Å and seemed to be smaller by 0.5-1 Å than the values reported in the literature.

The variation of the ion pair structure with the temperature could be described by three models. The first model describes the alkali ion and the radical ion as forming a more or less stable contact ion pair in which the alkali ion performs a vibration of which the amplitude

varies with the temperature. The second one assumes the existence of two different ion pair species in solution which are involved in an equilibrium of which the equilibrium constant may vary with the temperature. The third model considers only one ion pair species of which the structure alters as a result of a change in the solvation of the alkali ion as the temperature is changed.
The experimental results found in this study could be explained the best on the basis of the third model. To obtain a consistent explanation of the experimental results it appeared necessary to assume that also in the so-called contact ion pairs the solvation of the alkali ion by molecules of the solvent still plays an important role in determining the properties of the ion pair.

(v). General remarks

For the study of radical ion pairs in solution the NMR method has the following advantages.

1 The NMR method is suited to study the behaviour of alkali radical salts in solution in the concentration range of 0.1-1.0 M.

2 Sign and magnitude of the h.f.s.c. of a given nucleus can be inferred directly from sign and magnitude of the contact shift measured in the NMR spectrum of the nucleus.
As each group of equivalent nuclei in a radical ion pair is characterized by only one single NMR signal, the NMR spectrum of a radical ion pair will in most cases be more easily interpretable than the corresponding ESR spectrum of the ion pair.
A special advantage is that the signals of nuclei with a small h.f.s.c. can be measured easily by the NMR method, because the signals of these nuclei stay relatively sharp in the NMR spectrum of the radical ion pair. Therefore, hyperfine splitting constants which fall outside the range of resolution of an ESR spectrometer can be easily measured by the NMR method.

3 The study of the linewidths in the proton NMR spectrum of a radical provides an excellent means to study the behaviour of the electron spin correlation time in concentrated radical solutions.

4 The study of the linewidths in the alkali NMR spectrum of a radical ion pair provides information about the intramolecular interaction parameters of the alkali nuclei. This in turn may give information about the structure of the ion pair.

5 In the NMR spectrum of a given solution the signals of paramagnetic and diamagnetic species can be studied at the same time provided the interconversion between the different species is slow.

These advantages of the NMR method are attended by the following disadvantages.

1 As the use of high radical concentrations is necessary in order to obtain sufficiently short electron spin correlation times, the applicability of the method is limited to the study of systems of which solutions can be prepared with radical concentrations in the order of magnitude of 1 M.

2 The use of high concentrations may cause the appearance of complicating effects, like the formation of multiple ion clusters, which are usually absent in ESR experiments.

3 In the alkali NMR experiments the choice of a proper diamagnetic reference solution constitutes a problem. The difference between the shielding constants of a given nucleus in the reference and in the sample solution may affect the value of the contact shift to an unknown extent. However, this will possibly introduce a serious systematic error in the determination of the contact shift and thus of the hyperfine splitting constant only if the observed contact shift is small.

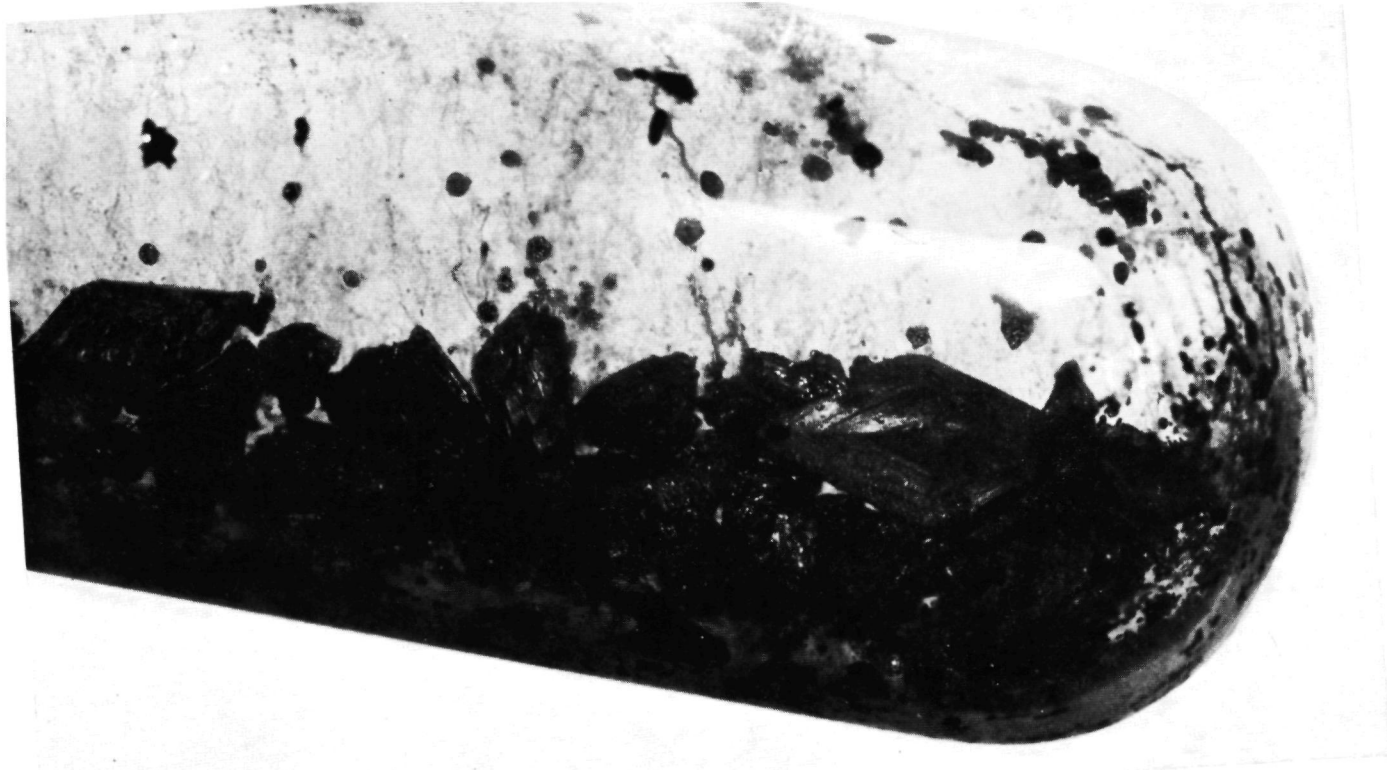

Fig. 58. Crystals of $LiBpTHP_5$. The actual dimension of the edge of the crystal in the lower right corner of the tube amounts to 14 mm.

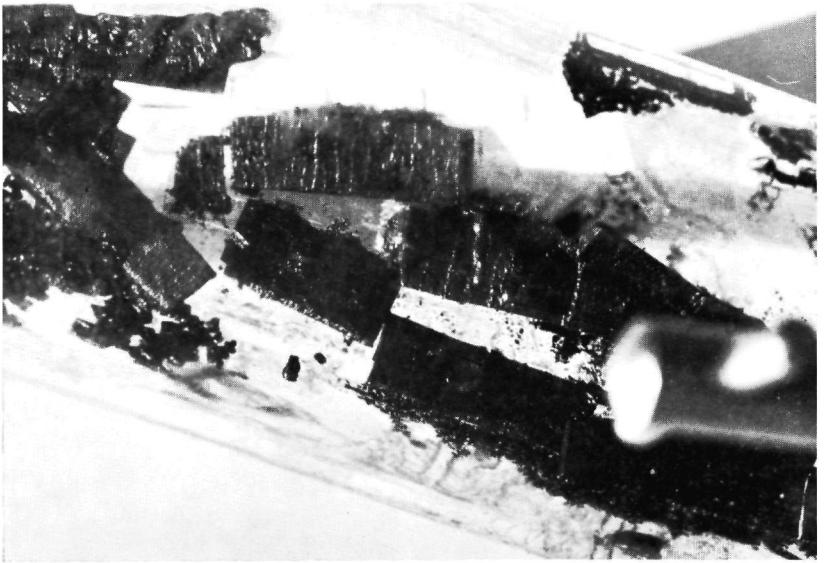

Fig. 59. Crystals of $Na_2Bp_2Tg_5$. At the top of the figure a division in centimeters is weakly visible.

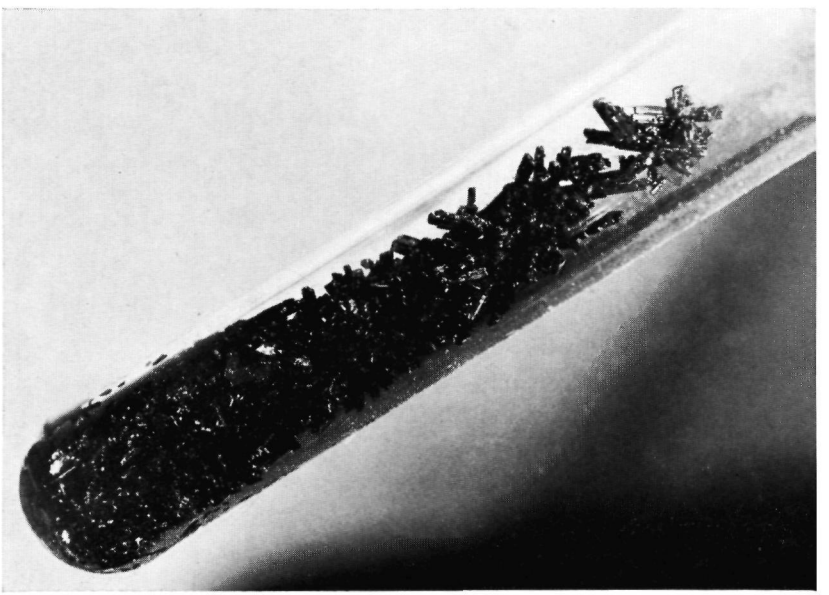

Fig. 60. Crystals of Rb Bp Ttg_3. The dimensions of the crystals can be inferred from a comparison with the diameter of the tube containing the crystals, which amounts to 2.5 cm.

PART II

CHAPTER 7

INVESTIGATIONS ON SINGLE CRYSTALS OF ALKALI RADICAL ION PAIRS

(i). Introduction

During the experiments on solutions of radical ion pairs described in the foregoing chapters, it appeared that in some cases a crystalline precipitate was deposited from the solutions. It was known that organic alkali salts, like Li fluorenyl, can be obtained in a crystalline form [96]. These crystals can be considered as being built up of ions, but they do not show a paramagnetism. On the other hand it was known that neutral free radicals like diphenylpicrylhydazil (DPPH) may form single crystals which are paramagnetic, but which are not built up of ions [97]. Therefore, it was of interest to investigate the possibility to prepare single crystals of paramagnetic alkali radical salts, particularly because the structure of these crystals might give more insight in the structure of alkali radical ion pairs in solution.
Up till now single crystals have been prepared of the systems Li Bp THP, Na Bp Tg, K Bp Ttg and Rb Bp Ttg. The results of preliminary investigations on these crystals are reported in the paragraphs two to six of this chapter: paragraph two contains a description of the preparation of the crystals, paragraph three deals with the composition of the crystals, in paragraph four the physical properties of the crystals and the results of preliminary ESR and NMR experiments are reported, and finally a short discussion and a conclusion are presented in respectively paragraph five and paragraph six.

(ii). Preparation of the crystals

For the preparation of the single crystals solutions of 0.5-1.0 M Bp in the appropriate ether were made and reduced according to hte

methods outlined in sec. 3.2. The glassware apparatus was constructed of vessels with a diameter of 2.5-5 cm and a length of 15-20 cm. The quantities of solvent used for the preparation of the solutions, varied from 20-200 ml. Except for the Li Bp solutions the reduction was performed at elevated temperatures ($\leqslant$ 50° C) and in most cases the reduction took 2-4 hours. Crystals were grown by allowing a reduced solution to come at rest at room temperature during a few days. The crystals were dried by pouring off the solution in a side arm, distilling the remaining solvent and melting off the side arm. In this way the LiBp crystals could be easily dried, but the crystals of the other salts could not always be completely freed of adhering solvent.

(iii). Composition of the crystals

As the alkali salts of Bp decompose in the presence of oxygen and moisture, the crystals had to be handled in an inert atmosphere. For that purpose an evacuable glove box was used, which was filled and flushed with nitrogen. The nitrogen was dried over molecular sieves. In this atmosphere the crystals decomposed only slowly.
The chemical analysis of the crystals was performed by dissolving a weighed amount of crystals in cyclohexane and decomposing it by adding a small amount of water. From the NMR spectrum of the hexane solution the concentrations of the Bp and the ether solvent, which appeared to be always included in the crystals, could be determined by integrating the respective NMR signals and comparing the integrals with those of a standard. After extraction of the hexane solution with water the hexane layer was diluted and the Bp concentration was once again determined by measuring the optical extinction of the solution at the first UV absorption maximum of Bp and comparing the measured extinction with the extinction of a standard solution. In the aeqeous extract the amount of alkali hydroxide was determined by a titration. The method was tested by analysing samples consisting of a mixture of weighed amounts of alkali metal, Bp and ether solvent. The results showed that the relative error for one single determination usually amounted to less than $\pm$ 5%.
The experimentally determined percentages of the components of the alkali Bp crystals are presented in table 15 together with the experimental uncertainties, which are indicated directly behind the quoted percentages. Theoretical percentages calculated on the basis

of a guessed composition, which is indicated in column two of table 15, are shown in parentheses behind the corresponding experimental percentages.

	proposed composition	metal, % [1])	biphenyl, % [1])	solvent, % [1])	total, %
Li Bp THP	1:1:5	1.3±0.1 (1.18)	27 ±1 (26.1)	72±3 (72.8)	99.3 (100)
Na Bp Tg	2:2:5	3.8±0.1 (3.7)	23.1±0.6 (24.8)	64±2 (71.5)	91.3 (100)
K Bp Ttg	1:1:3	5.0±0.3 (4.6)	16.2±0.5 (17.9)	70±2 (77.4)	91.2 (100)
Rb Bp Ttg	1:1:3	9.0±1 (9.4)	16.3±0.8 (17.0)	66±3 (73.5)	91.2 (100)

[1]) The quoted experimental uncertainties are equal to three times the root mean square deviation.

Table 15. Results of the chemical analysis of the alkali Bp crystals. The numbers in parentheses represent theoretical weight percentages based on the proposed composition in the second column.

(iv). Physical properties and magnetic resonance experiments

The crystals of the alkali Bp salts all show a deep blue-black colour. Li Bp THP and Na Bp Tg crystallize in the form of respectively diamond shaped and rectangular shaped plates (figs. 58 and 59), K Bp Ttg crystallizes in the form of closely packed small plates and the crystals of Rb Bp Ttg exhibit the form of 1 mm thick and 5-7 mm long needles (fig. 60). The NaBp crystals melt at 65-67°C, while the crystals of the other three systems decompose before melting, while they loose solvent upon heating.

Preliminary ESR and NMR experiments were performed on crystals of Na Bp Tg. The ESR spectrum consisted of a single strong signal at $g=2$ with a derivative peak-peak width of 0.3-0.4 g. No half field signal was observed. NMR spectra were measured on a polycrystalline sample. The proton spectrum consisted of three peaks namely a strong signal, which was shifted slightly upfield (0.07 g or 300 cps) from the signal of pure Tg and which exhibited a derivative peak-peak width of 0.1 g, a second weak and broad signal at the same position as the first signal with a derivative peak-peak width of 6 g and a third signal, equally broad as, but still weaker than than the second signal, which was shifted upfield from the former two signals by an amount of 4 g.

The Na NMR spectrum consisted of one signal with a derivative peak width of 4-6 g, which was shifted upfield from the Na signal of a 1 M solution of NaCl in H_2O by an amount of 5-6 g.

(v). Discussion

Comparing the experimental and theoretical percentages of the different components of the alkali Bp crystals, quoted in table 15, it appears that for Li Bp THP the experimentally determined percentages are within the experimental uncertainty equal to the proposed theoretical percentages. For the other systems this appears to be true only for the metal percentages. The experimental percentages of Bp and glyme appear to be too low by respectively 0.7-1.7% and 7-7.5%, while also the total amount of material found at the end of the analysis is 8-9% smaller than the amount which was weighed in. These discrepancies may be caused by a slight decomposition and a polymerization of the Bp and of the polyethers at the start of the analysis, when the crystals are decomposed by the addition of a small amount of water [2, 98]. Therefore, the observed discrepancies can be considered as being inherent to the applied method of analysis, so that they do not need to affect the final conclusion that the composition of the crystals mentioned in the second column of table 15 is correct. Thus the composition of the crystals can be given by the stoechiometric formulae Li Bp THP_5, $Na_2Bp_2Tg_5$, K Bp Ttg_3 and Rb Bp Ttg_3.

The composition of the crystals makes it clear that the solvent plays an important role in the formation of the crystals. Probably the solvation of the alkali ions is the main cause for the thermodynamic stability of the crystals. The importance of the solvation energy for the formation of stable ion pairs and stable crystals may become apparent also from the observations 1. that it is impossible to reduce Bp completely with Na in poor solvating agents like THP and MTHF [48, 50, 68] (see also sec. 3.1), 2. that the alkali Bp crystals decompose as soon as the solvent is extracted from the crystals either by evaporation ($LiBpTHP_5$, by extraction with a non-polar solvent like *n*-hexane ($Na_2Bp_2Tg_5$, see also ref. [2]) or by heating (K Bp Ttg_3 and Rb Bp Ttg_3), and 3. that NaBp and KBp form crystals with those solvents which are known to

solvate the respective alkali ions specifically [52, 77] (see also sec. 5.1.2).
The presence of solvent molecules in the crystals makes it improbable that the crystals can be considered as purely ionic crystals. The soft consistency of the crystals, the low melting point of $Na_2Bp_2Tg_5$ and the ease with which the solvent can be removed from the crystals of the other three systems characterize them as Van der Waals-type or molecular crystals.

The ESR and NMR experiments on the $Na_2Bp_2Tg_5$ crystals show that there exists a strong exchange interaction between the unpaired electrons in the crystal: the width of 0.3 g observed for the ESR signal of the crystal is typical for an exchange narrowed ESR line. Similar phenomena have been observed for crystals which are built up of neutral free radicals. For instance, for DPPH. C_6H_6 an exchange narrowed ESR line has been observed with a width of 3 g. From the width of this signal a value of 10^{-11} s has been estimated for the electron exchange time in those crystals [98]. Considering the value of 0.3-0.4 g measured for the $Na_2Bp_2Tg_5$ crystals, it is expected that the electron exchange time in these crystals will have a value between 10^{-11} and 10^{-12} s.
Regarding the Na NMR spectrum of the crystals, the relative sharpness of the signal shows that the anisotropic dipolar interaction of the metal nucleus with the unpaired electron is probably averadged out by the electron exchange. Furthermore the absence of a quadrupolar fine structure may indicate that the solvent molecules are chelated in a symmetric configuration around the metal ions.
The sharp peak in the proton spectrum of the $Na_2Bp_2Tg_5$ crystals is ascribed to the Tg molecules. This peak exhibits an unexpectedly small width. Even if the anisotropic dipolar interaction between the protons and the unpaired electrons would be averadged out completely by the electron exchange one would expect the dipolar interactions between the protons themselves to cause the proton signal to be broader than 0.1 g. It may be supposed that the Tg molecules in the crystal have still some motional degree of freedom, so that they are able to rotate in the crystal. This may result in motional narrowing of the corresponding proton signals. The remaining two broad signals in the proton spectrum of the $Na_2Bp_2Tg_5$ crystals may be ascribed to the protons of the Bp radical ions. The broad signal at high field may originate from the para protons, while the other signal,

which did not show a notable shift, may originate from the ortho and the meta protons.

(vi). Conclusion

From the results presented in this chapter it is concluded that it is possible to prepare single crystals of the paramagnetic alkali salts of Bp. It was found that solvent molecules are taken up in the crystals in stoechiometric well defined proportions probably as chelating agents of the alkali ions.

Preliminary NMR and ESR experiments on $Na_2Bp_2Tg_5$ crystals showed that between the unpaired electrons in the crystals exchange occurs with a virtual time constant of 10^{-11}—10^{-12} s. Moreover the experiments indicated that the solvent molecules have probably some motional degree of freedom in the crystal.

Future study of the properties and the structure of these crystals, especially an X-ray structure determination, may give further information about the structure of the alkali radical ion pairs in the solid state and in solution.

SUMMARY

The experiments described in this study were started to investigate the applicability of the NMR method for the study of alkali radical ion pairs in solution. The results of these investigations are presented in Part I of this study.
In the course of the experiments it proved possible to prepare single crystals of these ion pairs. Part II of this study contains an account of preliminary investigations on these crystals.

The experiments described in Part I of this study have shown that it is possible to observe the NMR signals of protons as well as of alkali nuclei like ^{6}Li, ^{7}Li, ^{23}Na, ^{39}K, ^{85}Rb, ^{87}Rb and ^{133}Cs from solutions of the paramagnetic alkali salts of aromatic compounds like biphenyl, fluorenone, phenanthrene and naphthalene.
The NMR spectra provided information 1. about sign and magnitude of the proton and the alkali hyperfine splitting constants (h.f.s.c.), 2. about the relaxation mechanisms of the protons and the alkali nuclei and the corresponding correlation times, and 3. about the structure of the ion pairs.

1 Regarding the h.f.s.c. of the protons the results of the NMR experiments agreed with the results of ESR measurements and theoretical calculations.
Regarding the h.f.s.c. of the alkali nuclei the experimental results proved that the h.f.s.c. may be negative as well as positive and that in some systems the alkali h.f.s.c. may change sign upon a change of the temperature. A description of the spin density at the alkali nucleus was given on the basis of a zero order M.O. calculation and a first order configuration interaction calculation.

2 The relaxation of the protons and the alkali nuclei proved to be determined by intramolecular interactions.
For the aromatic protons the magnitudes of these interactions could be calculated a priori. The results were used to calculate values for the electronic and the rotational correlation times from the proton linewidths. For both correlation times values between 2×10^{-10} and 2×10^{-11} s were found for concentrated radical solutions at room temperature.
For the alkali nuclei the magnitudes of the intramolecular inter-

actions could be calculated from the alkali linewidths by using the correlation times calculated from the proton experiments. From the values of the interaction parameters conclusions could be drawn about the structure of the ion pairs and its change with the temperature.

3 Regarding the structure of the ion pairs, the best fit with the experimental results was obtained if the ion pairs were described by a static model. Furthermore the experimental results led to the assumption that also in so-called contact ion pairs solvent molecules play an important role in determining the properties and the structure of the ion pairs. A value of 1-2 Å was calculated for the "van der Waals radius" of an aromatic ion.

For the investigations which are described in Part II of this study single crystals of a number of alkali biphenyl (Bp) salts were prepared, which proved to have the following stoechiometric composition: Li Bp THP_5, Na_2 Bp_2 Tg_5, K Bp Ttg_3 and Rb Bp Ttg_3. The abbreviations THP, Tg and Ttg denote respectively the ethers tetrahydropyran, triglyme and tetraglyme. In the crystals, which show the characteristics of molecular crystals, exchange between the unpaired electrons of the radicals occurs with a virtual time constant of 10^{-11}—10^{-12} s. NMR experiments showed that the solvent molecules have still some motional degrees of freedom in the crystal lattice.

SAMENVATTING

Het in dit proefschrift beschreven onderzoek is opgezet om na te gaan in hoeverre de methode der kernspinresonantie (nuclear magnetic resonance, N.M.R.) toegepast kan worden voor het onderzoek aan oplossingen van ionenparen bestaande uit alkali-ionen en aromatische radicaalionen. De resultaten van dit onderzoek zijn vastgelegd in deel I van dit proefschrift.
In de loop van het onderzoek bleek dat het mogelijk is één-kristallen van deze ionenparen te bereiden. Aangezien deze mogelijkheid tot dan toe onbekend was en onderzoek aan deze kristallen nieuwe informatie zou kunnen opleveren over de structuur van dergelijke ionenparen, werd een aantal voorlopige experimenten aan deze kristallen uitgevoerd. De resultaten hiervan zijn vastgelegd in deel II van dit proefschrift.

De in deel I beschreven experimenten hebben aangetoond dat het mogelijk is niet alleen de signalen van de protonen, maar ook die van alkali-isotopen als ^{6}Li, ^{7}Li, ^{23}Na, ^{39}K, ^{85}Rb, ^{87}Rb en ^{133}Cs waar te nemen aan oplossingen van de paramagnetische alkalizouten van verbindingen als bifenyl, fluorenon, fenantreen en naftaleen. De N.M.R.-spectra bleken informatie te verschaffen over 1. teken en grootte van de proton- zowel als van de alkali-koppelingsconstanten, 2. de relaxatiemechanismen van de bestudeerde kernen en de bijbehorende correlatietijden, en 3. de structuur van de ionenparen.

1 Wat de koppelingsconstanten van de protonen betreft bleken de tekens en de grootten hiervan meestal overeen te stemmen met de resultaten van theoretische berekeningen en de resultaten van E.S.R.-experimenten.
Het onderzoek naar teken en grootte van de koppelingsconstanten van de alkali-kernen leverde een bevestiging op van de hypothese van De Boer: zowel positieve als negatieve koppelingsconstanten werden gemeten en in een enkel geval werd een tekenomkering waargenomen bij een verandering van de temperatuur.
2 De bestudering van de relaxatie van verschillende kernen in de bovengenoemde ionenparen toonde aan dat deze relaxatie wordt beheerst door de drie volgende intramoleculaire wisselwerkingen:

de Fermi contact wisselwerking, i.e. de isotrope magnetische dipoolwisselwerking tussen de beschouwde kern en het ongepaarde electron, de anisotrope magnetische dipoolwisselwerking tussen de kern en het ongepaarde electron en de wisselwerking van het quadrupoolmoment van de kern met de veldgradient ter plaatse van de kern.

Voor de relaxatie van de protonen zijn alleen de twee eerstgenoemde wisselwerkingen van belang. De grootten hiervan konden berekend worden aan de hand van de gemeten koppelingsconstanten, respectievelijk met behulp van een computer. Op grond van de aldus berekende waarden konden uit de lijnbreedten in de protonspectra van de radicalen waarden bepaald worden voor de correlatietijd van de electronspin en de correlatietijd van de moleculaire rotatie. In geconcentreerde oplossingen bleken de waarden van beide correlatietijden te liggen tussen 2×10^{-10} en 2×10^{-11} sec.

Voor de relaxatie van de alkalikernen zijn in het algemeen de bovengenoemde wisselwerkingen alle drie van belang. Met behulp van de correlatietijden bepaald op grond van de protonexperimenten, konden de grootten van deze wisselwerkingen bepaald worden uit de lijnbreedten die werden gemeten in de alkalispectra van de oplossingen. De grootten van de Fermi contact wisselwerking en de anisotrope magnetische dipoolwisselwerking bleken voornamelijk bepaald te worden door de grootte van de afstand tussen het alkali-ion en het radicaalion in het ionenpaar. Daarentegen bleek de grootte van de quadrupoolwisselwerking vaak bepaald te worden door de oplosmiddelmoleculen in de solvatatiemantel van het alkali-ion.

3 Tenslotte konden uit de experimenteel bepaalde grootten van de verschillende wisselwerkingen conclusies worden getrokken aangaande de structuur van de ionenparen. De verandering in de grootte van de wisselwerkingen met de temperatuur bleek het beste beschreven te kunnen worden aan de hand van een statisch model voor de ionenparen. Hierbij moest worden aangenomen dat zowel voor de zgn. „contact" ionenparen als voor de zgn. „solvent separated" ionenparen oplosmiddelmoleculen steeds een belangrijke rol spelen bij het bepalen van de structuur en de eigenschappen van de complexen. Voor de „van der Waals straal" van een aromatisch ion, gemeten in een richting loodrecht op het vlak van een aromaatring, werd een waarde gevonden die varieerde

van 1 tot 2 Å, wat 0.5 tot 1 Å minder is dan de uit de litteratuur bekende waarden.

De in deel II beschreven experimenten omvatten in de eerste plaats een onderzoek naar de bereiding en de samenstelling van éénkristallen van een aantal alkalizouten van bifenyl (Bp). De kristallen die tot nog toe bereid konden worden, bleken de volgende stoechiometrische samenstelling te bezitten: Li Bp THP_5, Na_2 Bp_2 Tg_5, K Bp Ttg_3 en Rb Bp Ttg_3, waarin de afkortingen THP, Tg en Ttg respectievelijk de ethers tetrahydropyran, triglym en tetraglym aanduiden. De kristallen, die gekarakteriseerd kunnen worden als molecuulkristallen, vertonen een sterk paramagnetisme als gevolg van de aanwezigheid van ongepaarde electronen in het kristal. Uit E.S.R.-metingen bleek dat de „exchange" tussen deze electronen gekarakteriseerd wordt door een virtuele tijdsconstante van 10^{-11}—10^{-12} sec. Uit de N.M.R.-spectra bleek dat de oplosmiddelmoleculen in het rooster over één of meer vrijheidsgraden van beweging beschikken.
Toekomstig onderzoek, zoals een röntgenografische structuurbepaling, kan nadere informatie geven over de structuur van ionenparen van alkali-ionen en radicaalionen in de vaste fase en in oplossing.

REFERENCES

[1] BERTHELOT, Ann. de Chim., [4] **12**, 155, 1867; W. SCHLENK, J. APPENRODT, A. MICHAEL and A. THAL, Ber. der deutsch-chem. Gesellsch., **47**, 473, 1914; W. SCHLENK and E. BERGMANN, Liebigs Ann. Chem., **463**, 83 ff., 1928; W. HÜCKEL and H. BRETSCHNEIDER, *ibid.*, **540**, 157, 1939.

[2] N. D. SCOTT, J. F. WALKER and V. L. HANSLEY, J. Am. Chem. Soc., **58**, 2442, 1936.

[3] S. I. WEISSMAN, J. TOWNSEND, D. E. PAUL and G. E. PAKE, J. Chem. Phys., **21**, 2227, 1953; D. LIPKIN, D. E. PAUL, J. TOWNSEND and S. I. WEISSMAN, Science, **117**, 534, 1953.

[4] H. M. MCCONNELL, J. Chem. Phys., **24**, 632, 1956.

[5] E. DE BOER, *ibid.*, **25**, 190, 1956.

[6] E. DE BOER and S. I. WEISSMAN, J. Am. Chem. Soc., **80**, 4549, 1958.

[7] H. M. MCCONNELL and D. B. CHESNUT, J. Chem. Phys., **28**, 107, 1958.

[8] P. BROVETTO, and S. FERRONI, Nuovo Cimento, **5**, 142, 1957.

[9] A. D. MCLACHLAN, Mol. Phys., **3**, 233, 1960.

[10] N. M. ATHERTON and S. I. WEISSMAN, J. Am. Chem. Soc., **83**, 1330, 1961.

[11] A. C. ATEN, J. DIELEMAN and G. J. HOIJTINK, Disc. Farad. Soc., **29**, 182, 1960.

[12] E. DE BOER, Rec. Trav. Chim., **84**, 609, 1965.

[13] M. A. KOMARYNSKI, cited in ref. [11].

[14] P. GRACEFFA and T. R. TUTTLE, JR., J. Chem. Phys., **50**, 1908,1969.

[15] N. HIROTA, J. Am. Chem. Soc., **89**, 32, 1967.

[16] N. BLOEMBERGEN, J. Chem. Phys., **27**, 595, 1957.

[17] E. DE BOER and C. MACLEAN, Mol. Phys., **9**, 191, 1965; J. Chem. Phys., **44**, 1334, 1966.

[18] G. W. CANTERS, H. VAN WILLIGEN and E. DE BOER, Chem. Comm., **3**, 566, 1967.

[19] K. H. HAUSSER, H. BRUNNER and J. C. JOCHIMS, Mol. Phys., **10**, 253, 1966; R. KREILICK, J. Chem. Phys., **45**, 1922, 1966.

[20] G. W. CANTERS and E. DE BOER, Mol. Phys., **13**, 395, 1967.

[21] G. W. CANTERS, E. DE BOER, B. M. P. HENDRIKS and H. VAN WILLIGEN, Chem. Phys. Lett., **1**, 627, 1968.

[22] G. W. CANTERS, E. DE BOER, B. M. P. HENDRIKS and A. A. K. KLAASSEN, Proc. Coll. Ampère XV, P. Averbuch, ed., Amsterdam: North-Holland Publishing Co., 1969, p. 242.

[23] J. A. POPLE, W. G. SCHNEIDER and H. J. BERNSTEIN, High-resolution Nuclear Magnetic Resonance, New York: McGraw-Hill Book Company, Inc., 1959, Chap. 1.

[24] C. P. SLICHTER, Principles of Magnetic Resonance, New York: Harper & Row, 1963, Sec. 4.6.

[25] H. M. MCCONNELL, J. Chem. Phys., **28**, 1188, 1958.

[26] H. M. MCCONNELL and J. STRATHDEE, Mol. Phys., **2**, 129, 1959.

[27] A. ABRAGAM, The Principles of Nuclear Magnetism, Oxford: at the Clarendon Press, 1961, p. 313 ff.

[28] M. H. COHEN and F. REIF, "Quadrupole Effects in Nuclear Magnetic Resonance Studies of Solids", Solid State Phys., F. SEITZ and D. TURNBULL,

eds., New York: Academic Press, Inc., 1957, Vol. 5, p. 321 ff.; T. P. Das and E. L. Hahn, "Nuclear Quadrupole Resonance Spectroscopy", *ibid.*, 1958, Supplement 1.
[29] H. M. McConnell, J. Chem. Phys., **24**, 764, 1956.
[30] S. I. Weissman, *ibid.*, **25**, 890, 1956; S. I. Weissman, T. R. Tuttle, Jr. and E. de Boer, J. Phys. Chem., **61**, 28, 1957.
[31] D. A. Goodings, Phys. Rev., **123**, 1706, 1961.
[32] P. Kusch and H. Taub, *ibid.*, **75**, 1477, 1949; R. G. Schlecht and D. W. McColm, *ibid.*, **142**, 11, 1966.
[33] K. C. Brog, T. G. Eck and H. Wieder, *ibid.*, **153**, 91, 1967.
[34] M. L. Perl, I. I. Rabi and B. Senitzky, *ibid.*, **98**, 611, 1955. J. N. Dodd and R. W. N. Kinnear, Proc. Phys. Soc., **75**, 51, 1960; H. Ackermann, Z. Phys., **194**, 253, 1966; M. Baumann, W. Hartmann, H. Krüger and A. Oed, *ibid*, **194**, 270, 1966.
[35] P. Buck and I. I. Rabi, Phys. Rev., **107**, 1291, 1957.
[36] B. Senitzky and I. I. Rabi, *ibid.*, **103**, 315, 1956.
[37] H. A. Schüssler, Z. Phys., **182**, 289, 1965.
[38] C. Corvaja, private communication.
[39] D. N. Bhattacharyya, C. L. Lee, J. Smid and M. Szwarc, J. Phys. Chem., **69**, 608, 1965.
[40] C. Carvajal, K. J. Tölle, J. Smid and M. Swarcz, J. Am. Chem. Soc., **87**, 5548, 1965.
[41] R. V. Slates and M. Szwarc, J. Phys. Chem., **12**, 4124, 1965.
[42] P. Chang, R. V. Slates and M. Szwarc, *ibid.*, **70**, 3180, 1966.
[43] D. Nicholls, C. Sutphen and M. Szwarc, *ibid.*, **72**, 1021, 1968.
[44] S. Winstein, E. Clippinger, A. H. Fainberg and G. C. Robinson, J. Am. Chem. Soc., **76**, 2597, 1954; S. Winstein and G. C. Robinson, *ibid.*, **80**, 169, 1958.
[45] E. Grunwald, Anal. Chem., **26**, 1696, 1954.
[46] N. Hirota and R. Kreilick, J. Am. Chem. Soc., **88**, 614, 1966; N. Hirota, J. Phys. Chem., **71**, 127, 1967; A. Crowley, N. Hirota and R. Kreilick, J. Chem. Phys., **46**, 4815, 1967; N. Hirota, R. Carraway and W. Schook, J. Am. Chem. Soc., **90**, 3611, 1968.
[47] T. E. Hogen-Esch and J. Smid, J. Am. Chem. Soc., **87**, 669, 1965; *ibid.*, **88**, 307, 1966; *ibid.*, **88**, 318, 1966; *ibid.*, **89**, 2764, 1967.
[48] R. V. Slates nad M. Szwarc, *ibid.*, **89**, 6043, 1967.
[49] M. Szwarc, Makromolek. Chem., **89**, 44, 1965.
[50] A. I. Shatenstein and E. S. Petrov, Russ. Chem. Rev., **36**, 100, 1967.
[51] L. L. Chan and J. Smid, J. Am. Chem. Soc., **90**, 4654, 1968.
[52] L. L. Chan and J. Smid, *ibid.*, **89**, 4547, 1967.
[53] P. Biloen, Thesis, Amsterdam, 1968.
[54] N. Hirota and S. I. Weissman, J. Am. Chem. Soc., **86**, 2538, 1964.
[55] C. P. Slichter, *op. cit.*, Chap. 5.
[56] G. E. Pake, Paramagnetic Resonance, New York: W. A. Benjamin, Inc., 1962, Chap. 5.
[57] I. Solomon, Phys. Rev., **99**, 559, 1955.
[58] N. Bloembergen, J. Chem. Phys., **27**, 572, 1957.

[59] R. A. Bernheim, T. H. Brown, H. S. Gutowsky and D. E. Woessner, *ibid.*, **30**, 950, 1959.
[60] A. Abragam, *op. cit.*, Chap. 8.
[61] A. Carrington and A. D. McLlachlan, Introduction to Magnetic Resonance, New York: Harper and Row, 1967, Chap. 11.
[62] G. E. Pake and T. R. Tuttle, Jr., Phys. Rev. Lett., **3**, 423, 1959; M. T. Jones, J. Chem. Phys., **38**, 2892, 1963; W. Plachy and D. Kivelson, *ibid.*, **47**, 3312, 1967.
[63] F. J. Millero, J. Phys. Chem., **72**, 3209, 1968.
[64] W. Derbyshire, Mol. Phys., **5**, 225, 1962.
[65] R. M. Sternheimer, Phys. Rev., **146**, 140, 1966.
[66] R. M. Sternheimer, Int. J. Quant. Chem., **1S**, 67, 1967.
[67] J. A. Pople, W. G. Scheider and H. J. Bdrnstein, *op. cit.*, Sec. 10-2.
[68] A. Rembaum, A. Eisenberg, R. Haack and R. F. Landel, J. Am. Chem. Soc., **89**, 1062, 1967.
[69] J. A. Pople, W. G. Schneider and H. J. Bernstein, *op. cit.*, Sec. 4-9.
[70] C. Deverell and R. E. Richards, Mol. Phys., **10**, 551, 1966.
[71] G. E. Maciel, J. K. Hancock, L. F. Lafferty, P. A. Mueller and W. K. Musker, Inorg. Chem., **5**, 554, 1966.
[72] L. Petrakis, J. Chem. Educ., **44**, 432, 1967.
[73] O. E. Meyers and E. J. Putzer, J. Appl. Phys., **30**, 1987, 1959; G. W. Smith, *ibid.*, **35**, 1217, 1964.
[74] M. Shporer, G. Ron, A. Loewenstein and G. Navon, Inorg. Chem., **4**, 358, 1965.
[75] J. C. Danner, Thesis, Brandeis Univeristy, Waltham (Mass.), 1967.
J. G. Powles and M. H. Mosley, Proc. Phys. Soc., **78**, 370, 1961.
[76] T. Schaefer and W. G. Schneider, Can. J. Chem., **41**, 966, 1963.
[77] M. Shinohara, J. Smid and M. Szwarc, J. Am. Chem. Soc., **90**, 2175, 1968.
[78] P. A. Speight and R. L. Armstrong, Can. J. Phys., **45**, 2493, 1967.
[79] A. Streitweiser, Jr., Molecular Orbital Theory for Organic Chemists, New York: John Wiley & Sons, Inc., 1961, Chap. 5.
[80] R. Dehl and G. K. Fraenkel, J. Chem. Phys., **39**, 1793, 1963.
[81] N. Hirota, "Metal Ketyls and Related Radical Ions-Electronic Structures and ion pair equilibria", Radical Ions, E. T. Kaiser and L. Kevan, eds., New York: Interscience Publishers, 1968, Chap. 2.
[82] J. P. Colpa and J. R. Bolton, Mol. Phys., **6**, 273, 1963.
[83] D. C. Reitz and S. I. Weissman, J. Chem. Phys., **33**, 700, 1960.
[84] N. Hirota, J. Am. Chem. Soc., **90**, 3603, 1968.
[85] C. L. Dodson and A. H. Reddoch, J. Chem. Phys., **48**, 3226, 1968.
[86] I. C. Calder, T. McL. Spotswood and C. I. Tanzer, Australian J. Chem., **20**, 1195, 1967.
[87] L. Pauling, The Nature of the Chemical Bond, New York: Cornell University Press, 1960, Sec. 13-2; see also: J. A. A. Ketelaar, Chemical Constitution, Amsterdam: Elsevier Publishing Company, 1958, Paragraph 4.
[88] L. Wharton, L. P. Gold and W. Klemperer, Phys. Rev., **133**, B270, 1964.
[89] G. J. Ritter and G. W. Series, Proc. Roy. Soc. (London), **238A**, 473, 1957.
[90] U. Meyer-Berkhout, Z. Phys., **141**, 185, 1955.
[91] P. Buck, I. I. Rabi and B. Senitzky, Phys. Rev., **104**, 553, 1956.

[92] H. Bucka, H. Kopferman and E. W. Otten, Ann. Phys., **4**, 39, 1959; H. Bucka and G. von Oppen, *ibid.*, **10**, 119, 1962; K. Althoff and H. Krüger, Naturwissenschaften, **47**, 368, 1954.
[93] H. V. Carter, B. J. McClelland and E. Warhurst, Trans. Far. Soc., **56**, 455, 1960.
[94] F. C. Adam and S. I. Weissman, J. Am. Chem. Soc., **80**, 1518, 1958.
[95] N. Hirota and S. I. Weissman, *ibid.*, **86**, 2537, 1964.
[96] J. A. Dixon, P. A. Gwinner and D. C. Lini, *ibid.*, **87**, 1379, 1965; A. K. Banerjee, A. J. Layton, R. S. Nyholm and M. R. Truter, Nature, **217**, 1147, 1968.
[97] G. E. Pake, *op. cit.*, Chap. 4.
[98] J. L. Down, J. Lewis, B. Moore and G. Wilkinson, J. Chem. Soc., 1959, 3767.

STELLINGEN

I

De deuterium kernspinresonantie-spectra van gedeutereerde aromatische radicalen in oplossing zijn bij gegeven uitwendig magnetisch veld aanmerkelijk beter opgelost dan de protonspectra van de overeenkomstige niet-gedeutereerde verbindingen, terwijl onder de gebruikelijke experimentele omstandigheden de signaal-ruisverhouding voor beide typen van spectra van dezelfde orde van grootte is.

II

Over de relaxatieprocessen van de kernspins en de electronenspins van een radicaal in oplossing kan gedetailleerde informatie verkregen worden door met elkaar te vergelijken het protonspectrum en het deuterium kernspinresonantie-spectrum van een oplossing die een mengsel bevat van de ongedeutereerde en de volledig gedeutereerde verbinding.

III

De door Espersen en Kreilick gebruikte benadering voor de anisotrope wisselwerking tussen het magnetisch moment van een atoomkern en dat van een ongepaard electron in een radicaal leidt tot een door hen berekende waarde voor de parameter Q_{FF}, die een factor 1,8 te groot is.

W. G. Espersen en R. W. Kreilick, Mol. Phys., **16**, 577, 1969.

IV

Het optreden van radicalen bij de reactie van t-butylhypochloriet met kalium-t-butanolaat zou verklaard kunnen worden via een redoxreactie door de vorming van een ladingsoverdrachtcomplex als eerste stap in de reactieketen aan te nemen.

C. Walling en J. Kjellgren, J. Org. Chem., **34**, 1487, 1969.

V

Byfleet c.s. maken onvoldoende aannemelijk, dat voor de beschrijving van de g- en de A-tensor in het door hen bestudeerde molybdaatcomplex gebruik gemaakt mag worden van een hogere symmetrie dan die van de puntgroep van het complex.

C. R. Byfleet, F. G. Herring, W. C. Lin, C. A. McDowell en D. J. Ward, Mol. Phys., **15**, 239, 1968.

VI

De voorstellen van de commissie-van Os tot wijziging van de structuur van het wetenschappelijk corps komen niet tegemoet aan de door de commissie gesignaleerde gebreken in de bestaande structuur.

Structuur van het wetenschappelijk corps, Publicatie nr. 9 van de Academische Raad, 's-Gravenhage: Staatsuitgeverij, 1968, pargr. II, III en IV.

VII

De ethiek van de wetenschapsbeoefening verdient een plaats in de studieprogramma's voor de verschillende studierichtingen in de faculteit der Wiskunde en Natuurwetenschappen.

VIII

Het is de vraag of de met de invoering van de wet op het voortgezet onderwijs van kracht geworden en van kracht wordende wijzigingen in het leerplan van het V.W.O. en het A.V.O. op de juiste manier tegemoet komen aan de behoefte aan een verbeterde sociale opvoeding van leerlingen van het voortgezet onderwijs enerzijds en aan de stijgende vraag naar geschoolde arbeidskrachten in bijvoorbeeld de chemische industrie anderzijds.

IX

De mogelijkheid een proefschrift te doen verschijnen via een vereenvoudigde procedure wordt geopend, indien de voorschriften tot regeling van de promotie worden gewijzigd in die zin, dat

1 de beoordeling van het proefschrift wordt opgedragen aan een commissie van drie leden,
2 de van universiteitswege verplicht gestelde minimum-oplage van het proefschrift wordt verlaagd tot maximaal 5 exemplaren,
3 de verplichting tot het doen drukken van het proefschrift komt te vervallen.

X

De volksvertegenwoordiger die verklaart de vervulling van zijn politieke functies te beschouwen als vrije-tijdsbesteding, diskwalificeert hiermee het niveau van het politieke bedrijf in Nederland.

Prof. dr. J. W. van Hulst, Dagblad „Trouw", 10/9/'69, 15/9/'69.

Nijmegen 3 oktober 1969
G. W. Canters